Albert Ernest Smith

candidate for the degree of

Doctor of Philosophy

Dissertation: The Effect of the Source Aperture on Diffraction Grating Images

Outline of Studies

Major subject: Physics

Minor subject: Mathematics

Biographical Items

Born, November 1, 1927, Windham, Vermont

Undergraduate Studies, Atlantic Union College, 1944-49

Graduate Studies, Michigan State College, 1949 - 1954

Experience: Graduate Assistant, Michigan State College, 1949-1953; Instructor in Physics, Michigan State College, 1953-1954; Assistant Professor of Physics, Union College, 1954 -

THE EFFECT OF THE SOURCE APERTURE ON DIFFRACTION GRATING IMAGES

By

Albert Ernest Smith

AN ABSTRACT

Submitted to the School of Graduate Studies of Michigan State College of Agriculture in partial fulfillment of the requirements for the degree of

DOCTOR OF PHILOSOPHY

Department of Physics and Astronomy

1954

Approved Robert D Spence

In a previous work Smith and Hause (1) derived an expression for the intensity distribution in the Fraunhofer pattern of a diffraction grating with N apertures as a function of the breadth of the illuminating aperture where the source aperture was illuminated in the noncoherent mode. Almost simultaneously Takeyama, et al. (2) arrived at the corresponding expression for a grating with a small number of apertures illuminated in the coherent mode. Both of these expressions were extremely cumbersome in case of a diffraction grating with a large number of apertures. No experimental verification existed for the coherent mode, and the verification for the noncoherent mode was limited to the behavior of the subsidiary maxima as a function of source breadth in the case of a grating with a small number of apertures.

In this work both expressions mentioned were simplified so that they could readily be used to find the intensity distribution in the image formed by the diffraction grating of many apertures. Particular attention was given to the intensity distribution in the principal maxima.

The results obtained for the diffraction grating were compared with the results which Van Cittert (3)

obtained in his calculations of the intensity distribution in the images formed by a single diffracting aperture. Within the limits of the assumptions used to simplify the grating theory no differences were found. In the grating theory it was assumed that the source aperture was located on the axis of the grating and that the angle subtended by the source aperture was sufficiently small that the first order approximation could be used for the sine of the angle and that N was large.

These results were verified in the laboratory by direct measurement of the intensity in the grating image. Two different gratings were used of different N values and measurements taken over a wide range of values of the source aperture breadth. The results obtained were compared graphically with the theoretical results. Three different modes of illumination as suggested by Stockbarger and Burns (4) were used and the results of the comparison were interpreted in terms of the degree of coherence or noncoherence of the source aperture. Measurements were also made on the image formed by the single aperture as a means of verifying Van Cittert's calculations

and of checking the conclusion of the present calculation that the two theories give the same result. No difference was evident.

(1) Smith A. E., and C. D. Hause, Fraunhofer Multiple Slit Diffraction Patterns with Finite Sources, J. Opt. Soc. Am. 42, 426-430, (1952)

(2) Takeyama, H., T. Kitahara, and T. Matubayasi, On the Mathematical Treatment of the Effect of the Width of the Slit on Fraunhofer's Diffraction Phenomenon (Part II), J. Sci. Hirosima Univ. (S.A.) 15, 139-146, (1951)

(3) Van Cittert, P.H., Zum Einfluss der Spaltbreite auf die Intensitatsverteilung in Spektrallinien. Z. Physik 65, 547-563, (1930)

(4) Stockbarger, D. C. and L. Burns, Line Shape as a Function of Spectrograph Slit Irradiation. J. Opt. Soc. Am. 23, 379-384, (1933)

THE EFFECT OF THE SOURCE APERTURE ON DIFFRACTION GRATING IMAGES

By

Albert Ernest Smith

A THESIS

Submitted to the School of Graduate Studies of Michigan State College of Agriculture in partial fulfillment of the requirements for the degree of

DOCTOR OF PHILOSOPHY

Department of Physics and Astronomy

1954

5/28/57
g 1269

ACKNOWLEDGEMENT

The author wishes to express his appreciation to Dr. C. D. Hause, at whose suggestion this work was undertaken, for his constant encouragement and guidance in its completion. He is also grateful to Dr. R. D. Spence for his suggestions and for checking the final report.

Albert E. Smith

TABLE OF CONTENTS

LIST OF FIGURES

I. INTRODUCTION

The problem of predicting the characteristics of the image formed by an aberrationless optical system is one which depends to a large extent on the diffraction effects produced by the components of the system. If the amplitude and phase distributions in one cross section of an optical system are known together with the geometry of the components which follow this cross section, it is possible, at least in principle, to determine the intensity distribution for any other cross section desired. In practice, however, the problem may be extremely difficult except for certain definite planes of the system.

With these ideas in mind there are three places of interest, places at which computation is reasonably simple, in the system to be considered: the object or source element, the diffracting or image-forming element, and the image or focal plane. In this work the problem will be taken as one in Fraunhofer diffraction, where a plane wave, or set of plane waves, from the object source is incident on a diffracting element and the resulting disturbance is focused on an image plane to be examined.

A technique which has been commonly used is to calculate the pattern produced by a diffracting ele-

ment when illuminated by a point or line source. This method results in an expression which is a function of the characteristics of the diffracting element and of the angles of incidence and of observation. If the source has finite dimensions, it is then treated as being made up of a large number of elementary sources of infinitesimal dimensions, each of which contributes to the final image. The manner in which the elementary sources contribute to the final image depends on their relative phases. Two limiting cases exist for which the pattern may readily be calculated. The source may be radiating as a unit, all elements having the same phase, in which case the amplitudes are additive, or there may be a random distribution of phases in the source, in which case the intensities are additive. These usually are referred to respectively as the coherent and noncoherent modes of illumination.

The ideas expressed here have been used by Van Cittert (1) and others (2-4) to determine the characteristics of the image formed by a single diffracting aperture in a Fraunhofer system as a function of the mode of illumination and of the dimensions of the object source. The results of this study have been applied to predict the line-shape characteristic of a prism spectroscope (5) and to predict the image-

forming properties of the microscope.

The double slit diffracting system has been treated extensively (6, 7) and the characteristics of the images formed have been applied to the problem of determining the diameters of stellar (8) and microscopic objects (9).

It has often been tacitly assumed by spectroscopists that the single-aperture results apply equally well to the far more complicated system of the diffraction grating. The problem considered here is the calculation of the intensity distribution in the grating image as a function of source dimensions for both coherent and noncoherent illumination and a comparison of these calculations with experimental results. The results, both theoretical and experimental, indicate to a very close approximation that grating apertures do behave as single apertures when the gratings have large numbers of lines. The work has been done only for small incidence angles.

In a former work (10) the problem of a grating with a small number of lines and a noncoherent source was treated with particular reference to the behavior of the subsidiary maxima as the breadth of the source was increased. A theoretical treatment of the corresponding coherent case was carried out almost simultaneously (11) with interesting predictions as to the

variation of the intensity in the center of the principal maxima as a function of source width; but apparently no experimental verification exists.

The formal techniques for extending the problem to the diffraction grating with any number of slits was essentially complete with the treatment of the small grating. In fact, in the treatment of the grating with a small number of slits expressions were found which, although extremely cumbersome, were equally valid for a large number of apertures. It therefore seemed of interest to carry out the computations for a grating consisting of a large number of apertures and to attempt to simplify to such an extent that it would be suitable for rapid computation.

The computations were carried out as a two dimensional problem assuming rectangular sources which are either completely coherent or completely noncoherent. Since these conditions are not realizable experimentally the results of the theory and the experiment cannot be expected to agree completely. This and other sources of difficulty will be discussed later. There is, however, a considerable range of agreement and the experimental results found can be taken as verification of the principal predictions of the theory.

II. THEORY

The optical system under consideration consists of a source of finite breadth W located in the focal plane of the collimating lens. The collimator is followed by the diffracting element, a grating of N slits in the case studied, and the pattern produced is imaged in the focal plane of the camera lens.

The source subtends an angle $\alpha = W/f$ at the collimator and hence the plane waves from the source are incident on the grating with angles ranging from $+\alpha/2$ to $-\alpha/2$. The source radiates monochromatic light of wavelength λ. The separation of the apertures in the grating, the grating constant, will be s.

To find the effect produced in the image plane by a line element of the object a method is used which is similar to that of Born (12).

From a single element of the source a plane wave with an amplitude $a = a_0 e^{jkr}$ is incident on the grating at an angle i. Where $j = \sqrt{-1}$, $k = 2\pi/\lambda$ and r is the distance parameter. The amplitude at an observation point P in the image plane will be, if the angle of observation of the diffraction is θ, the result of summing the contributions from all the grating apertures:

$$a = a_0 e^{jkr} \sum_{m=0}^{m=N-1} e^{jmks(\sin\theta + \sin i)} \qquad (1)$$

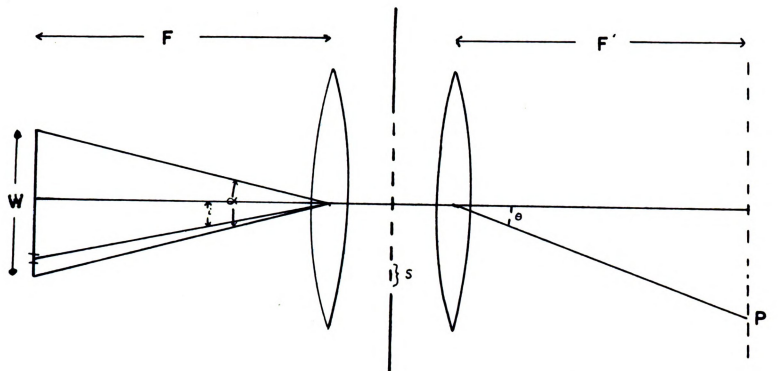

Fig. 1 The general optical set up. The angle of incidence for a line element of the source is designated as i. This angle takes on values from $-\alpha/2$ to $+\alpha/2$, where $\alpha = w/F$. The angle of diffraction is designated as θ.

The manner of finding the intensity expected at the point P depends upon the phase relations between the object elements. In the coherent case it will be assumed that the source radiates as a unit with all elements in the same phase and having the same amplitude. When this is true the resultant intensity is found to be

$$I = |A|^2, \text{ where } A = \int_{-\alpha/2}^{+\alpha/2} a \, di \qquad (2)$$

whereas in the noncoherent case there is a completely random distribution of phases and the intensity can be written

$$I = \int_{-\alpha/2}^{+\alpha/2} |a|^2 \, di \; . \qquad (3)$$

If the angles θ and i are assumed to be small, it is possible to substitute for the sines of the angles the angular values themselves. Simultaneously the exponent involving r may be omitted as a constant multiplying factor. Thus equation (1) is simplified to read

$$a = a_0 \sum_{m=0}^{m=N-1} e^{im k s(\theta+i)} \qquad (1')$$

A. COHERENT ILLUMINATION

A different set of numbers may be used to denote the grating apertures, and equation (1'), when rewritten in terms of these new numbers, becomes without changing its value

$$a = a_0 \sum_{n=-M}^{n=M} e^{jnk_s(\theta+i)} \qquad \text{where } M = \frac{N-1}{2} \qquad (4)$$

Since n is always an integer N must be an odd number. This restriction would appear to limit the generality of the theory. It will be seen later, however, that if N is large the contribution from the correction involved if N-1 is used in place of N has an absolute value less than 1/N of the total.

In order to obtain the amplitude from the complete source, equation (4) is substituted into equation (2) with the result

$$A = a_0 \int_{-\alpha/2}^{\alpha/2} \sum_{n=-M}^{n=M} e^{jnk_s(\theta+i)} \, di \; .$$

Since this is a finite series it is possible to interchange the order of the operations without changing the value

$$A = a_0 \sum_{n=-M}^{n=M} e^{jnk_s\theta} \int_{-\alpha/2}^{\alpha/2} e^{jnk_s i} \, di \; .$$

Expanding the exponential terms and integrating

$$A = \frac{2a_0}{k_s}\left[\sum \cos\frac{nk_s\theta \sin nk_s\alpha/2}{n} + j\sum_{n=-M}^{n=M} \frac{\sin nk_s\theta \sin nk_s\alpha/2}{n}\right].$$

The imaginary terms may be seen to vanish if rearranged, since

$$\frac{\sin(-nx)\sin(-ny)}{(-n)} + \frac{\sin(nx)\sin(ny)}{(n)} = 0 \quad , \quad \left.\frac{\sin nx \sin ny}{n}\right]_{n=0} = 0$$

The remaining term can be expanded to read

$$A = \frac{a_0}{k_s}\left[\sum_{m=-M}^{m=M} \frac{\sin m\frac{k_s}{2}(\alpha+2\theta)}{m} + \sum_{m=-M}^{m=M} \frac{\sin m\frac{k_s}{2}(\alpha-2\theta)}{m}\right] \quad (5)$$

This expression may be simplified by letting

$$\alpha' = \frac{k_s\alpha}{2}\ ,\ \theta' = \frac{k_s\theta}{2}\ . \quad (6)$$

In which case

$$A = \frac{a_0}{k_s}\left[\sum_{m=-M}^{m=M} \frac{\sin m(\alpha'+2\theta')}{m} + \sum_{m=-M}^{m=M} \frac{\sin m(\alpha'-2\theta')}{m}\right] \quad (7)$$

or

$$A = \frac{a_0}{k_s}\left[\sum_{m=-M}^{m=M} \frac{\sin mx^+}{m} + \sum_{m=-M}^{m=M} \frac{\sin mx^-}{m}\right] \quad (8)$$

where

$$x^+ = \alpha'+2\theta'\ ,\quad x^- = \alpha'-2\theta'\ . \quad (9)$$

Making use of the facts that

$$\frac{\sin(-mx)}{(-m)} + \frac{\sin(+mx)}{(+m)} = 2\frac{\sin mx}{m}\ ,\ \left.\frac{\sin mx}{m}\right]_{m=0} = x$$

it is seen that

$$A = \frac{a_0'}{\pi}\left[\alpha' + \sum_{m=1}^{m=M} \frac{\sin mx^+}{m} + \sum_{m=1}^{m=M} \frac{\sin mx^-}{m}\right] \quad (10)$$

where $a_0' = \frac{2a_0\pi}{k_s}$. The factor π is introduced to simplify a later result.

The series of the form $\sum_1^M \frac{\sin mx}{m}$ which appears twice in the expression for the amplitude is too cumbersome to evaluate exactly when M (or N) is large. The remainder of this analysis will be devoted to an attempt to arrive at a reasonably close approximation to its value in a more tractable form. Although the first two

steps that follow are not necessary to the logic of the final result they are helpful in understanding the approximation which is being made.

Consider a function defined as follows:

$$f(x) = \frac{\pi - x}{2} \quad , \quad 0 < x < 2\pi$$
$$f(x \pm 2\pi) = f(x) \quad , \quad x \neq 0, 2\pi, \ldots, 2l\pi \quad , \quad l = 1, 2, \ldots \tag{11}$$

The Fourier development for f(x) is the infinite series

$$\sum_{m=1}^{\infty} \frac{\sin mx}{m} \tag{12}$$

A theorem proved by Bôcher (13) states that the Fourier development of the function f(x) converges to the value f(x) at all points where the function is continuous and to the value $1/2\left[f(x+o) + f(x-o)\right]$ at all points where the function is discontinuous. It converges uniformly throughout any interval which does not include or reach up to a point of discontinuity.

The function f(x) consists of a series of straight lines with negative slopes and with finite discontinuities occurring at intervals of x that are multiples of 2π. If as a first approximation M is set equal to infinity in equation (10) the result should give an approximation to the amplitude.

$$A \simeq \frac{a_0'}{\pi} \left[\alpha' + \sum_{m=1}^{\infty} \frac{\sin mx^+}{m} + \sum_{m=1}^{\infty} \frac{\sin mx^-}{m} \right] . \tag{13}$$

This becomes upon substitution of equation (12)

$$A \simeq \frac{a_o'}{\pi}\left[\alpha' + f(x^+) + f(x^-)\right] . \qquad (14)$$

If (11), the definition of (12), is now inserted, the result obtained is

$$A \simeq \frac{a_o'}{\pi}\left[\alpha' + \pi - \tfrac{x^+}{2} - \tfrac{x^-}{2}\right], \text{ where } \left\{\begin{array}{l} 0 < x^+ < 2\pi \\ 0 < x^- < 2\pi \end{array}\right\} \quad (15)$$

which becomes by use of (9)

$$A \simeq \frac{a_o'}{\pi}\left[\alpha' + \pi - \left(\frac{\alpha'+2\theta'}{2}\right) - \left(\frac{\alpha'-2\theta'}{2}\right)\right], \left\{\begin{array}{l} 0 < \alpha'+2\theta' < 2\pi \\ 0 < \alpha'-2\theta' < 2\pi \end{array}\right\} \quad (16)$$

This expression, when plotted as a function of θ', consists of two series of straight lines with opposite slopes displaced from the origin by an amount $\alpha'/2$ as in Fig. 2. The result as seen either graphically or analytically will be a series of rectangular images at values of θ' equal to multiples of π as in Fig. 3. Making use now of the periodic nature of the function f(x) to evaluate the amplitude outside of the region between $+\alpha'/2$ and $-\alpha'/2$, for example with positive values to the right of $+\alpha'/2$

$$A \simeq \frac{a_o'}{\pi}\left[\alpha' + \left(\frac{\pi - x^+}{2}\right) + \left(\frac{-\pi - x^-}{2}\right)\right], \left\{\begin{array}{l} 0 < x^+ < 2\pi \\ -2\pi < x^- < 0 \end{array}\right\}$$

which becomes by equation (9)

$$A \simeq \frac{a_o'}{\pi}\left[\alpha' - \left(\frac{\alpha'+2\theta'}{2}\right) - \left(\frac{\alpha'-2\theta'}{2}\right)\right], \left\{\begin{array}{l} 0 < \alpha'+2\theta' < 2\pi \\ -2\pi < \alpha'-2\theta' < 0 \end{array}\right\} \quad (17)$$

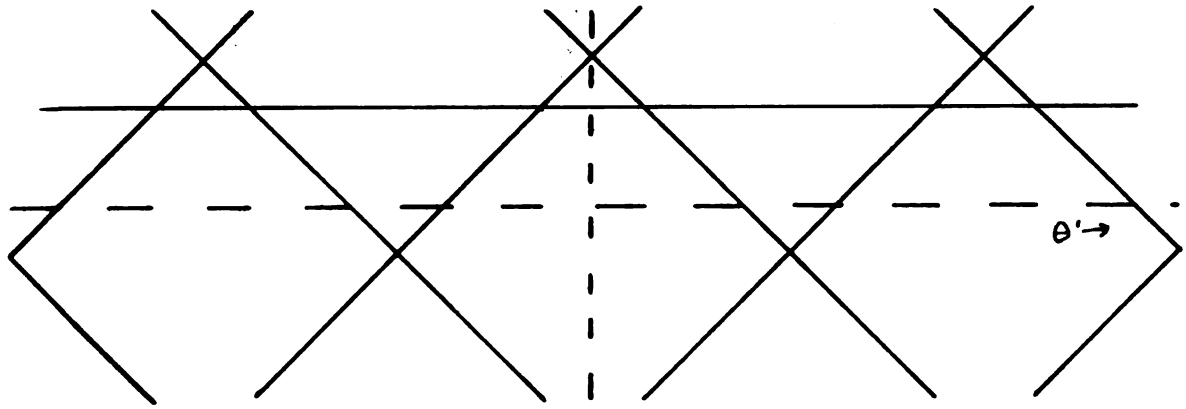

Fig. 2 The components of the rectangular amplitude function.

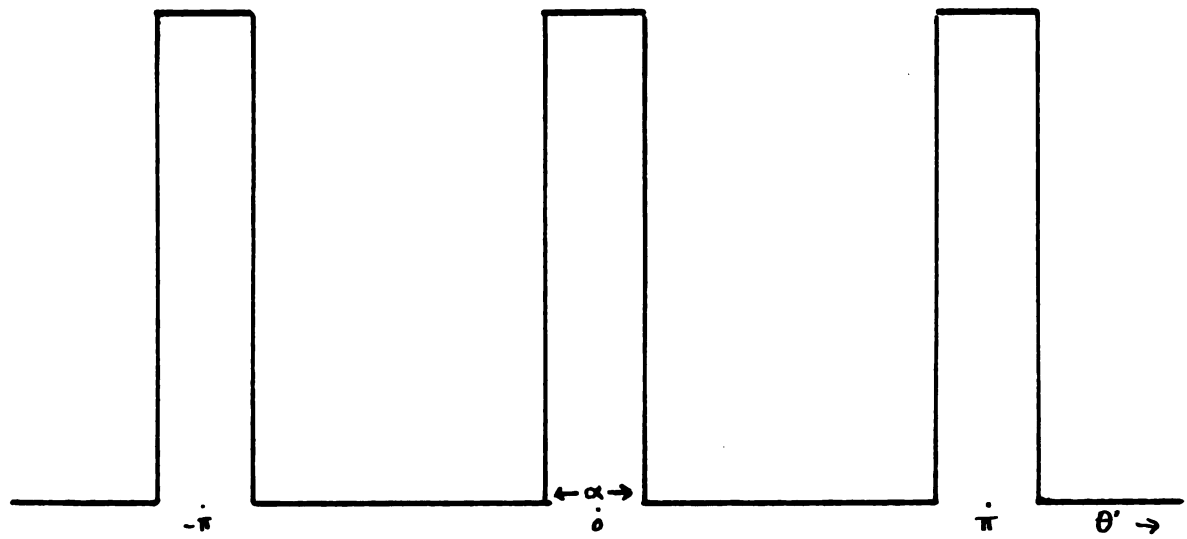

Fig. 3 The rectangular amplitude function with no account taken of the Gibbs phenomenon.

It is now possible to sum up the results obtained in equations (16) and (17) in a form which describes the rectangular images.

$$A \simeq a_0' \quad , \quad -\alpha'/2 < \theta' < \alpha'/2$$

$$A \simeq 0 \quad , \quad -\pi + \alpha'/2 < \theta' < -\alpha'/2 \quad \text{and} \quad \alpha'/2 < \theta' < \pi - \alpha'/2 .$$

It can be seen from the periodic nature of the Fourier series that this pattern will repeat itself in such a fashion that the images appear at intervals of π along the θ' axis. This picture, rough though it is, corresponds in some particulars to the anticipated grating image, and it would appear that there might be some uses for such an approximation.

In treating the whole as a rectangular image, the behavior of the approximation at the points of discontinuity has thus far been ignored. It is, however, well known that in the limit, as M approaches infinity, the value of the Fourier series approaches the value of the function only at points where there are no discontinuities, and at points where there are discontinuities it exceeds the value of the function by an amount which depends on the value of the discontinuity. This means that instead of the simple rectangular images pictured in Fig. 3 the images would have local maxima at points close to the points of discontinuity. This behavior comes under the general heading of the Gibbs phenomenon,

which also describes the behavior of the finite series $\sum_{m=1}^{M} \frac{\sin mx}{m}$. It is possible to progress further with the approximation by a method which follows.

For any partial series (finite number of terms) the sum oscillates about the value of the function with deviations the magnitudes of which increase as the point of discontinuity is approached. If M is allowed to increase, the number of oscillations increases, and as has been noted the partial sum converges to the value of the function except at the discontinuities. It is possible by the method which follows to locate the places of maximum deviation and to evaluate by another approximation the difference between the partial sum and the value of the function. From points located in this manner a curve can be drawn which represents the amplitude distribution more closely than does the rectangular image. Or, alternatively, the intensity distribution can be constructed directly from the expression obtained.

From equation (12)

$$S_M(x) = \sum_{m=1}^{m=M} \frac{\sin mx}{m} \tag{19}$$

$$S_M(x) = \sum_{m=1}^{m=M} \int_0^x \cos mx \, dx = \int_0^x \left[\sum_{m=1}^{m=M} \cos mx \right] dx$$

But $$\sum_{m=1}^{M} \cos mx = -1/2 + \frac{\sin (M+1/2)x}{2 \sin x/2} ,$$

and from (4) $M + \frac{1}{2} = N/2$, from which it follows that

$$S_N(x) = \int_0^x \left[-1/2 + \frac{\sin Nx/2}{2 \sin x/2} \right] dx$$

$$= -x/2 + \int_0^x \frac{\sin Nx/2}{2 \sin x/2} dx . \qquad (20)$$

The difference between the partial sum $S_N(x)$ and the function $f(x)$ will be given by

$$R_N(x) = S_N(x) - f(x) \qquad (21)$$

$$R_N(x) = -x/2 + \int_0^x \frac{\sin Nx/2}{2 \sin x/2} dx - \left(\frac{\pi - x}{2} \right)$$

$$= -\pi/2 + \int_0^x \frac{\sin Nx/2}{2 \sin x/2} dx \qquad (22)$$

As previously stated, the partial sum oscillates about the value of the function so that $R_N(x)$ is alternately positive and negative. The maximum values of $|R_N(x)|$ measured in a direction perpendicular to the x-axis will occur when $\frac{dR_N(x)}{dx} = 0$.

$$\frac{dR_N(x)}{dx} = \frac{\sin Nx/2}{2\sin x/2} = 0, \quad \text{when } x = x_\ell = \frac{2\ell\pi}{N}, \ell = 1,2,3,\ldots \quad (23)$$

The evaluation of the integral involved in equation (21) follows that of Bocher. Addition and subtraction of the term $\int_0^x \frac{\sin Nx/2}{x}\,dx = \int_0^{N\pi/2} \frac{\sin x}{x}\,dx$ to the right side of equation (21) gives the result that

$$R_N(x) = -\pi/2 + \int_0^{Nx/2} \frac{\sin x}{x}\,dx + \int_0^x \left[\frac{\sin Nx/2}{2\sin x/2} - \frac{\sin Nx/2}{x}\right] dx,$$

or,

$$R_N(x) = -\pi/2 + \int_0^{Nx/2} \frac{\sin x}{x}\,dx + B_N(x). \quad (24)$$

where

$$B_N(x) = 1/2 \int_0^x \sin Nx/2 \left(\frac{1}{\sin x/2} - \frac{2}{x}\right) dx. \quad (25)$$

An integration of equation (25) by parts gives the result

$$B_N(x) = 1/N \left\{ \left[\cos Nx/2 \left(2\frac{\sin x/2}{x \sin x/2} - x\right)\right]_0^x + \int_0^x \cos Nx/2 \left(x^2/2 \frac{\cos x/2}{x^2 \sin^2 x/2} - 2\sin^2 x/2\right) dx \right\}. \quad (26)$$

The two functions which occur here,

$$2\frac{\sin x/2 - x}{x \sin x/2} \quad \text{and} \quad x^2/2 \frac{\cos x/2 - 2\sin^2 x/2}{x^2 \sin^2 x/2}$$

both become infinite when $x = 2\pi$. But in an interval $0 < x < b$ where $b < 2\pi$ both functions are continuous except at the point $x = 0$ where they are not defined and they both ap-

proach finite limits as x approaches zero. It is therefore possible to find a positive constant K such that

$$\left|\frac{2\sin x/2 - x}{x\sin x/2}\right| < K \quad , \text{ and } \int_0^x \left|\frac{x^2\cos x/2 - 2\sin^2 x/2}{x^2\sin x/2}\right| < K$$

for $0 < x < b$, where $b < 2\pi$.

It then follows that

$$|B_N(x)| < 2K/N \quad , \text{ when } \quad 0 < x < b \qquad (27)$$

This inequality shows that $B_N(x)$ approaches zero as N tends to infinity for all values of x which satisfy the restrictions. In the case of the grating, however, there is the difficulty that N remains finite, although large, and therefore $B_N(x)$ does not necessarily go to zero. But if a further condition is put on b, that b may never come close to 2π, that is to say that x must remain small, then it follows that K will never become very large and $B_N(x)$ will be negligible in comparison with the other terms in equation (24). $R_N(x)$ can then be rewritten omitting the last term.

$$R_N(x) = -\pi/2 + \int_0^{Nx/2} \frac{\sin x}{x}\, dx$$

or

$$R_N(x) = -\pi/2 + Si\left(Nx/2\right) \qquad (28)$$

It is now possible to do two things which give information as to the behavior of the resulting pattern. First the values of the extrema of $R_N(x)$ can be evaluated at the points $x_i = \frac{2i\pi}{N}$.

$$R_N(x_\ell) = -\pi/2 + Si(\ell\pi) \quad ; \quad \ell = 1, 2, 3, \ldots$$

There will be two such differences, one for x^+ and the other for x^-. When these differences are added to $f(x^+)$ and to $f(x^-)$ at the intervals of $2\pi/N$ and a smooth curve is constructed through the points thus located, the result is two curves with a set of local maxima and minima. When plotted on the θ'-axis the origins of the two curves, $x^+=0$ and $x^-=0$, are displaced from $\theta'=0$ by amounts of $-\alpha'/2$ and $+\alpha'/2$ respectively. The resulting amplitude is then the sum of these two curves. As the value of α' is increased the two curves slide over each other introducing variations in the amplitude distribution. It is readily seen that the maximum value of the amplitude and thus of the intensity occurs when the two first maxima of the two curves coincide at $\theta'=0$, that is when $\alpha'=2\pi/N$. If α' is increased beyond this value, the intensity at the center decreases and passes through a minimum, after which it oscillates as a function of α' but never again attains its first value. For the larger values of α' the maximum values of the intensity in the image pattern occur at the sides of the image. They also oscillate as a function of α, but at a higher level than the central values.

Alternatively it is possible to substitute equation (28) directly into equation (21) and the result

into equation (10).

$$S_N(x) = R_N(x) + f(x) \tag{21}$$

$$S_N(x) \simeq -\pi/2 + Si(Nx/2) + \left(\frac{\pi - x}{2}\right)$$

$$\simeq -x/2 + Si(Nx/2)$$

$$A \simeq \alpha_0'/\pi \left[\alpha' - x^+/2 - x^-/2 + Si(Nx^+/2) + Si(Nx^-/2)\right]. \tag{10}$$

By use of equation (9), this becomes

$$A \simeq \alpha_0'/\pi \left[Si\{N/2(\alpha'+2\theta')\} + Si\{N(\alpha'-2\theta')/2\}\right]$$

or in terms of the original variables α and θ ,

$$A \simeq \alpha_0'/\pi \left\{Si\left[\frac{Nks}{4}(\alpha+2\theta)\right] + Si\left[\frac{Nks}{4}(\alpha-2\theta)\right]\right\} \tag{30}$$

The intensity then follows as

$$I \approx \left\{Si\left[\frac{Nks}{4}(\alpha+2\theta)\right] + Si\left[\frac{Nks}{4}(\alpha-2\theta)\right]\right\}^2 \tag{31}$$

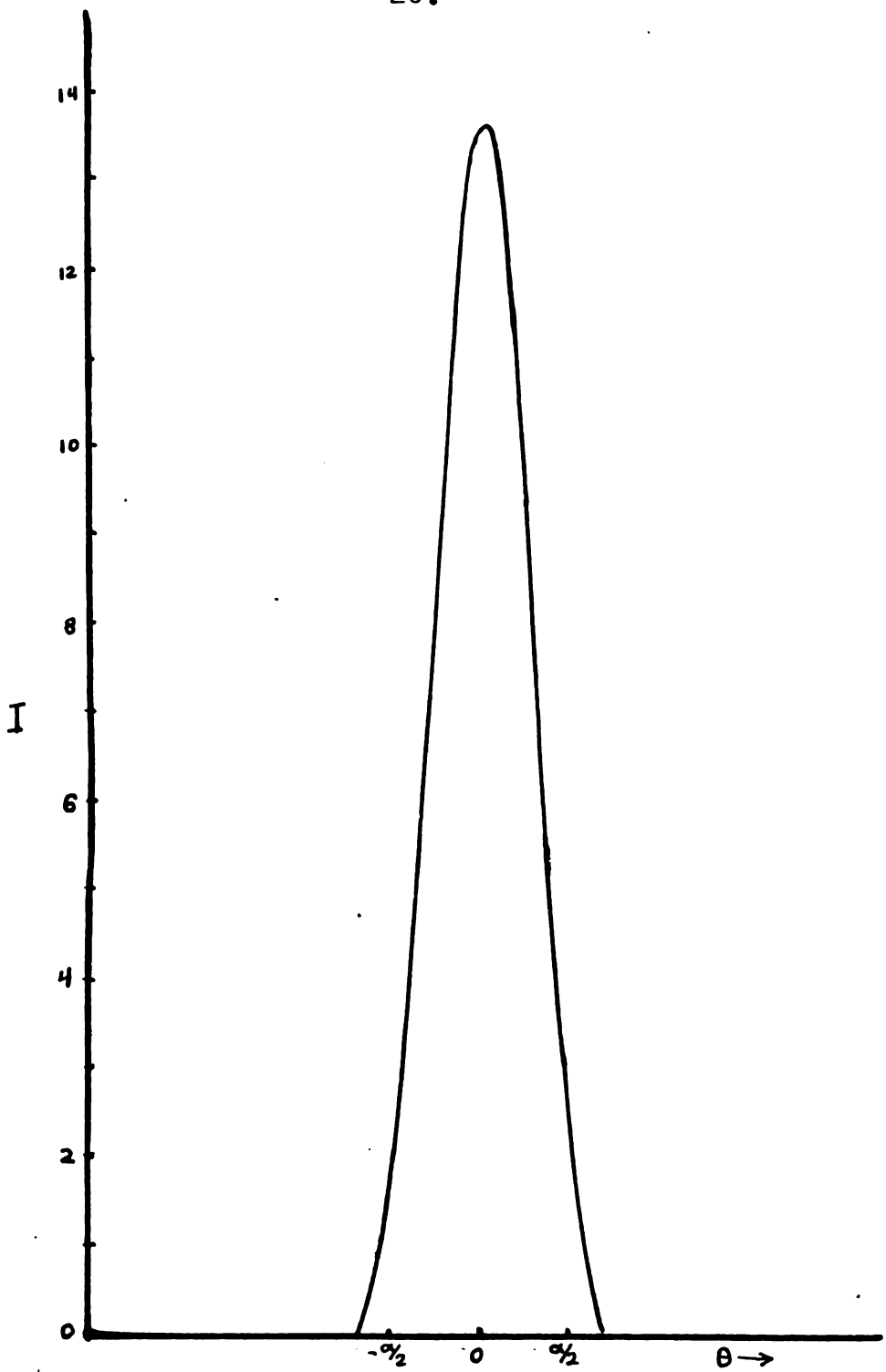

Fig. 4 Theoretical distribution of intensity in the image of the coherent source of angular width $\alpha = 2\lambda/Ns$.

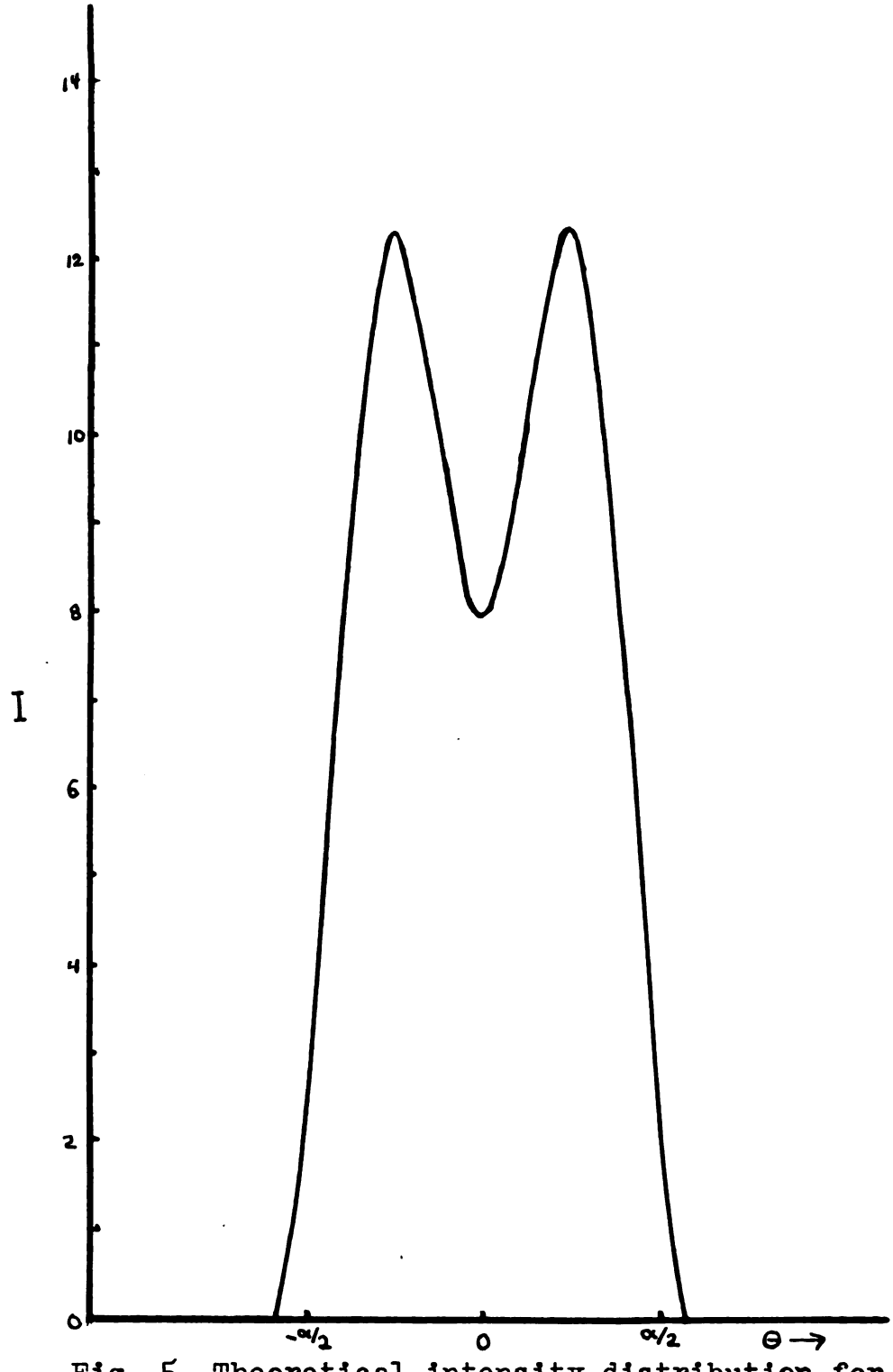

Fig. 5 Theoretical intensity distribution for a coherent source of angular width $\alpha = 4\lambda/Ns$.

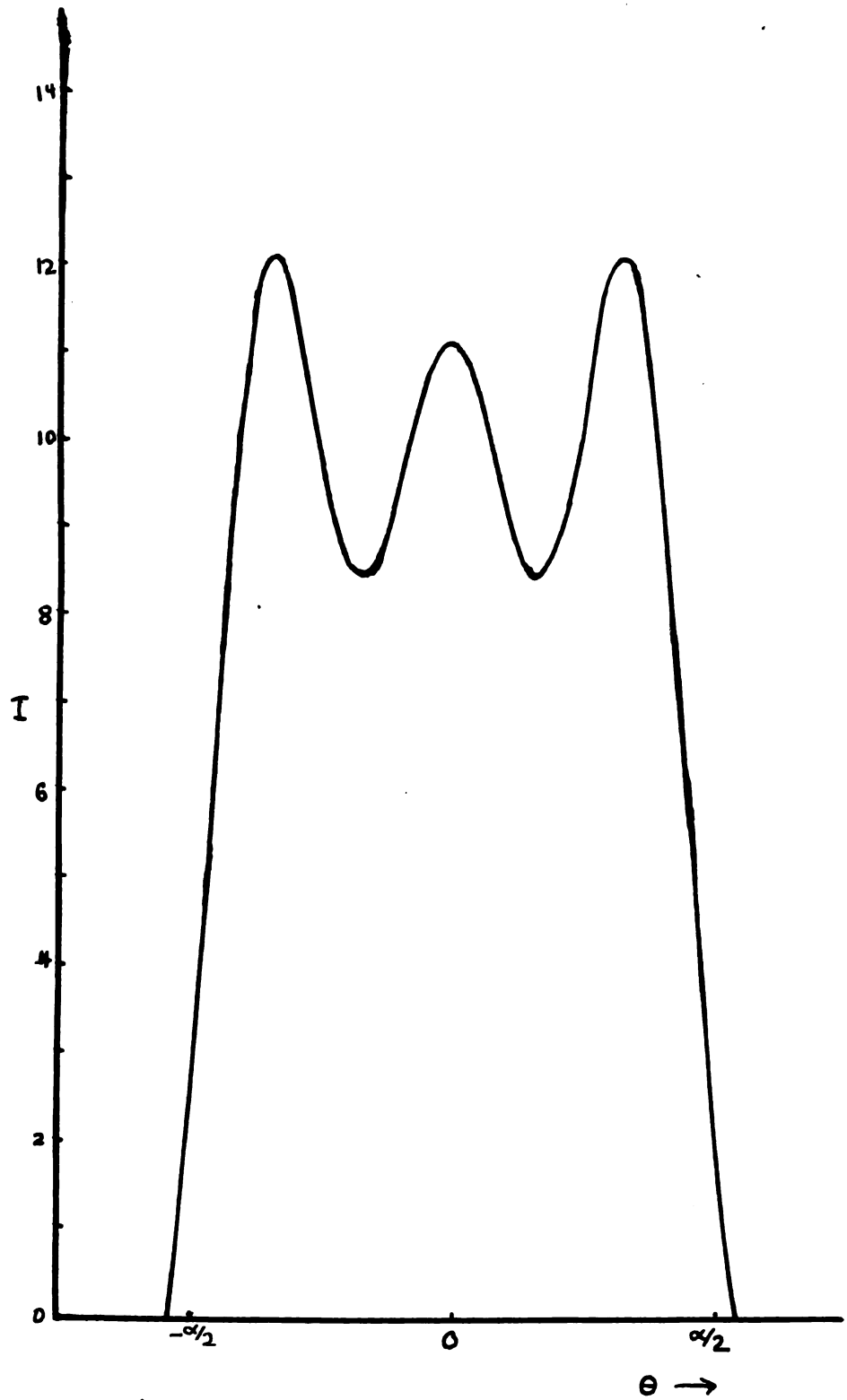

Fig. 6 Theoretical intensity distribution for the coherent source of angular width $\alpha = 6\lambda/Ns$.

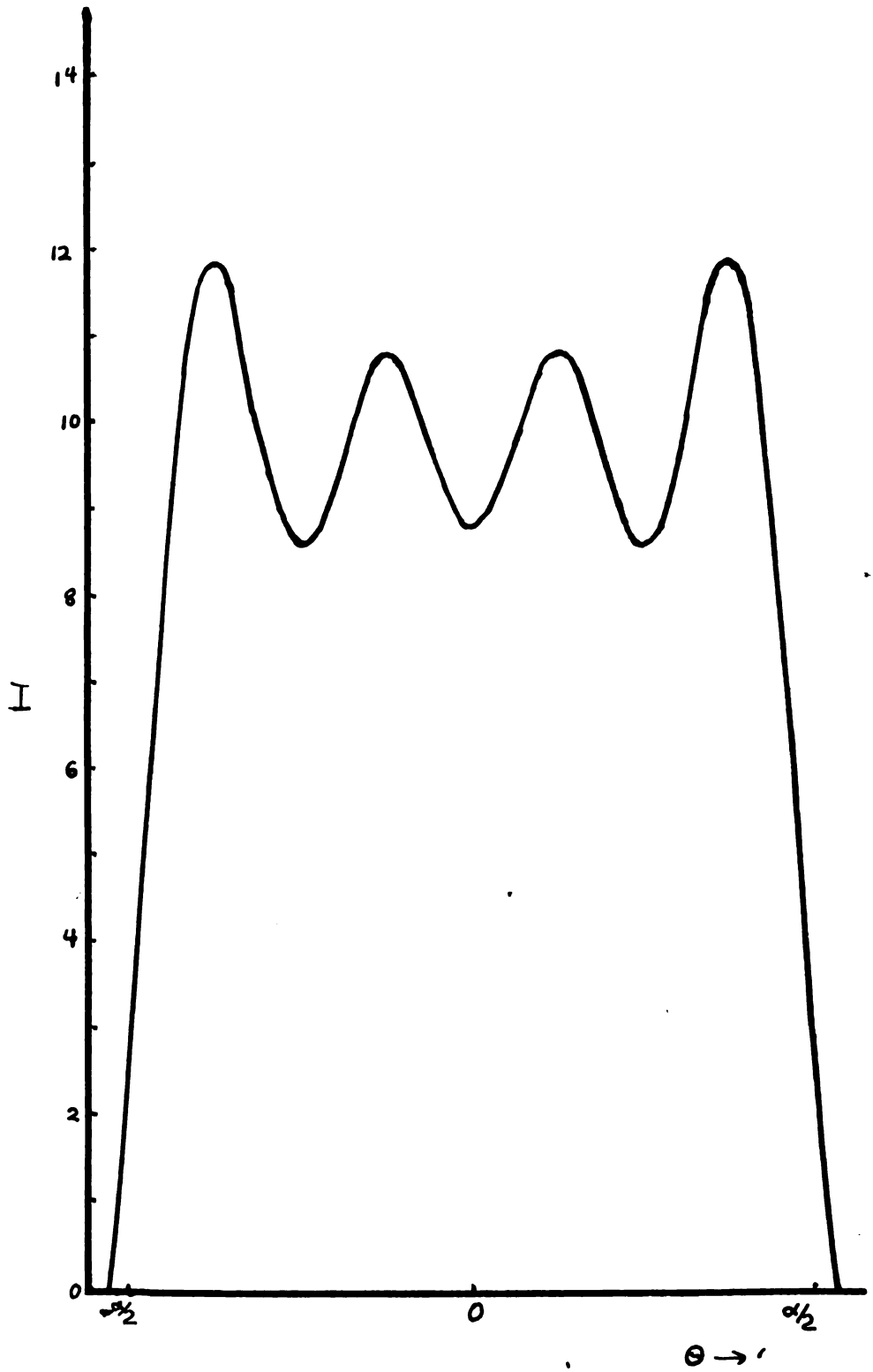

Fig. 7 Theoretical intensity distribution for the coherent source of angular width $\alpha = 8\lambda/Ns$.

B. NONCOHERENT ILLUMINATION

The equation (1') for the amplitude contribution from a single line element of the source,

$$a = a_o \sum_{m=0}^{m=N-1} e^{jmks(\theta+i)} \qquad (1')$$

may be rewritten

$$a = a_o \frac{1 - e^{jNks(\theta+i)}}{1 - e^{jks(\theta+i)}} .$$

The intensity contribution from the line source will then be

$$|a|^2 = a_o^2 \left[\frac{1 - e^{jNks(\theta+i)}}{1 - e^{jks(\theta+i)}} \right] \cdot \left[\frac{1 - e^{-jNks(\theta+i)}}{1 - e^{-jks(\theta+i)}} \right]$$

$$= a_o^2 \frac{1 - \cos Nks(\theta+i)}{1 - \cos ks(\theta+i)}$$

$$= a_o^2 \frac{\sin^2 \frac{Nks}{2}(\theta+i)}{\sin^2 \frac{ks}{2}(\theta+i)}$$

$$= a_o^2 \left[N + 2 \sum_{m=1}^{m=N-1} (N-m) \cos Nks(\theta+i) \right] . \qquad (32)$$

The intensity at the angle θ from the entire source of angular width α will then be given by equation (3).

$$I = \int_{-\alpha/2}^{\alpha/2} |a|^2 \, di \qquad (3)$$

$$I = \int_{-\alpha/2}^{\alpha/2} a_o^2 \left[N + 2 \sum_{m=1}^{m=N-1} (N-m) \cos N k s (\theta + i) \right] di. \qquad (33)$$

The order of operations may be interchanged, and upon expanding the cosine of the sum of two angles,

$$I = N\alpha + 2 \sum_{m=1}^{m=N-1} (N-m) \int_{-\alpha/2}^{\alpha/2} \left[\cos m k s \theta \cos m k s i - \sin m k s \theta \sin m k s i \right] di .$$

When the indicated integration is carried out the result is

$$I = N\alpha + 4/ks \sum_{m=1}^{m=N-1} \left(\frac{N-m}{m} \right) \cos m k s \theta \sin m k s \alpha/2 .$$

Using equation (6) and writing in terms of the sum and difference of angles

$$I = N\alpha + 2/ks \sum_{m=1}^{m=N-1} \left(\frac{N-m}{m} \right) \left[\sin m(\alpha' + 2\theta') + \sin m(\alpha' - 2\theta') \right]$$

The 2/ks may be removed as a multiplying factor and the term under the summation expanded as a group of sums.

$$I = N\alpha' + N\sum_{m=1}^{m=N-1} \frac{\sin m(\alpha'+2\theta')}{m} + N\sum_{m=1}^{m=N-1} \frac{\sin m(\alpha'-2\theta')}{m}$$

$$- \sum_{m=1}^{m=N-1} \sin m(\alpha'+2\theta') - \sum_{m=1}^{m=N-1} \sin m(\alpha'-2\theta') .$$

The sum of the last two terms is known.

$$I = N\alpha' + N\sum_{m=1}^{m=N-1} \frac{\sin m(\alpha'+2\theta')}{m} + \sum_{m=1}^{m=N-1} \frac{\sin m(\alpha'-2\theta')}{m}$$

$$- \frac{\sin[N(\alpha'+2\theta')/2]\ \sin[(N-1)(\alpha'+2\theta')/2]}{\sin[(\alpha'+2\theta')/2]}$$

$$- \frac{\sin[N(\alpha'-2\theta')/2]\ \sin[(N-1)(\alpha'-2\theta')/2]}{\sin[(\alpha'-2\theta')/2]} .$$

Rewriting in terms of equation (9),

$$I = N\alpha' + N\sum_{m=1}^{m=N-1} \frac{\sin mx^+}{m} + N\sum_{m=1}^{m=N-1} \frac{\sin mx^-}{m} \qquad (35)$$

$$- Y(x^+) - Y(x^-) ,$$

where

$$Y(x) = \frac{\sin Nx/2\ \sin(N-1)x/2}{\sin x/2} \qquad (36)$$

The two finite series which occur as the second and third terms are of the same form as those which

occurred in the coherent case. The contribution from these two plus the first term will be of the same form as the coherent amplitude expression. The one difference is the location of the extrema, which is controlled by the number of terms in the series.

The difference between the values of the rectangular image and that of the partial sum will be, as in equation (22),

$$R_N(x) = -\pi/2 + \int_0^x \frac{\sin(2N-1)x/2}{2\sin x/2} \qquad (37)$$

And the location of the extrema will be given by

$$\frac{dR_N(x)}{dx} = \frac{\sin(2N-1)x/2}{2\sin x/2} = 0$$

or

$$(2N-1)x_l/2 = l\pi \quad , \quad x_l = \frac{2l\pi}{2N-1} \quad , \quad l = 1,2,3,\cdots \qquad (38)$$

If, as is required by the approximations made, N is large and l is small, it will be found convenient later to make the location approximately

$$x_l \simeq l\pi/N$$

or

$$\theta_l' \simeq \frac{l\pi}{2N} - \alpha/2 \quad , \quad l = 1,2,3,\cdots \qquad (39)$$

Thus it is seen that the extrema occur here twice as often as in the coherent case. The value of the difference at these points of extrema will be the same

as in the coherent case except for the factor of N which multiplies all of the first three terms.

$$R_N(x) \simeq -\pi/2 + Si(Nx_\ell) \quad , \quad \ell = 1,2,3,\ldots \tag{28'}$$

The remaining part of the intensity distribution, the fourth and fifth terms, are still rather complex. A workable approximation may be found as follows:

$$Y(x) = \frac{\sin Nx/2 \sin (N-1)x/2}{\sin x/2} = \sum_{m=1}^{m=N-1} \sin mx \tag{35}$$

If x is small and N is large this may be rewritten

$$Y(x) \simeq 2 \frac{\sin^2 Nx/2}{x} \tag{40}$$

The extreme values of this expression are found when

$$\frac{dY(x)}{dx} \simeq 2\left[\frac{\sin^2 Nx/2 - x\,N \sin Nx/2 \cos Nx/2}{x^2}\right] = 0$$

$$\simeq 2 \sin Nx/2 \left[\sin Nx/2 - Nx \cos Nx/2\right] = 0 \tag{41}$$

This can be seen to be true when

$$Nx/2 = k\pi \quad , \; k = 1,2,3,\ldots \text{(a)} \quad \text{or} \quad Nx = \tan Nx/2 \text{ (b)} \tag{42}$$

A graphical analysis shows that equation (42 b) is satisfied when

$$Nx/2 \simeq (2k-1)\pi/2 \quad , \quad k = 1,2,3,\ldots \tag{42 b'}$$

Substitution of these results into (40) give the result

$$Y(x) = 0 \quad , \text{ when } \quad x = 2k\pi/N \quad , \quad k = 1, 2, 3, \ldots$$

$$Y(x) \simeq 2/x = 2N/(2k-1) \, , \text{ when } x = (2k-1)\pi/N \, , \tag{43}$$

or writing in terms of α' and θ',

$$Y(\alpha';\theta') = 0 \, , \text{ when } \theta' = k\pi/N - \alpha'/2 \, , \; \theta' = \alpha'/2 - k\pi/N$$

$$= 2N/(2k-1)\pi \, , \; \theta' = \frac{(2k-1)\pi}{2N} - \alpha'/2 \, , \; \theta' = \alpha'/2 - \frac{(2k-1)\pi}{2N} \tag{44}$$

The construction of intensity distribution from the results found follows the same procedure as was used to find the amplitude distributions of the coherent case. A rectangular image is described by the first three terms in equation (35). The subtraction of the Y terms at the points and of amounts given by equation (44) completes the picture.

It is seen that since the terms in Y are positive and at a maximum and are to be subtracted when R_N has a positive maximum value and are zero when R_N has a maximum negative value that the net result for the noncoherent case is going to be a rather smooth curve. A construction of the intensity distribution by drawing the curves bears out this result.

And again, alternatively, as in the coherent case, equation (10), the intensity distribution may be evaluated as

$$I \simeq N\alpha' + N S_N(x^+) + N S_N(x^-) - V(x^+) - V(x^-) \tag{45}$$

which becomes

$$I \simeq N\,Si\left[(N-1)x^+/2\right] + N\,Si\left[(N-1)x^-/2\right] - \frac{\sin^2 Nx^+/2}{x^+/2} - \frac{\sin^2 Nx^-/2}{x^-/2} \tag{46}$$

or

$$I \simeq N\,Si\left[(N-1)\frac{ks}{4}(\alpha+2\theta)\right] + N\,Si\left[(N-1)\frac{ks}{4}(\alpha-2\theta)\right] - \frac{\sin^2\left[N\frac{ks}{2}(\alpha+2\theta)\right]}{\frac{ks}{2}(\alpha+2\theta)} - \frac{\sin^2\left[N\frac{ks}{2}(\alpha-2\theta)\right]}{\frac{ks}{2}(\alpha-2\theta)} \tag{47}$$

The construction of the curves was made with the results as indicated in the accompanying figures. Figs. (4) - (7) and (11) are for the coherent case. Fig. (4) - (7) show the intensity distribution as a function of the observation angle θ. Each curve represents a different value of the source aperture and is calculated for the source width which will give the maximum visibility of the structure in the image. In addition to the curves for the intensity distribution in the image for a given source width it is possible to find the intensity in the center of the image, at $\theta = 0$, as a function of α. Thus equation (31) becomes for the intensity at the center

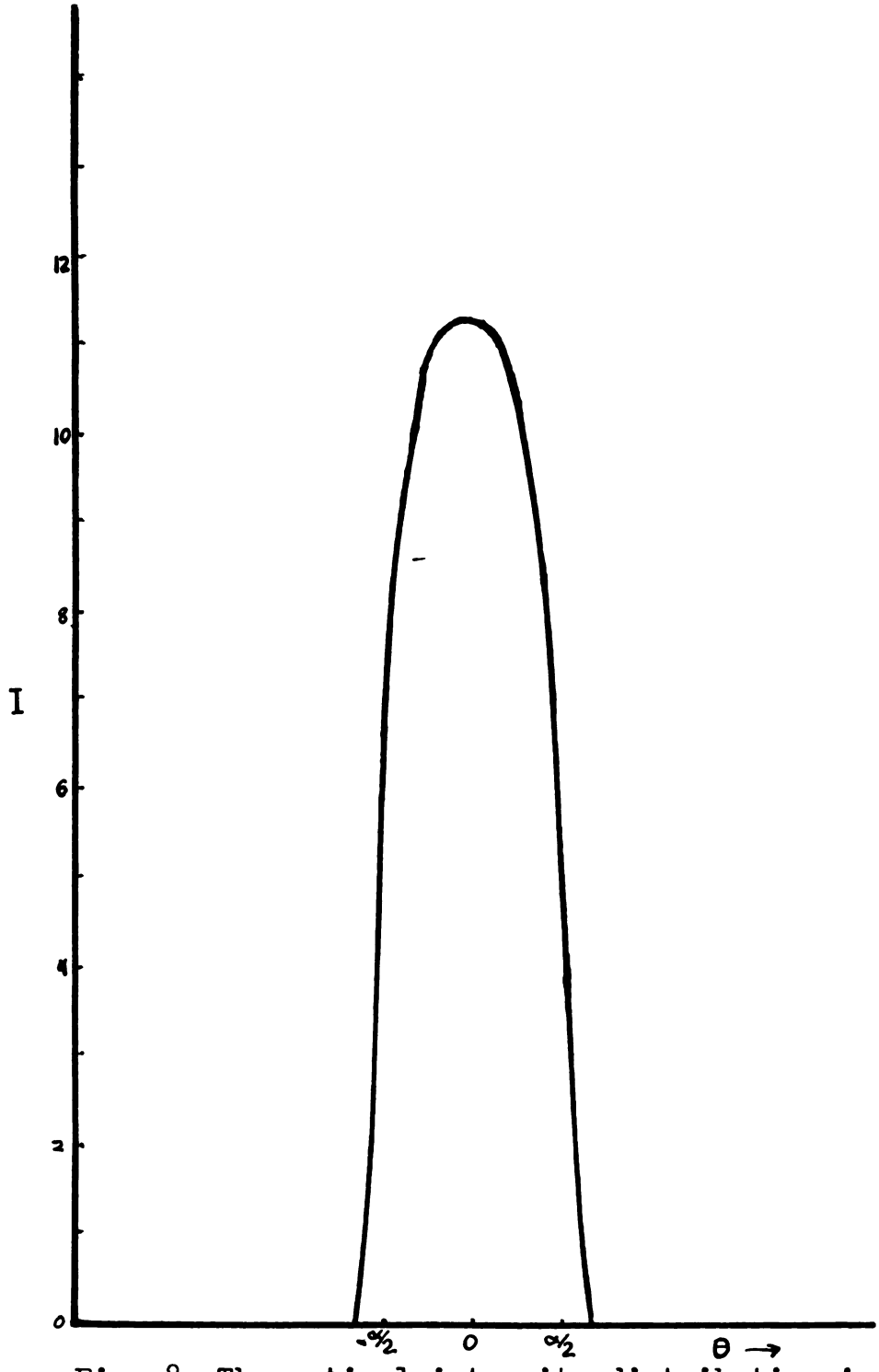

Fig. 8 Theoretical intensity distribution in the image of a noncoherent source of angular width $\alpha = 2\lambda/Ns$.

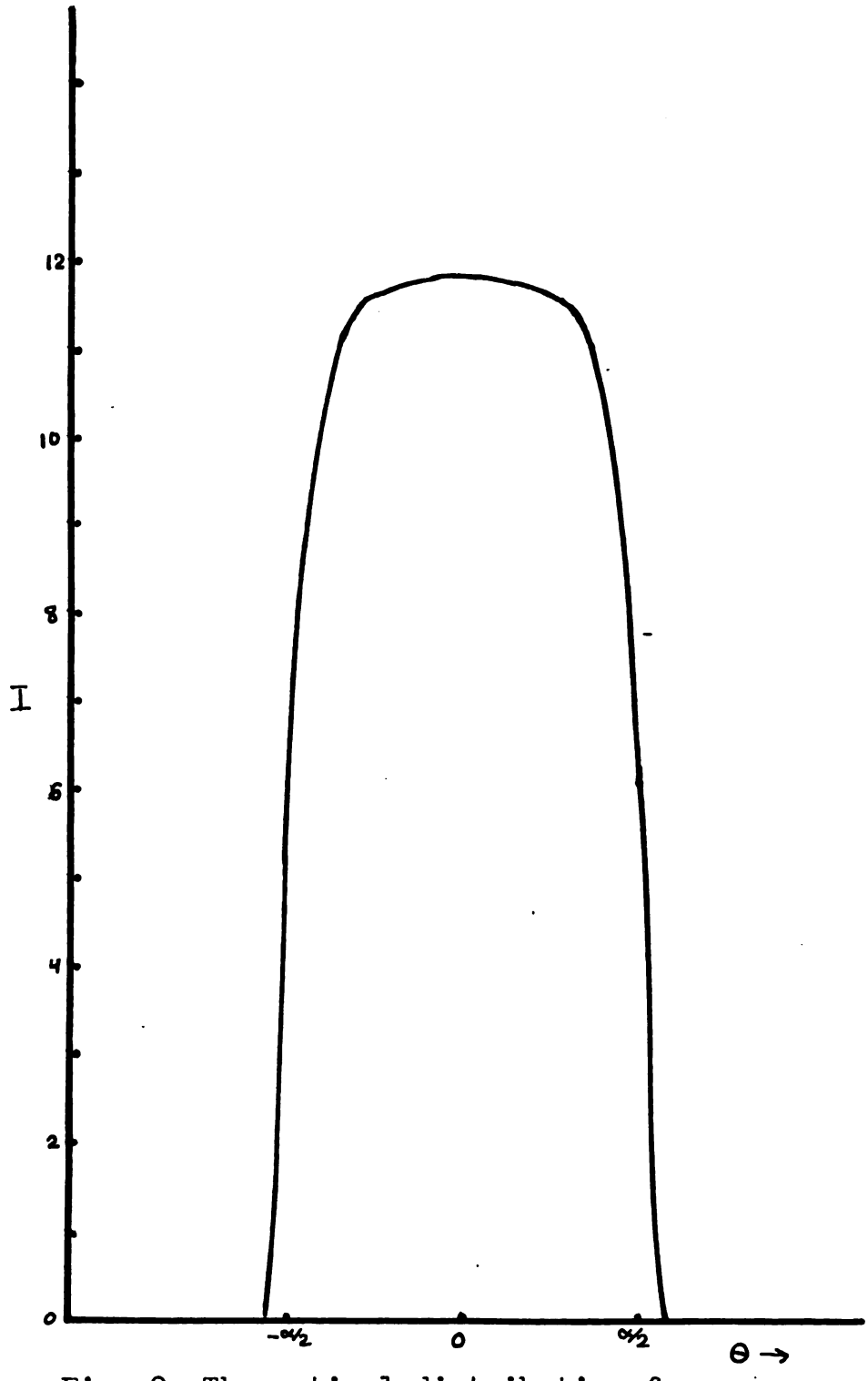

Fig. 9 Theoretical distribution for a non-coherent source with $\alpha = 4\lambda/Ns$.

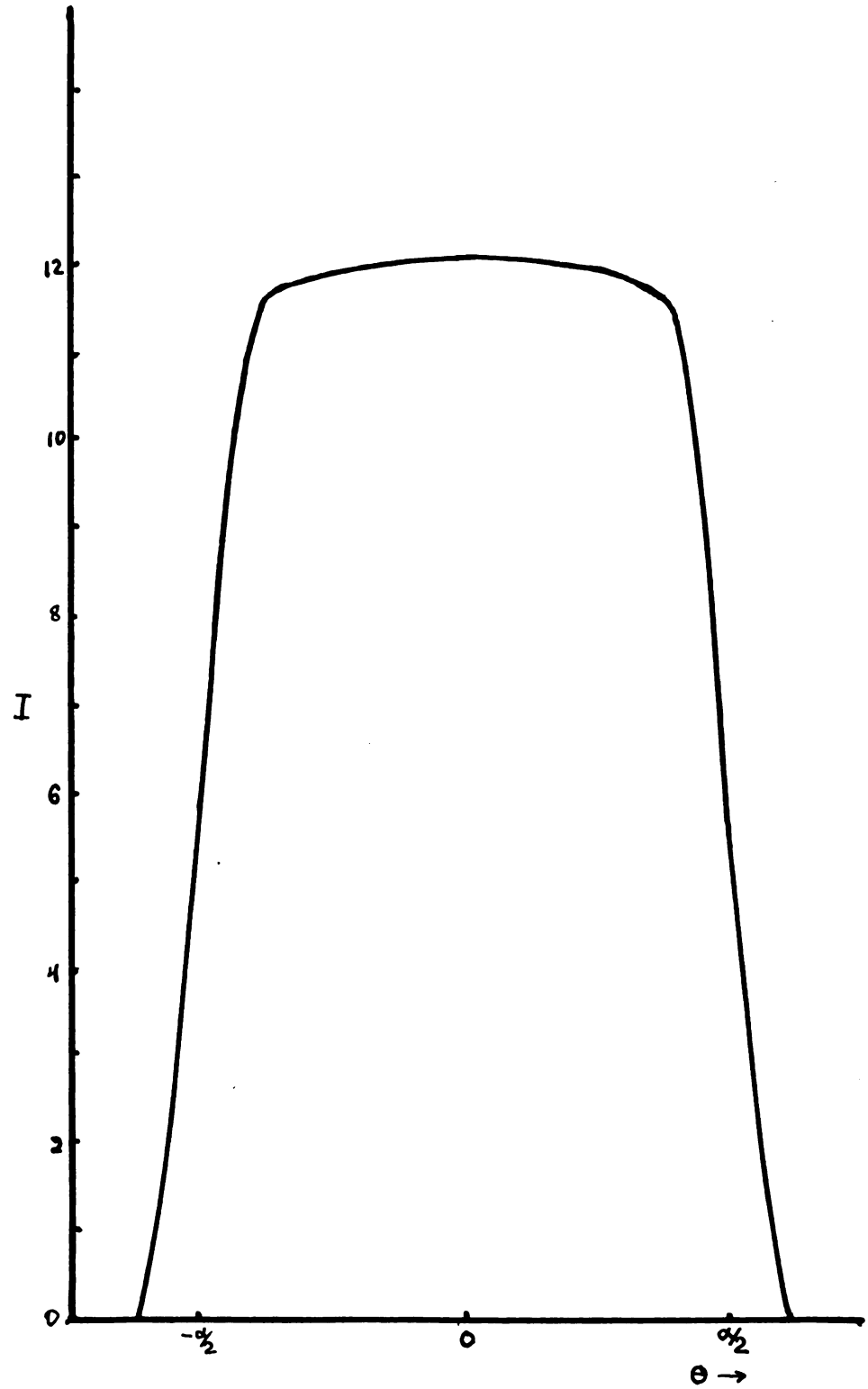

Fig. 10 Theoretical distribution for a non-coherent source with $\alpha = 6\lambda/Ns$.

$$I_c \simeq \left[2\, Si\left(N s k \alpha/4\right)\right]^2 \tag{48a}$$

Fig. (11) illustrates this result.

The construction for the noncoherent mode of illumination is illustrated in Figs. (8) - (10) and (12). The intensity at the center of the pattern is given by

$$I_c \simeq 2\, Si\left[(N-1) k s \alpha/2\right] - 2\,\frac{\sin^2\left[(N-1) k s \alpha/4\right]}{(N-1) k s \alpha/4} \tag{48b}$$

and the result is plotted in Fig. (12).

C. COMPARISON WITH THE SINGLE APERTURE

It is of interest to compare the results derived here for the diffraction grating with those given by Van Cittert, ~~equation~~ reference (1), for the single diffracting aperture. For the single aperture illuminated in the coherent mode the intensity distribution independent of constant multipliers is

$$I = \left[\, Si\,(\psi_0 - \phi)\, d \;+\; Si\,(\psi_0 + \phi)\, d\right]^2$$

This when translated into the terms which are used in this work becomes

$$I = \left\{ Si\left[D k (\alpha - 2\theta)/4\right] + Si\left[D k (\alpha + 2\theta)/4\right]\right\}^2 \tag{49}$$

Where D is the breadth of the diffracting aperture, the result for the noncoherent illumination becomes

$$I = Si\left[D k/2 (\alpha - 2\theta)\right] + Si\left[\frac{D k}{2}(\alpha + 2\theta)\right]$$

$$- \frac{\sin^2 \frac{D k}{4}(\alpha - 2\theta)}{\frac{D k}{4}(\alpha - 2\theta)} - \frac{\sin^2 \frac{D k}{4}(\alpha + 2\theta)}{D k/4 (\alpha + 2\theta)} \tag{50}$$

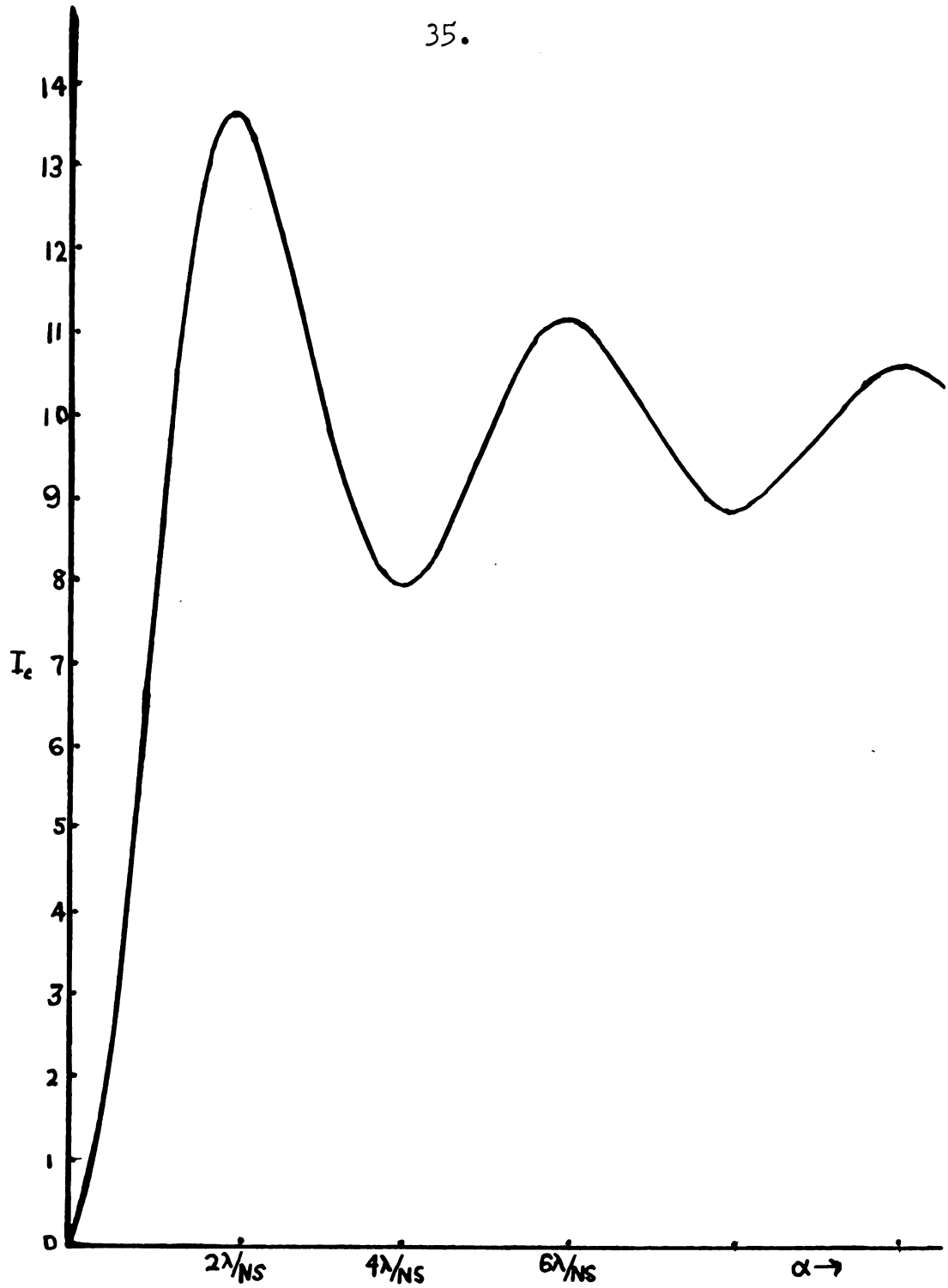

Fig. 11 The intensity at the center of the image of the coherent source as a function of the angular source width as calculated from the theory.

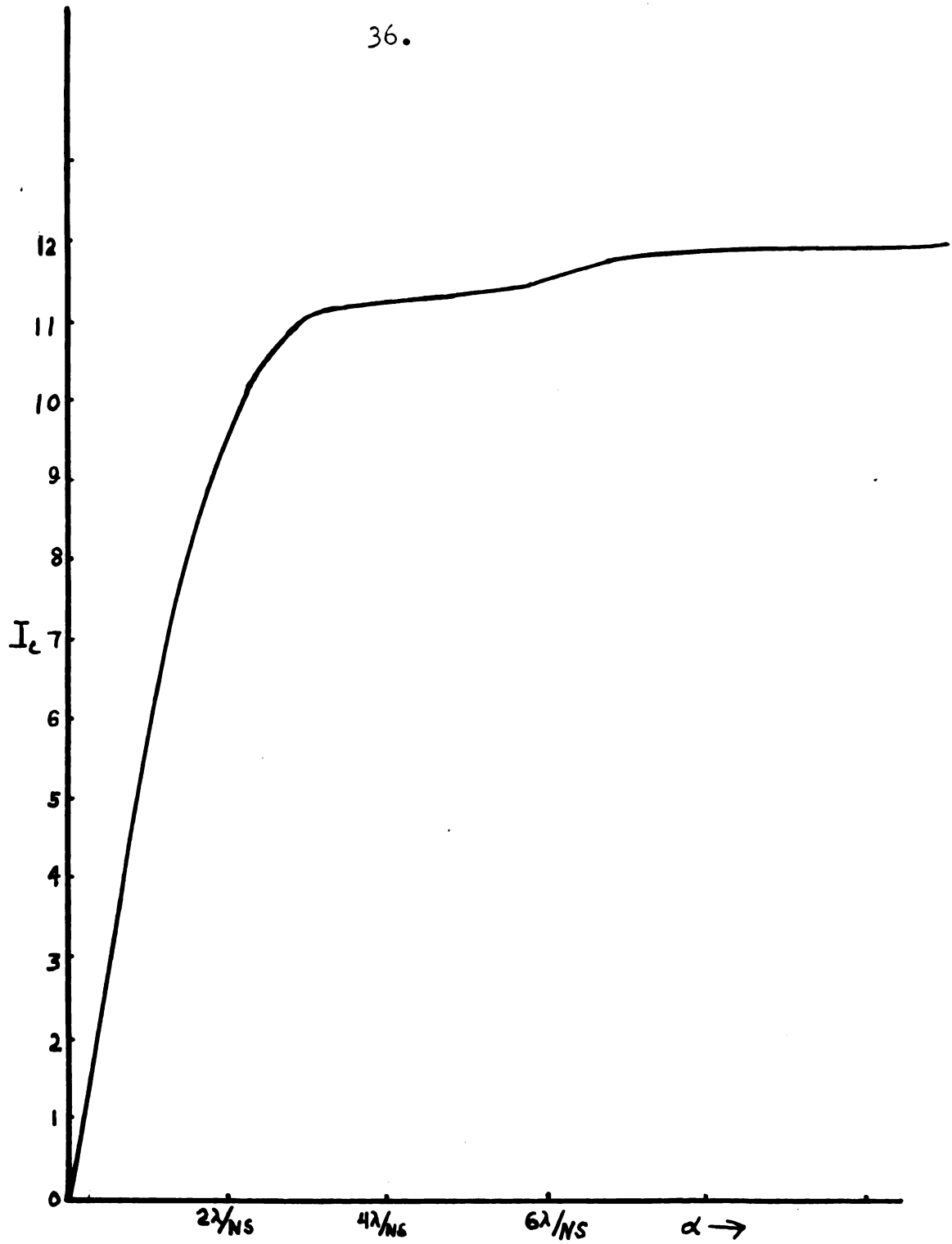

Fig. 12 The intensity at the center of the image from the noncoherent source, as a function of the angular source width as calculated from the theory.

These results should compare with equations (31) and (47). When cognizance is taken of the fact that the product $(N-1)s \simeq Ns$, which is equivalent to the D of the single aperture, is the total expanse of the grating aperture it is seen that the two appear to be identical. That is to say, the grating aperture acts within the limits of the approximations used as a single diffracting aperture. The results stated for the single aperture are subject only to the condition of small angles of incidence. For large N it would be expected that there would be no detectable difference between the single aperture and the grating in either of the two modes of illumination treated.

III. DESCRIPTION OF EXPERIMENT

The experimental techniques used to verify the preceding theory were essentially quite simple. The source of light was a high pressure mercury arc, air-cooled so that it could be operated for long periods in a light-proof housing. The slit used as a source aperture was a Spindler and Hoyer bilateral precision slit. The collimating and camera lenses were achromats of approximately one meter focal length. A 931-A photomultiplier tube in an American Instrument Company microphotometer was used to read the image intensity. The photomultiplier tube was located behind an exit slit constructed of a pair of razor blades with a separation of 0.015 mm. The readings of the intensity were taken from left to right on the image at intervals of 0.05 mm on a precision screw.

A. COHERENT

In order to achieve coherent illumination of the source aperture the lamp was placed at a distance of 10 meters from the aperture and a slit of less than 1 mm breadth was then placed about 10 cm from the lamp. With this arrangement a very small part of the light source was contributing to the excitation at the source aperture and hence it was reasonable to regard it as predominantly coherent.

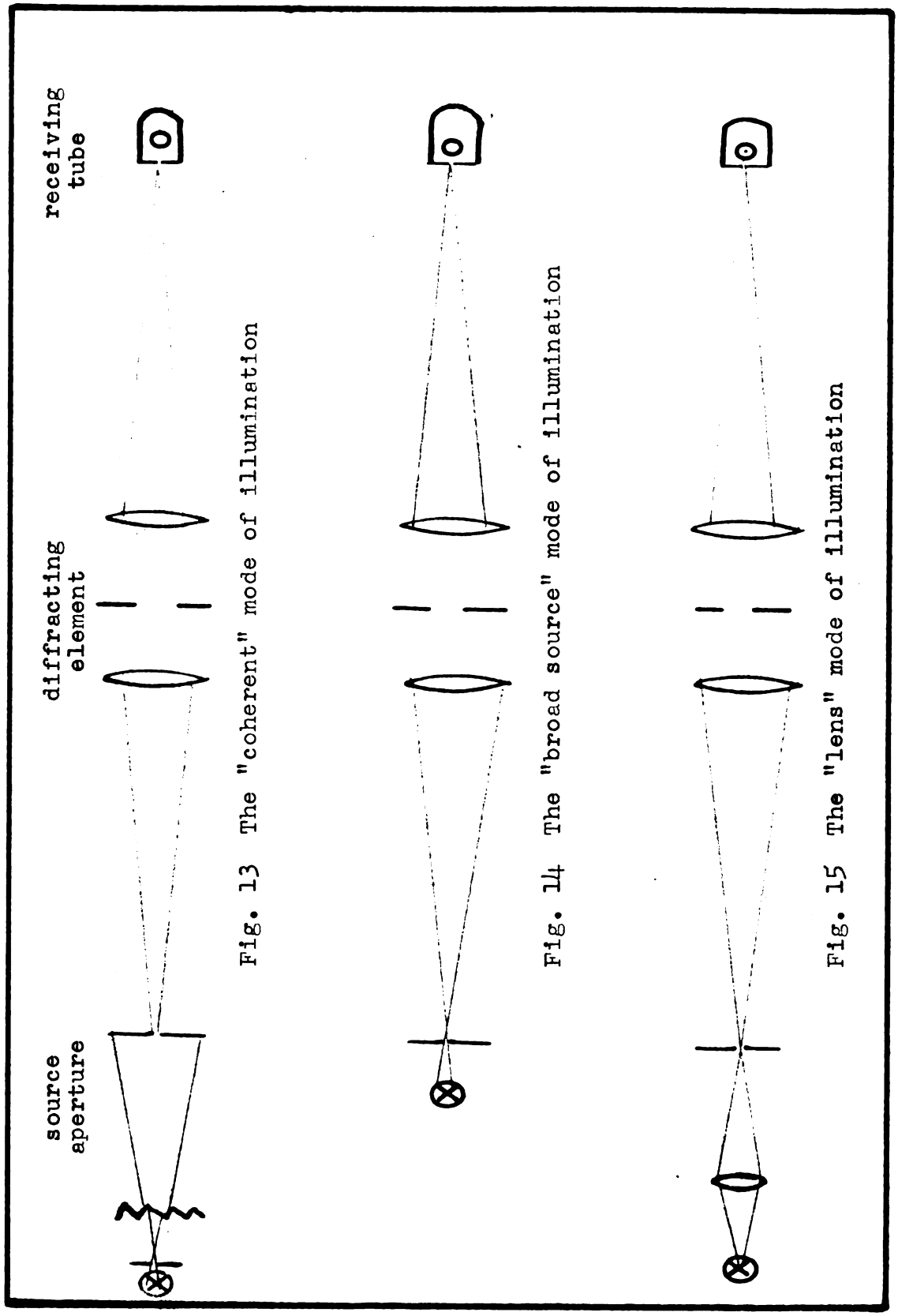

Fig. 13 The "coherent" mode of illumination

Fig. 14 The "broad source" mode of illumination

Fig. 15 The "lens" mode of illumination

Essentially this same arrangement was used by Stockbarger and Burns (5) in their work which was an outgrowth of Van Cittert's (1) theory. They used a distance of two meters between the source and source aperture and the curves which resulted were not examined in detail as to their comparison with theory. Particular notice was made of the resolving power of the instrument under different types of illumination and the general characteristics of the line shape which influence resolving power were noted.

Evidence that the arrangement is essentially correct exists in the fact that originally a distance of 5 meters was used between the source aperture and the source with the result of a systematic difference between the predicted patterns and the observed patterns. The structure visibility was much less than predicted and the positions of maximum visibility were displaced toward source apertures wider than predicted. These differences were markedly reduced with the increase of the separation to 10 meters. It was believed that little improvement would be noticed by increasing the separation beyond this point and the dimunition in light intensity would not be tolerable.

There are at least two ways in which the source aperture differs from the ideal coherent radiator assumed in the theoretical treatment: (1) It is not a

source in itself but a slit and as such has its own characteristic diffraction pattern. This was found to give little or no trouble for small openings of the source aperture, but as the breadth of the aperture was increased an effect was noticed which was the result of the edge of the aperture acting as a source. (2) There is some mixture of phases in the plane of the aperture, some incoherence. This effect does not lend itself to measurement, but from a study of the diffraction patterns it is seen to increase as the breadth of the source increases. The setup is illustrated in Fig.(13.)

B. NONCOHERENT

Two different methods of illumination are described in the literature (5) as approaching the noncoherent mode, a broad source placed before the source aperture (broad source mode) and an image of the light source focused on the source aperture (lens mode). The arrangement for the broad source mode is shown in Fig. (14) and the lens mode in Fig. (15). The same apparatus was used for the noncoherent as was used for the coherent case.

It is readily seen that complete noncoherence will not be achieved by either of these arrangements

since complete noncoherence would require that every point of the light source illuminate every point of the source aperture. The comparison between the theoretical and experimental results will indicate which mode more closely approximates noncoherence.

IV EXPERIMENTAL RESULTS

To obtain the results represented in Figs. (16)-(27) a Cenco transmission grating having 3000 lines/inch and covered with a mask which left an aperture of breadth 3.42 mm was used. The three different modes of illumination were employed as illustrated in Figs. (13) - (15).

The results for the coherent mode in Figs. (16)-(19) are to be compared with the calculated curves in Figs. (4) - (8). The experimental curves are constructed by interpolating between the experimental points. Sample sets of experimental points are included in Figs. (16a) - (20a). The other curves which follow are constructed in the same fashion but the experimental points are not included. There were very few instances when it was necessary to deviate from the experimental points in the interest of smoothing the resulting experimental curve. In no case did the deviation exceed $\pm 1\%$. The experimental images follow the predicted image in many respects. The changes in the pattern occur when predicted and the maximum visibility of the structure close to the source widths predicted. The biggest differences occur in the structure visibility which is not as great as would be predicted for the completely coherent source. The asymmetry which appears in Figs.(18) and (19) illustrates a characteristic of the

images of the coherent mode to be extremely sensitive to the alignment of the diffracting element in the beam. It is possible by rather laborious adjustments to obtain almost completely symmetric images. Some of these are shown later. The principal reason for the sensitivity is the narrow beam present in the coherent mode. For large values of the source aperture most of the radiation will be contained within a beam but little broader than the source aperture itself. The lack of structural visibility is without doubt a result of the mixture of noncoherent elements. This would tend to flatten out the image as seen by comparison with the noncoherent mode.

The curve for the intensity at the center of the image as a function of source width in Fig. (20) is to be compared with the curve in Fig. (8). As might be expected from the observations already made concerning the visibility of the structure in the image, the second minimum which occurs at the center will not be as great relative to the first maximum as predicted. In other respects the two appear to be the same. The curve is not carried beyond the place where the structure appears in the image.

The maximum value of the intensity can be predicted from equation (31) to occur at a source width $\alpha = 2\lambda/\pi s$ (51). The subsequent source widths

for maximum visibility of the structure occur at integral multiples of the above value.

In all of the graphs for the coherent case shown the first maxima occurs at the place predicted or extremely close to it. This was the case when the distance between the light source and the source aperture was ten meters. When a distance of five meters was used there appeared to be a systematic error in that the maximum always appeared at a value of source width somewhat greater than was predicted. A mixture of noncoherent elements would tend to produce such a deviation since in the noncoherent mode there is no definite maximum at the center; but a value which the central intensity appears to approach asymptotically.

The curve for the half-intensity breadth which occurs also in fig. (16) will be discussed later.

Figs. (20)- (23) for the broad source mode and Figs. (24)- (27) for the lens mode represent approaches to the noncoherent illumination and are to be compared with Figs. (9)- (12). In general it is seen that the broad source images have rounded tops and the central intensity quickly approaches an almost constant value. The lens mode apparently more closely approximates the noncoherent case with its square topped images and more slowly ascending central intensity.

Comparison of the half-intensity breadths in Figs. (16), (20), and (24) show some facts of interest. In the coherent case the half-intensity breadth remains at an almost constant value for a considerable range of source widths and then increases at a linear rate. In the broad source mode and in the lens mode the half-intensity breadth begins to increase much sooner. These facts in conjunction with the behavior of the central intensity become important in the choice of an optimum source width in a given spectral instrument and in some other optical instruments in which the diffraction properties of the image become important. It is often desired to obtain a maximum intensity and still retain a relatively narrow image. It can be seen from these graphs that there does exist an optimum source width which satisfies these conditions. Further the optimum width for the coherent case will be almost twice the value for the coherent mode that it will be for the lens mode. The broad source mode lies between the two only slightly greater than that for the lens mode. This would further substantiate the conclusion that the lens mode is more nearly noncoherent than the broad source mode.

These conclusions verify the predictions which Van Cittert (1) made for the half-intensity breadth of the image formed by a rectangular aperture.

The results represented in Figs. (28) - (40) were essentially duplicates of those shown in Figs. (16) - (17) except they were made with a different grating. The grating used was of the transmission type having 90 lines/mm. An area of 3.53 mm breadth was used to obtain the images observed. The details of these images are essentially the same as those obtained with the Cenco grating. There is some improvement as the asymmetry observed before is not as apparent in these images and the intensity at the center of the coherent image as shown in Fig. (28) follows the predicted curve more closely.

Measurements were also made with this grating in the first order images to find any difference which might occur as a result of the increase in diffraction angle. No observable effects appeared. This is as would be expected since the theory does not actually require any limitations on the angle θ. Sine θ could be used instead of θ without changing the form of the expressions.

The set of Figs. (41)- (53) were the result of measurements taken to find any differences which might appear between the single diffracting aperture and the diffraction grating. For the results pictured a rectangular aperture of 4.13 mm breadth was used as the

diffracting element. As predicted from the comparison of the grating theory with the aperture theory no significant difference is apparent when these images are compared with either of the previous sets.

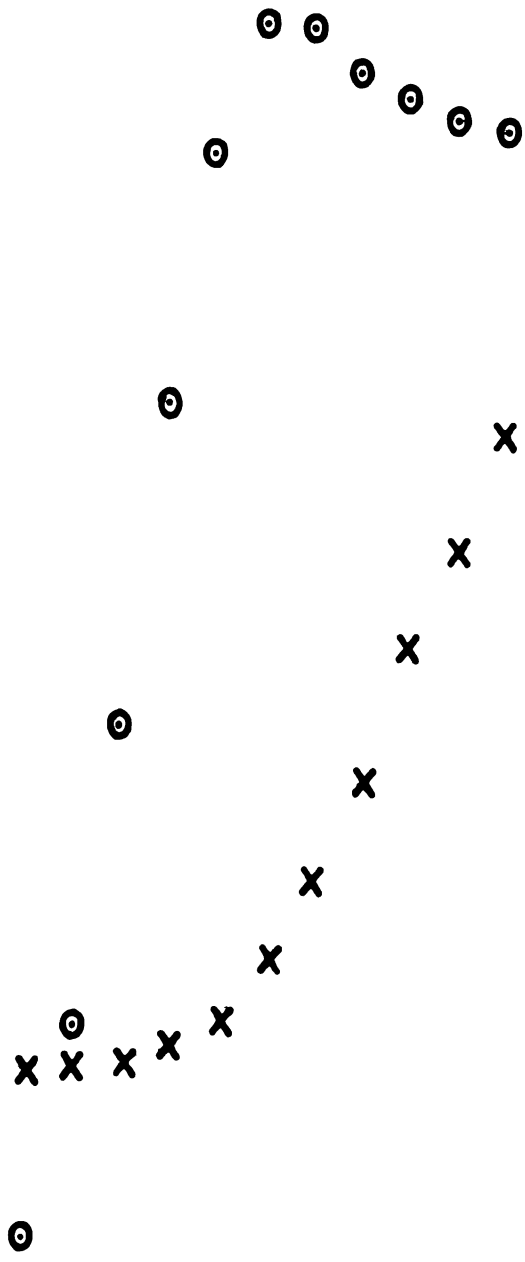

Fig. 16(a) Experimental points for Fig. 16

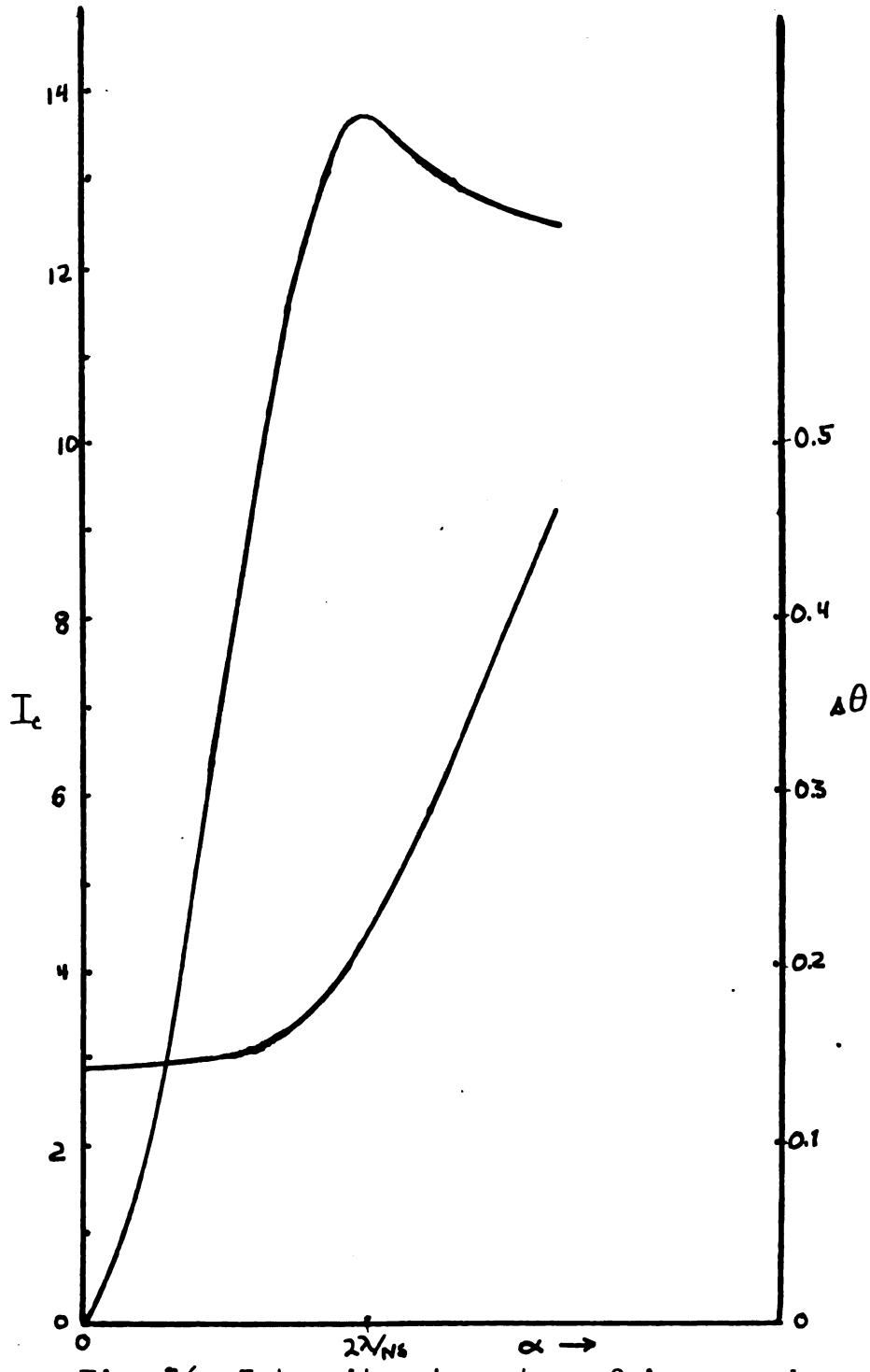

Fig. 16 Intensity at center of image and half-intensity breadth as functions of angular source breadth. Grating C - 3000 lines/inch; grating aperture, 3.42 mm; coherent mode. $\Delta\theta$ is expressed in units of 10^{-3} radians.

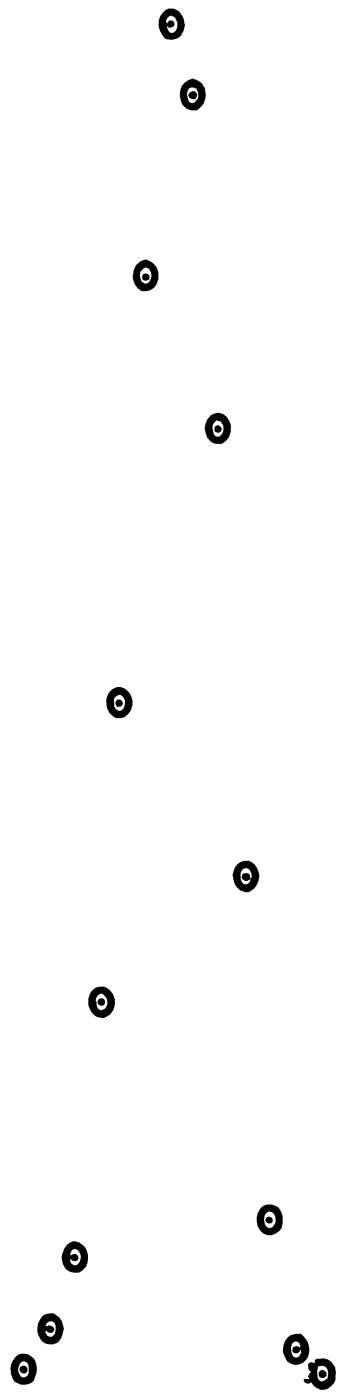

Fig. 17(a) Experimental points for Fig. 17

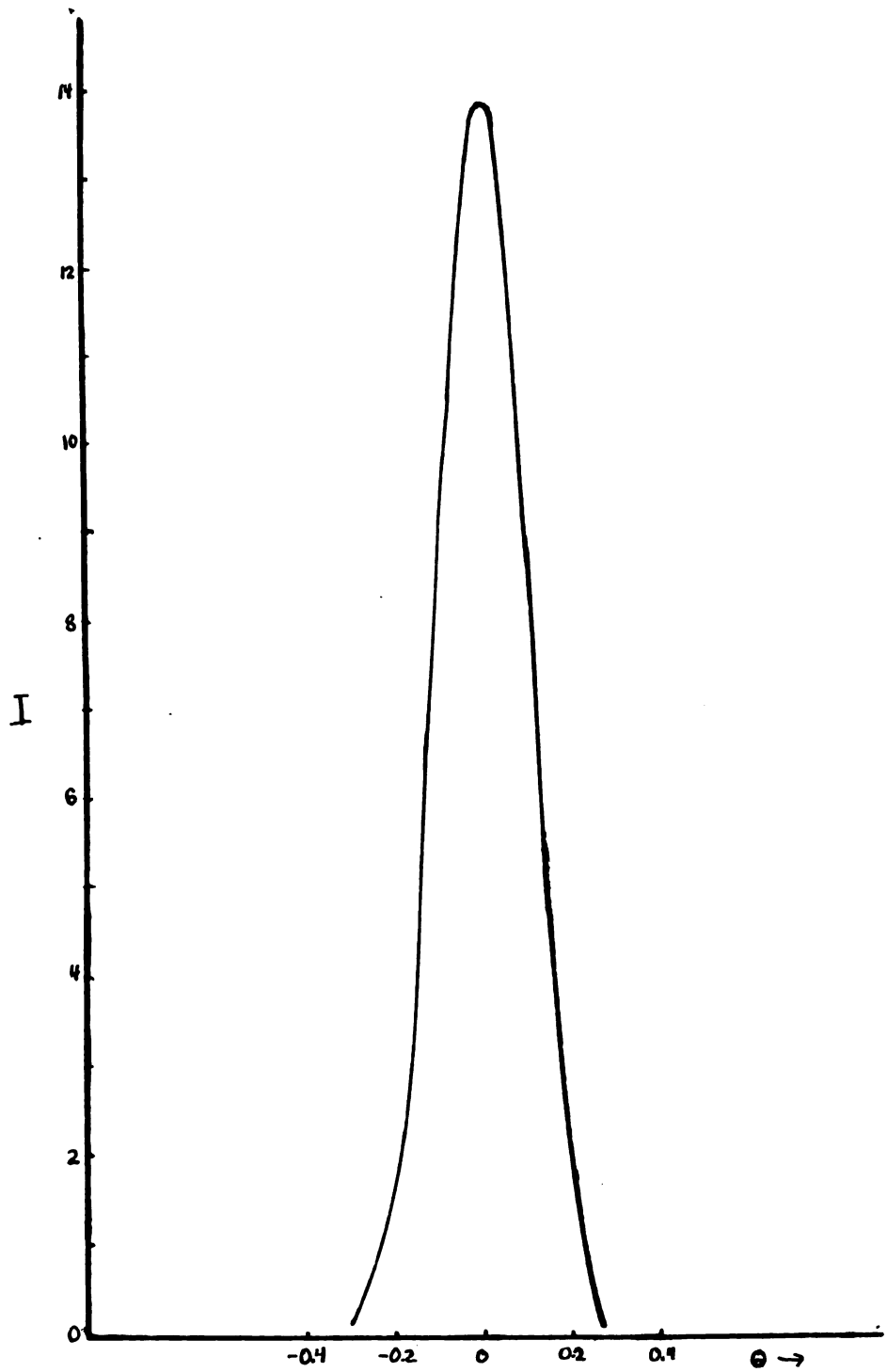

Fig. 17 Grating C - image formed by coherent mode. Source aperture of angular breadth $\alpha = 2\lambda/Ns$. θ is expressed in units of 10^{-3} radians.

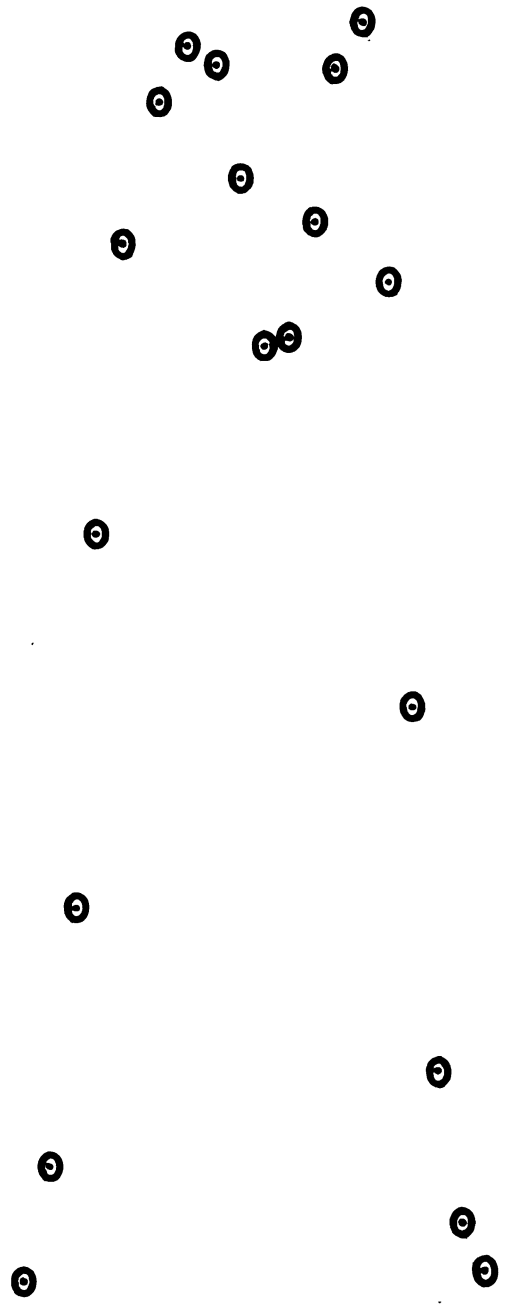

Fig. 18(a) Experimental points for Fig. 18

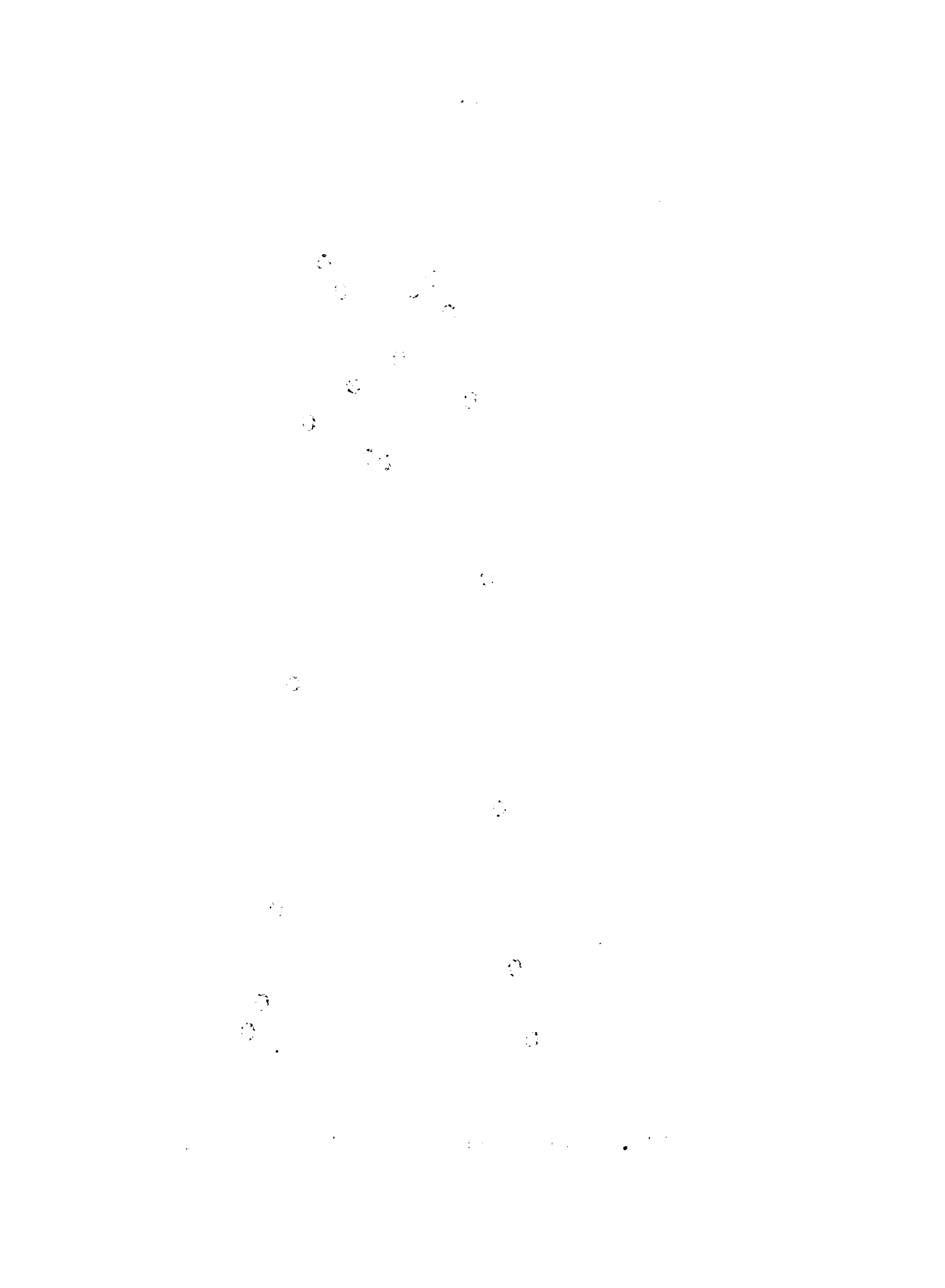

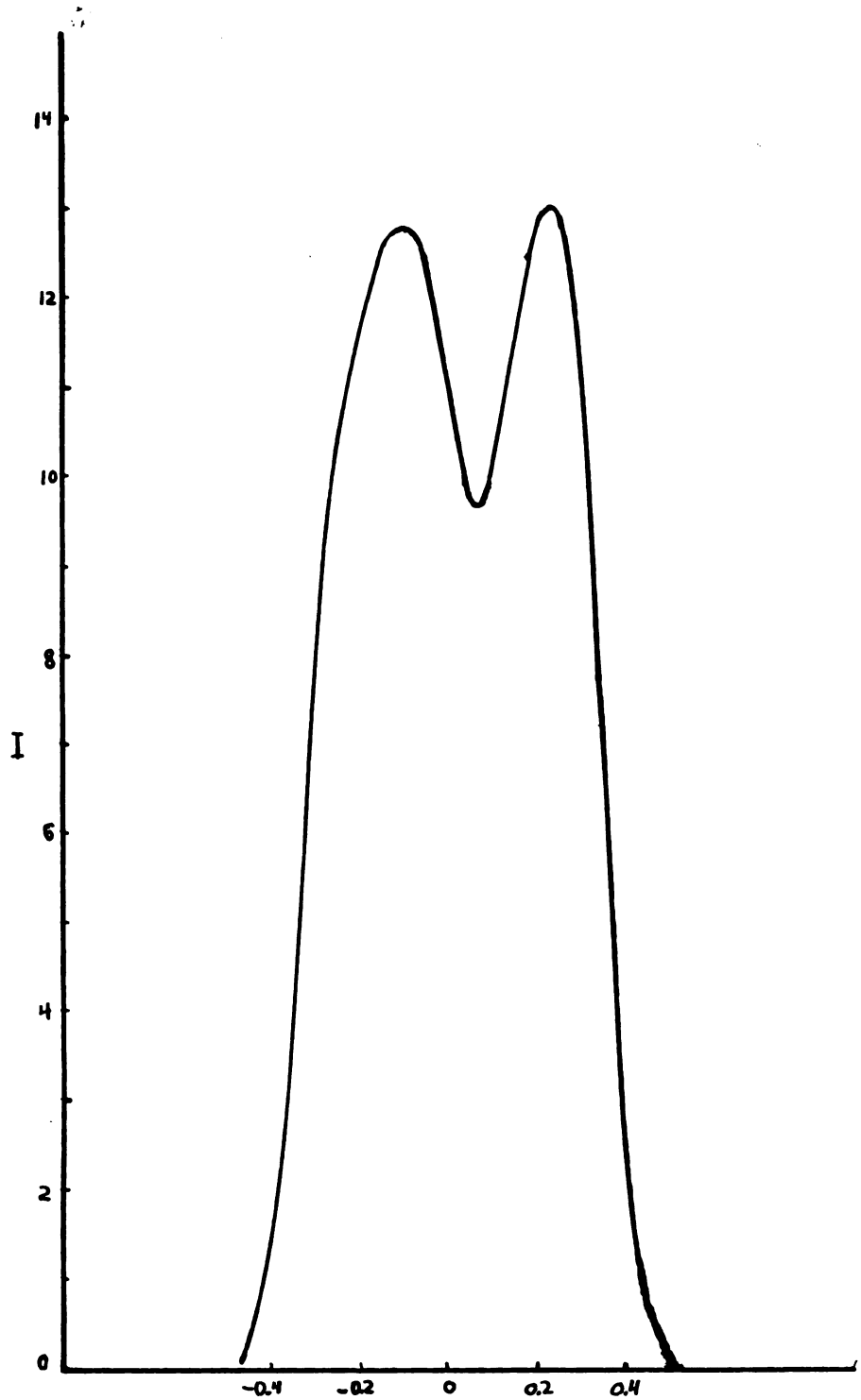

Fig. 18 Grating C. Coherent mode of illumination $\alpha = 2\lambda/Ns$.

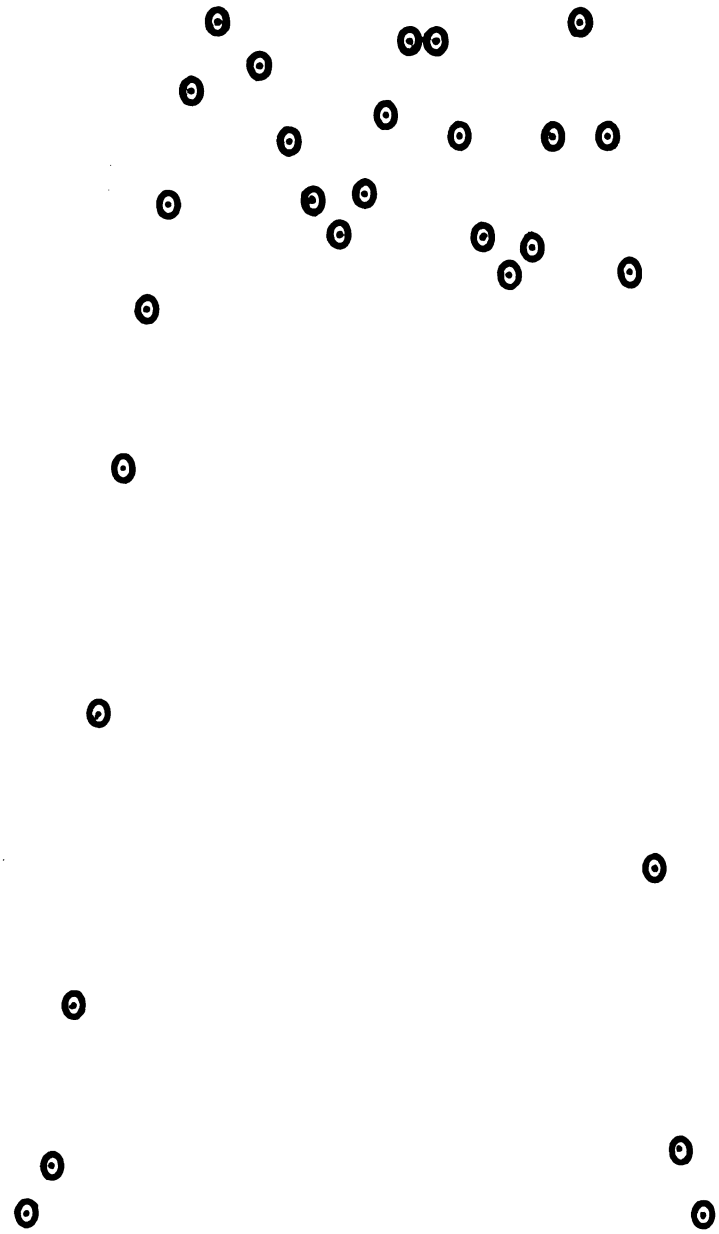

Fig. 19(a) Experimental points for Fig. 19

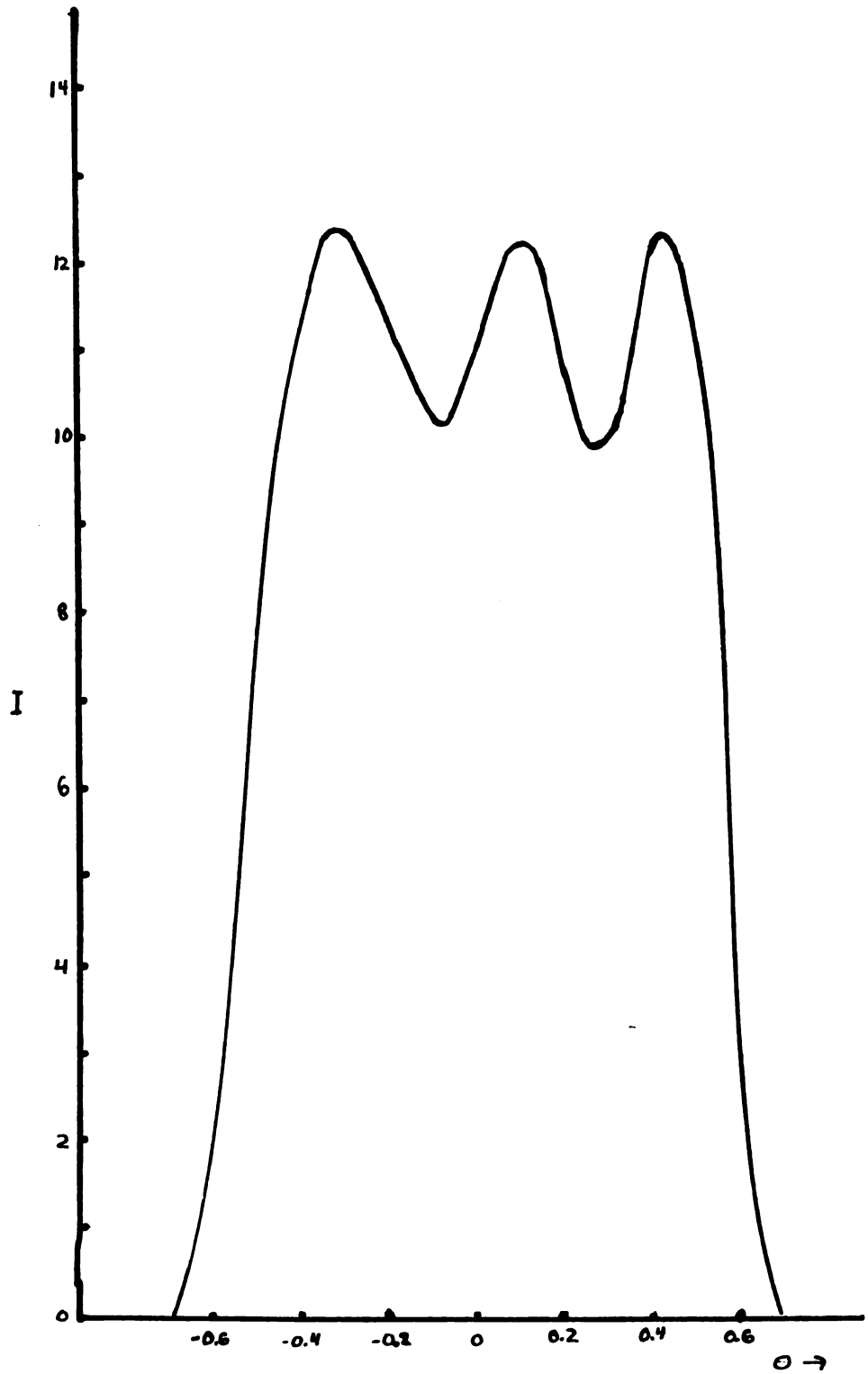

Fig. 19 Grating C. Coherent mode of illumination $\alpha = 6\lambda/Ns$.

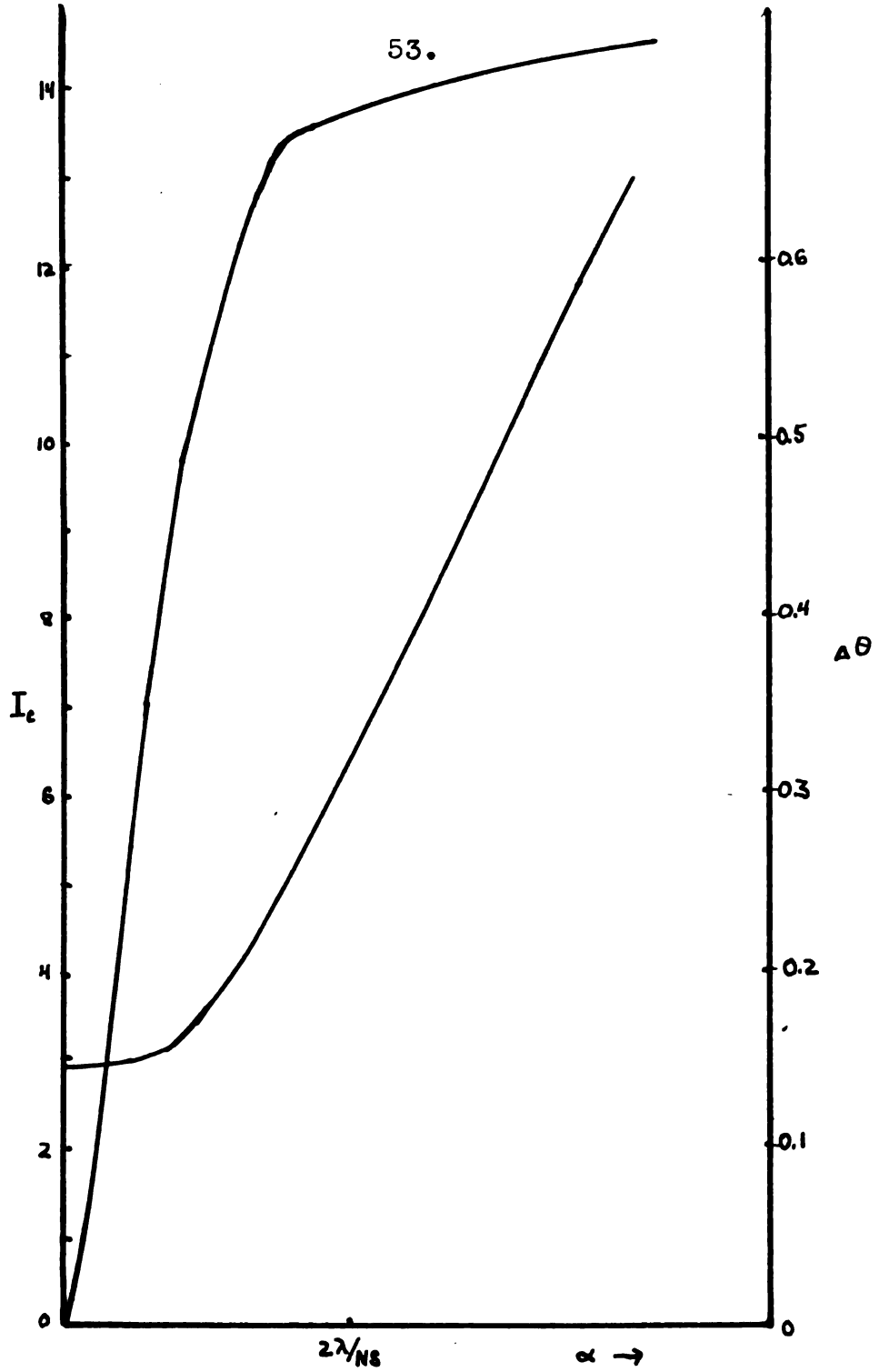

Fig. 20 Grating C, illuminated in the lens mode. Intensity at the center of the image and half-intensity breadth as functions of the source width.

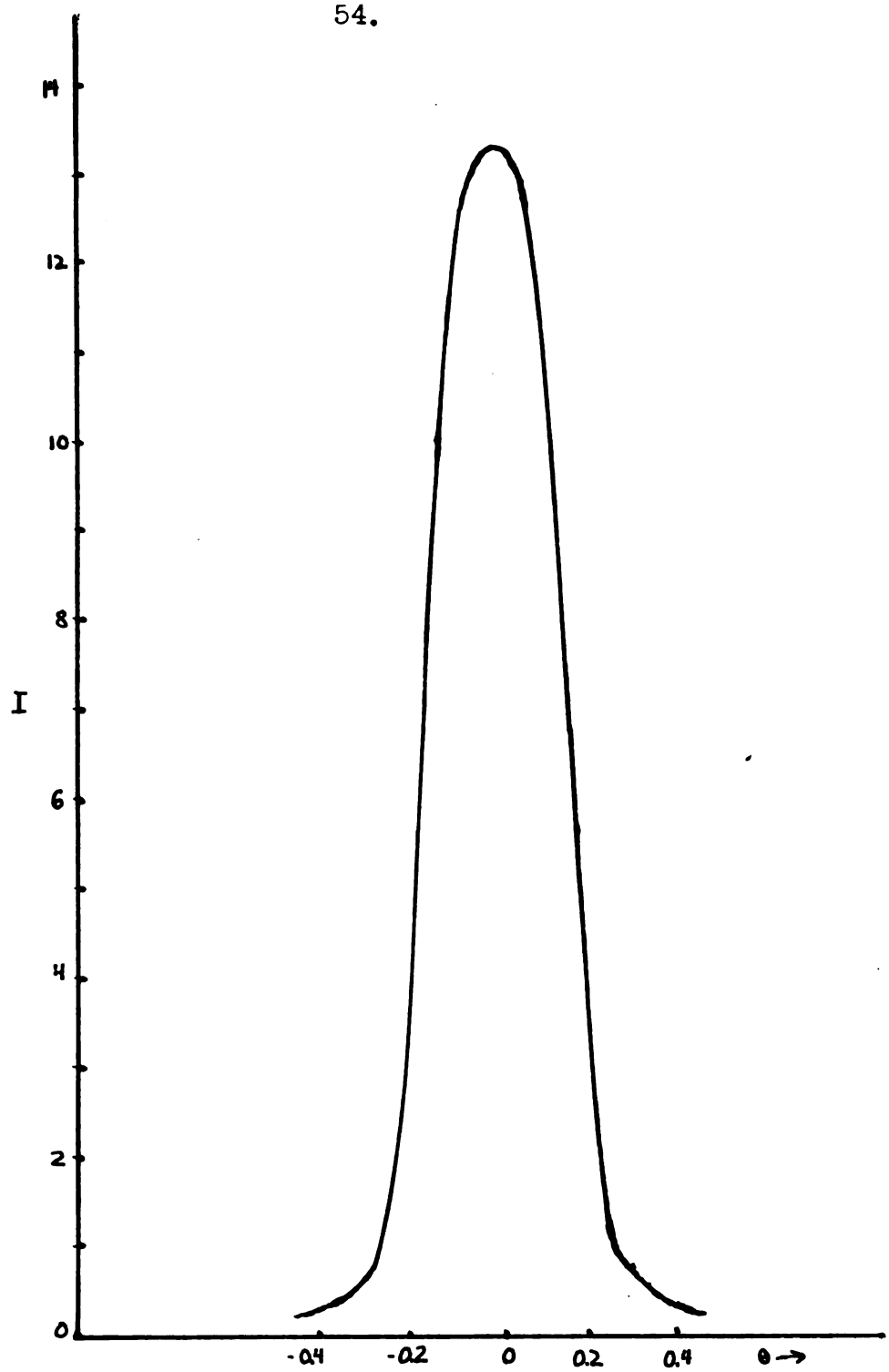

Fig. 21 Grating C. Lens mode of illumination $\alpha = 2\lambda/Ns$.

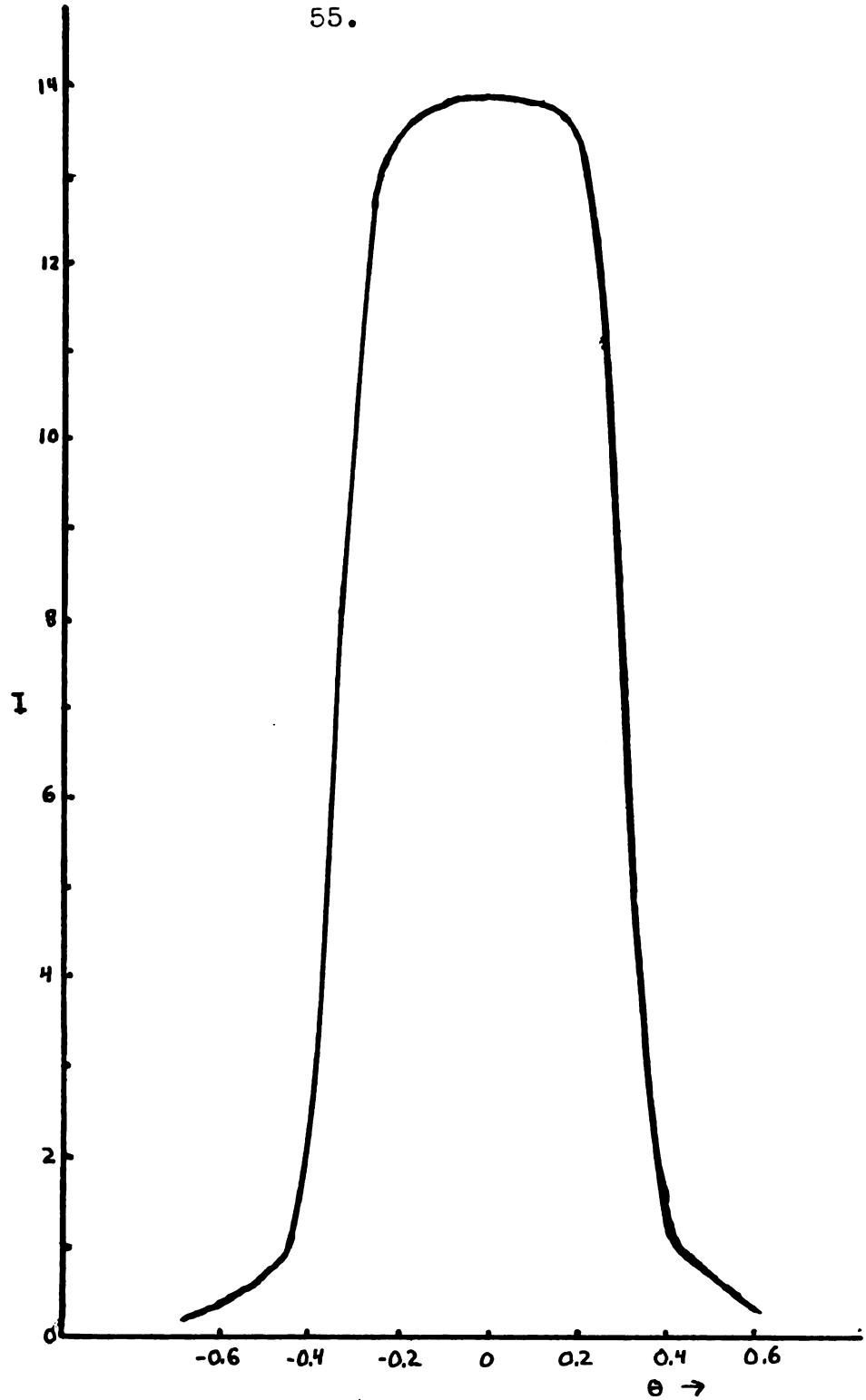

Fig. 22 Grating C. Lens mode of illumination $\alpha = 4\lambda/Ns$.

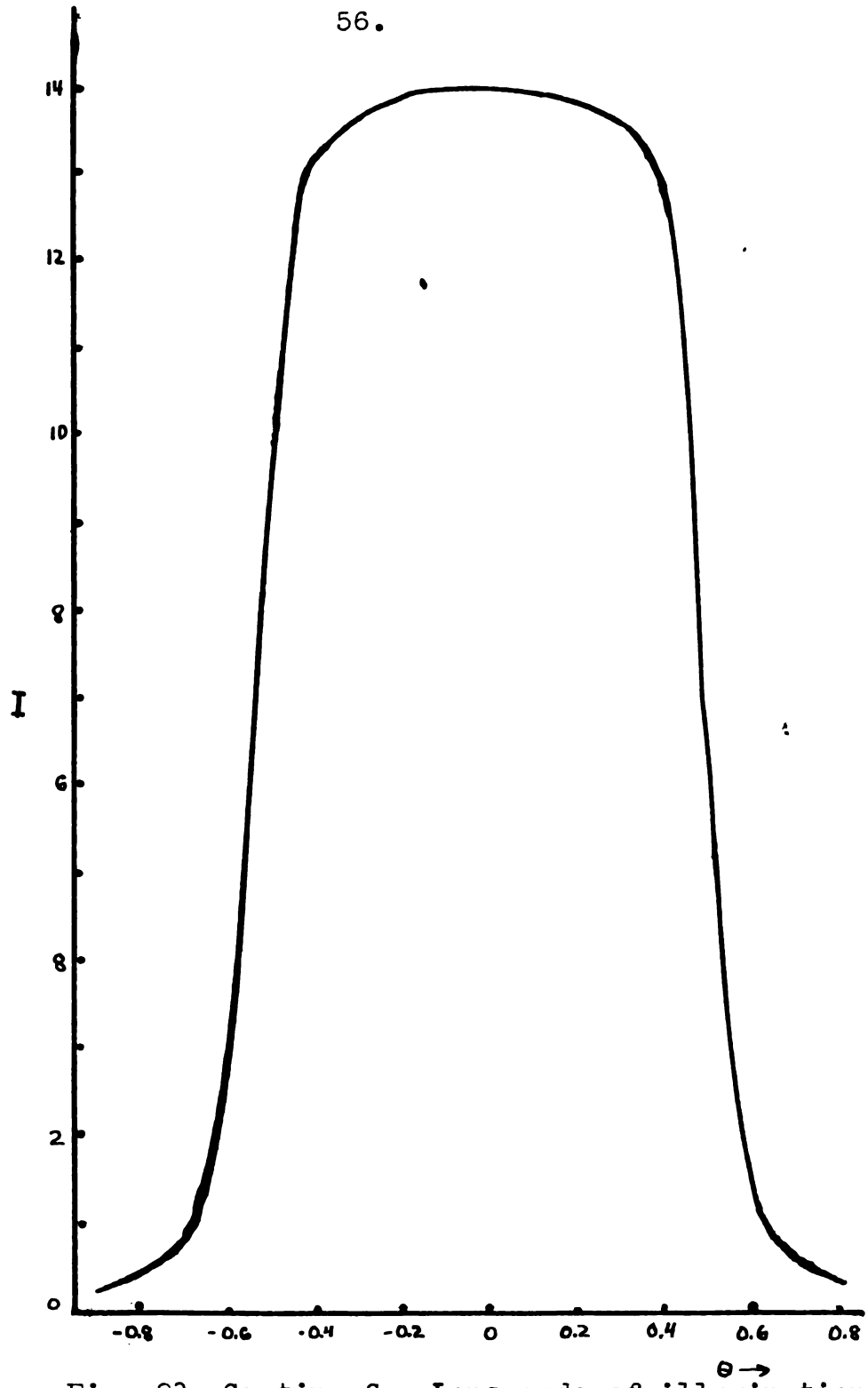

Fig. 23 Grating C. Lens mode of illumination $\alpha = 6\lambda/Ns$.

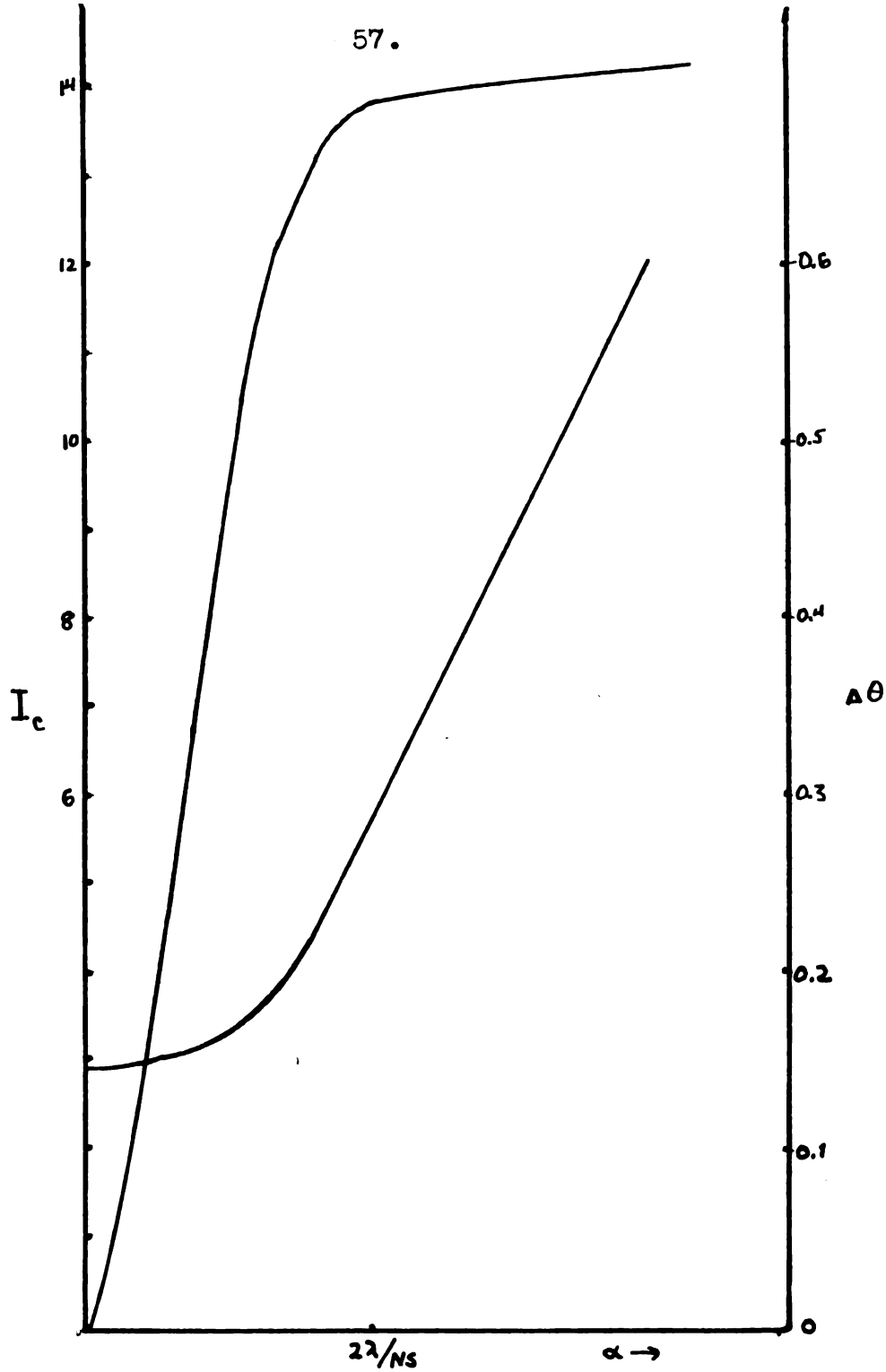

Fig. 24 Grating C illuminated in the broad source mode. Intensity in the center of the image and half-intensity breadth as functions of the source width.

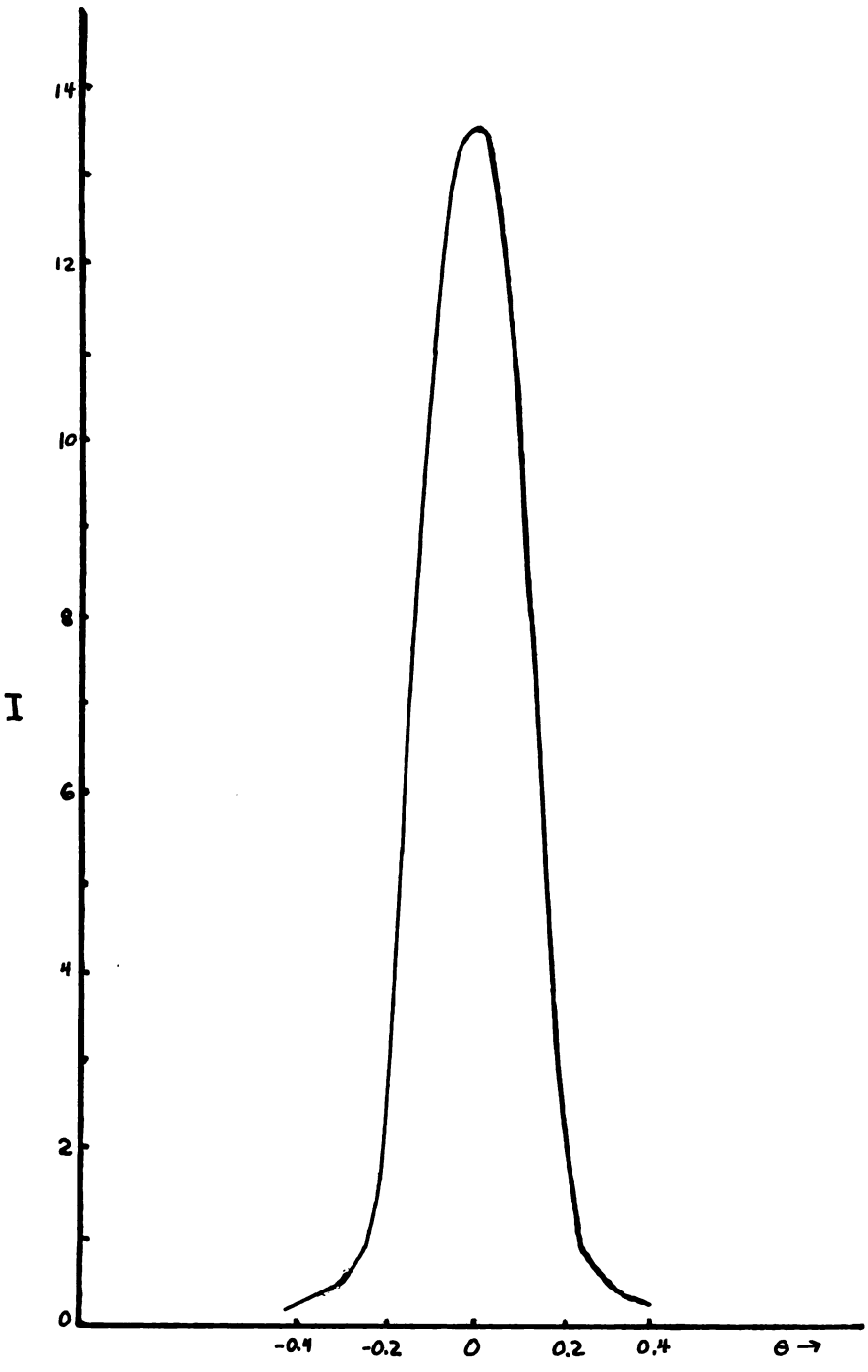

Fig. 25 Grating C. Broad source mode of illumination $\alpha = 2\lambda/Ns$.

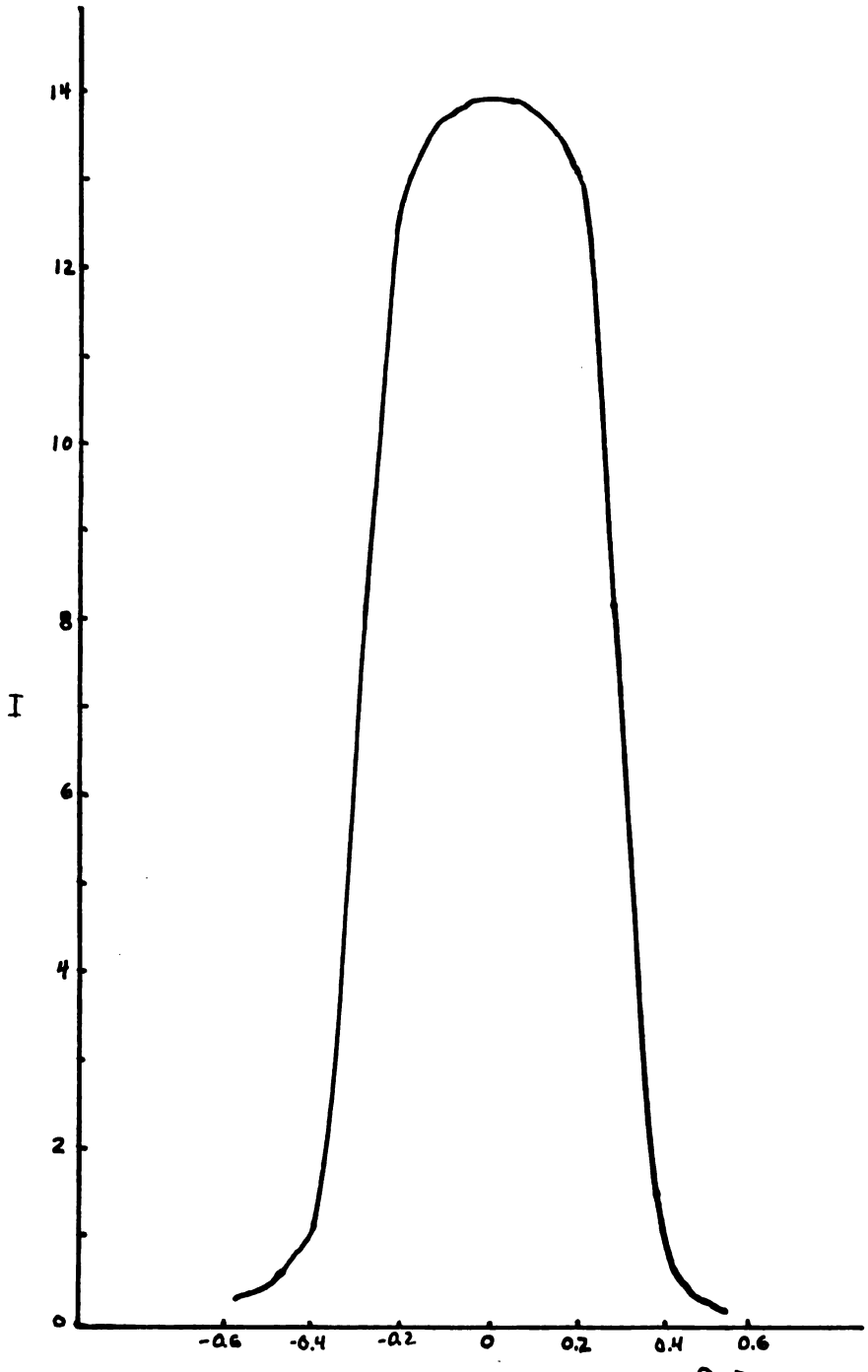

Fig. 26 Grating C. Broad source mode of illumination $\alpha = 4\lambda/Ns$.

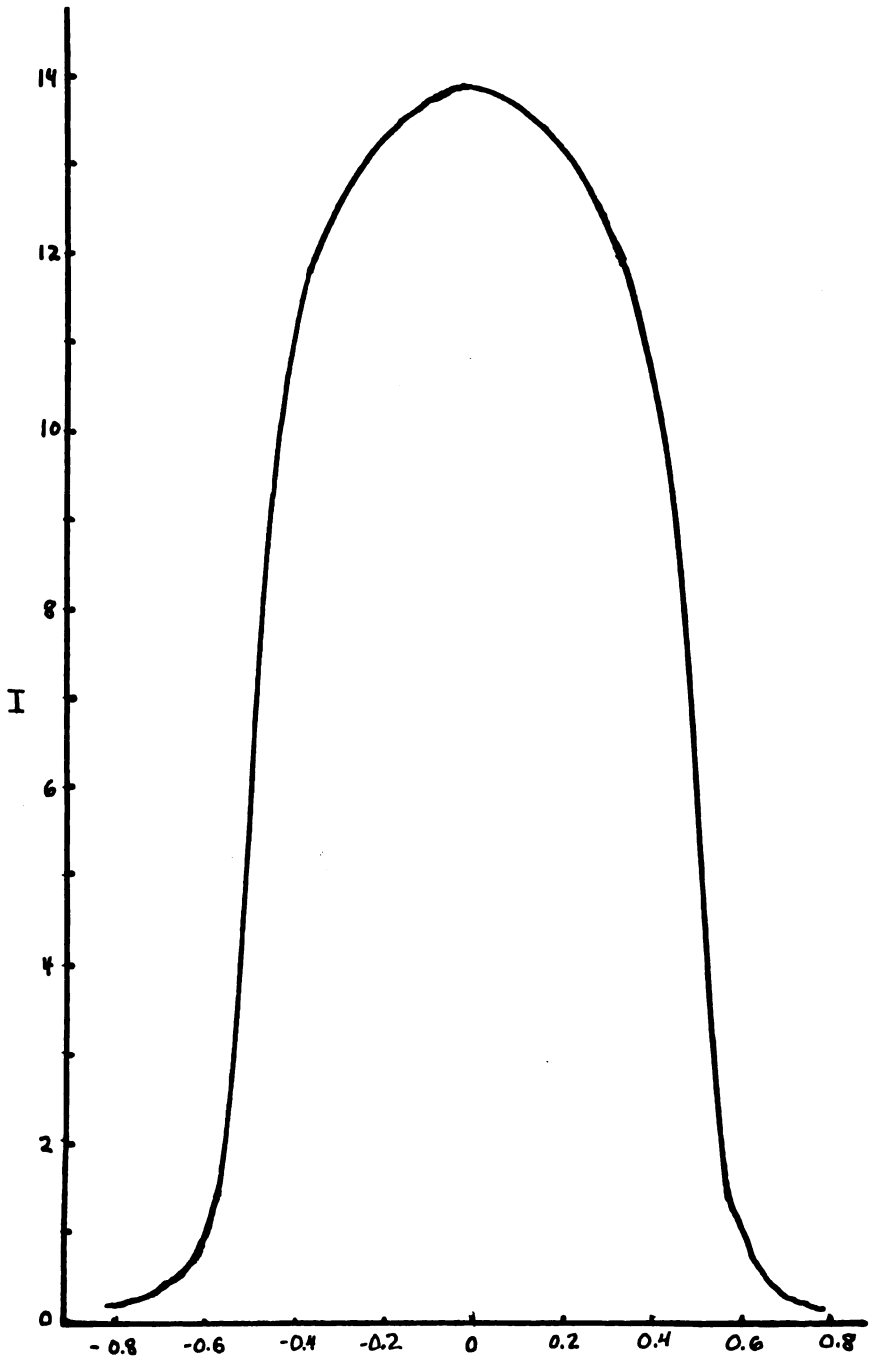

Fig. 27 Grating C. Broad source mode of illumination $\alpha = 6\lambda/Ns$.

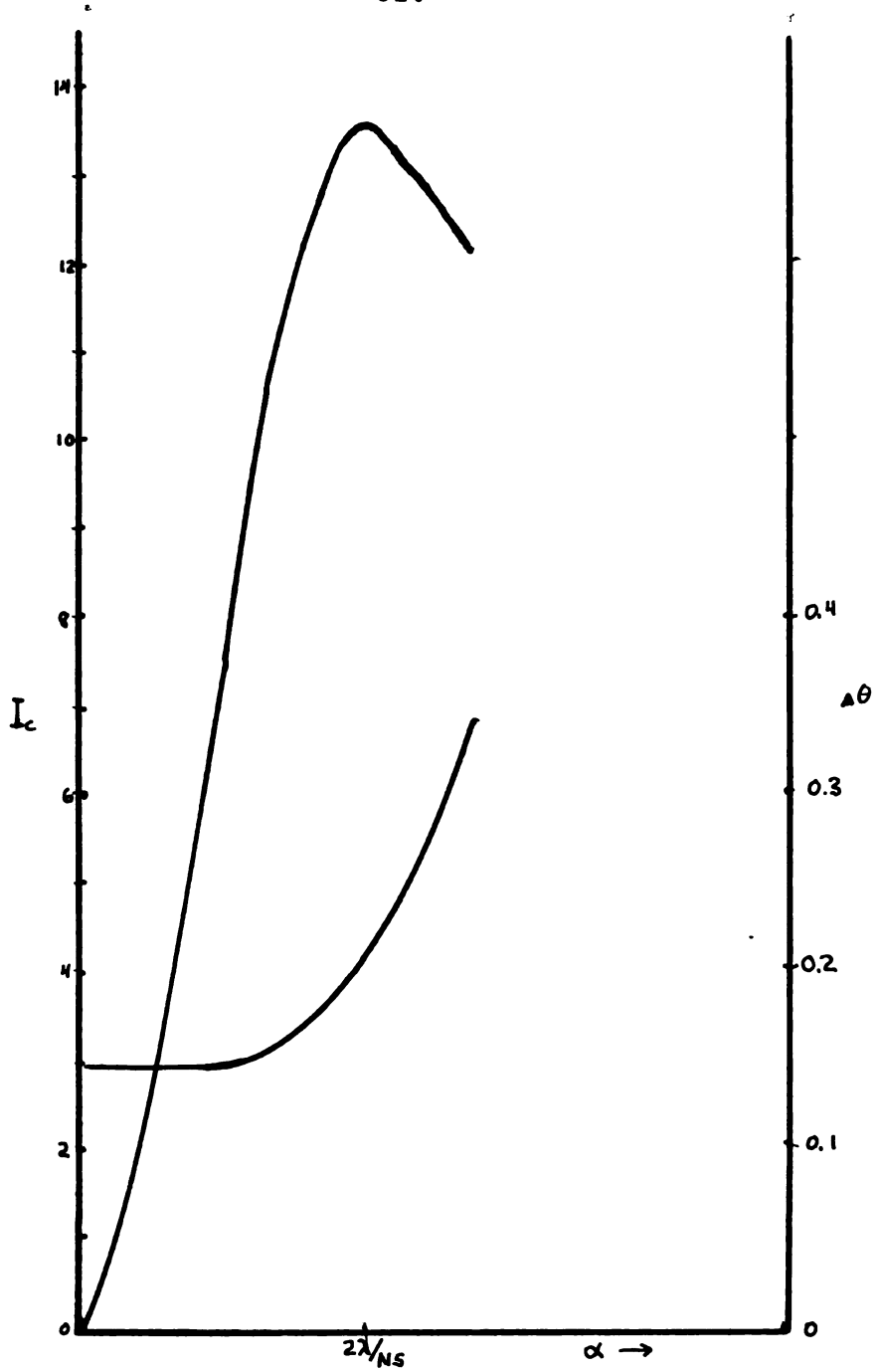

Fig. 28 Intensity at center of image and half-intensity breadth as functions of angular source breadth. Grating B - 90 lines/mm; grating aperture 3.50 mm; coherent mode. $\Delta\theta$ is expressed in units of 10^{-3} radians.

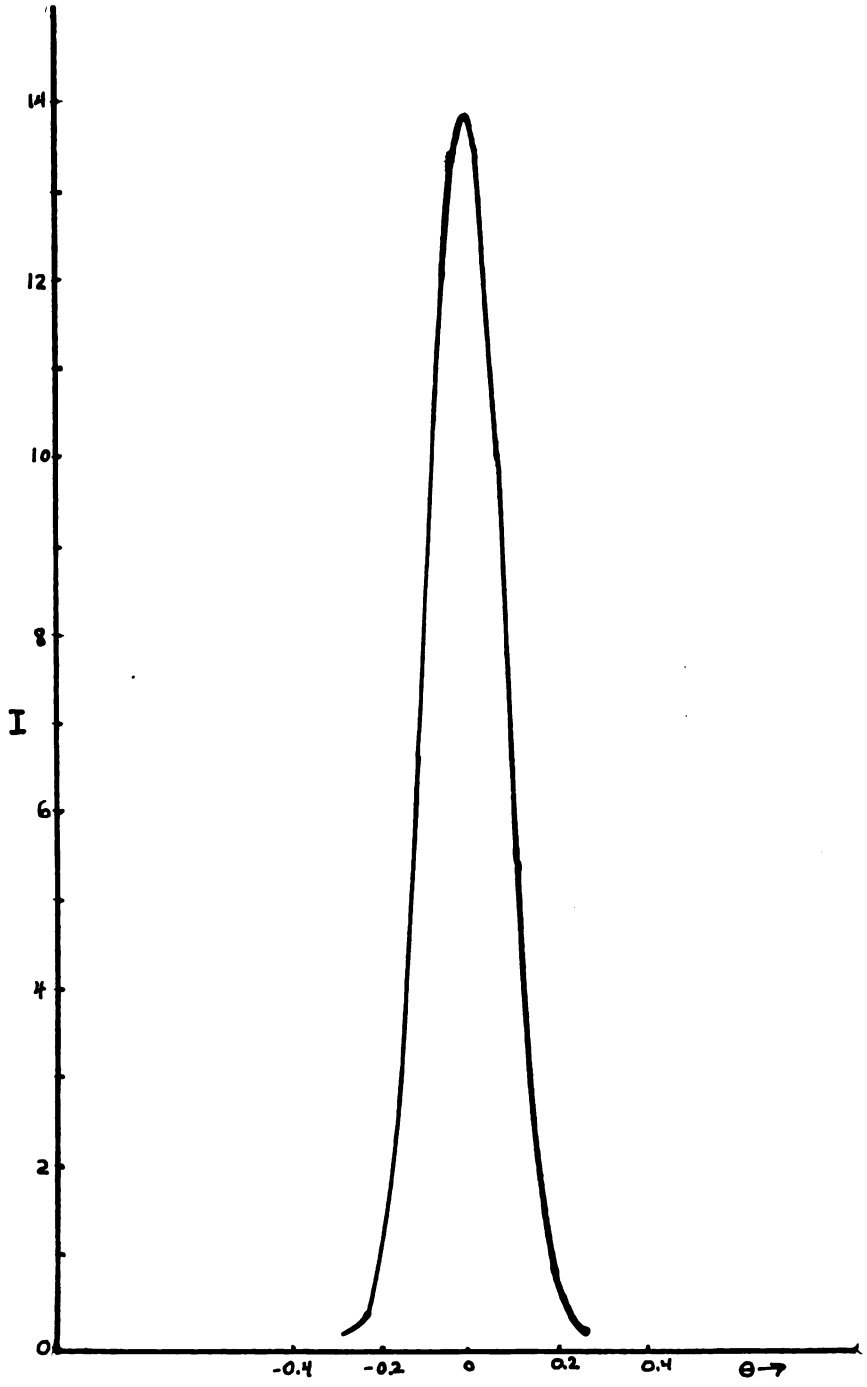

Fig. 29 Grating B. Image formed by coherent mode of illumination. Source aperture of angular breadth $\alpha = 2\lambda/Ns$. is expressed in units of 10^{-3} radians.

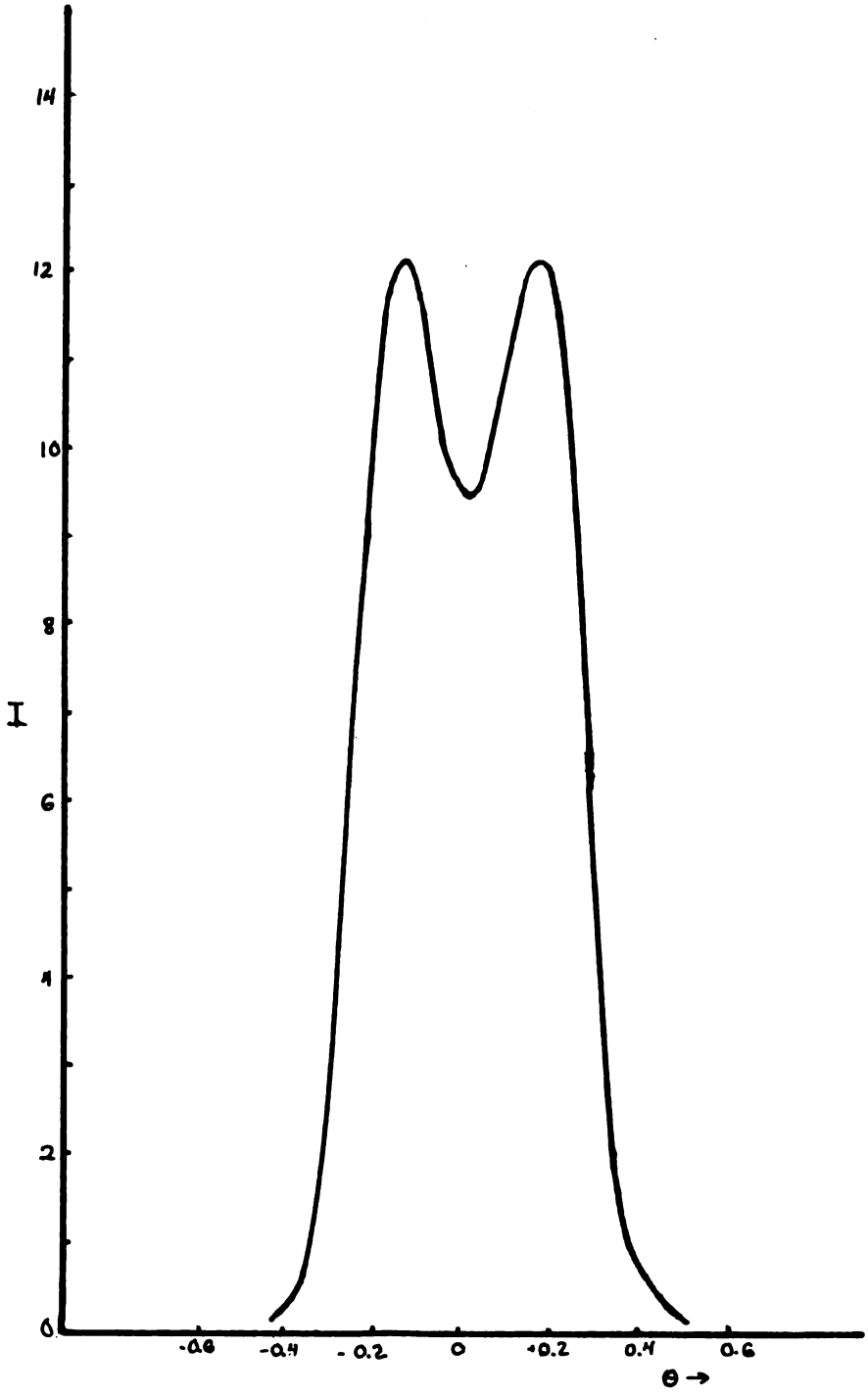

Fig. 30 Grating B. Coherent mode of illumination $\alpha = 4\lambda/Ns$.

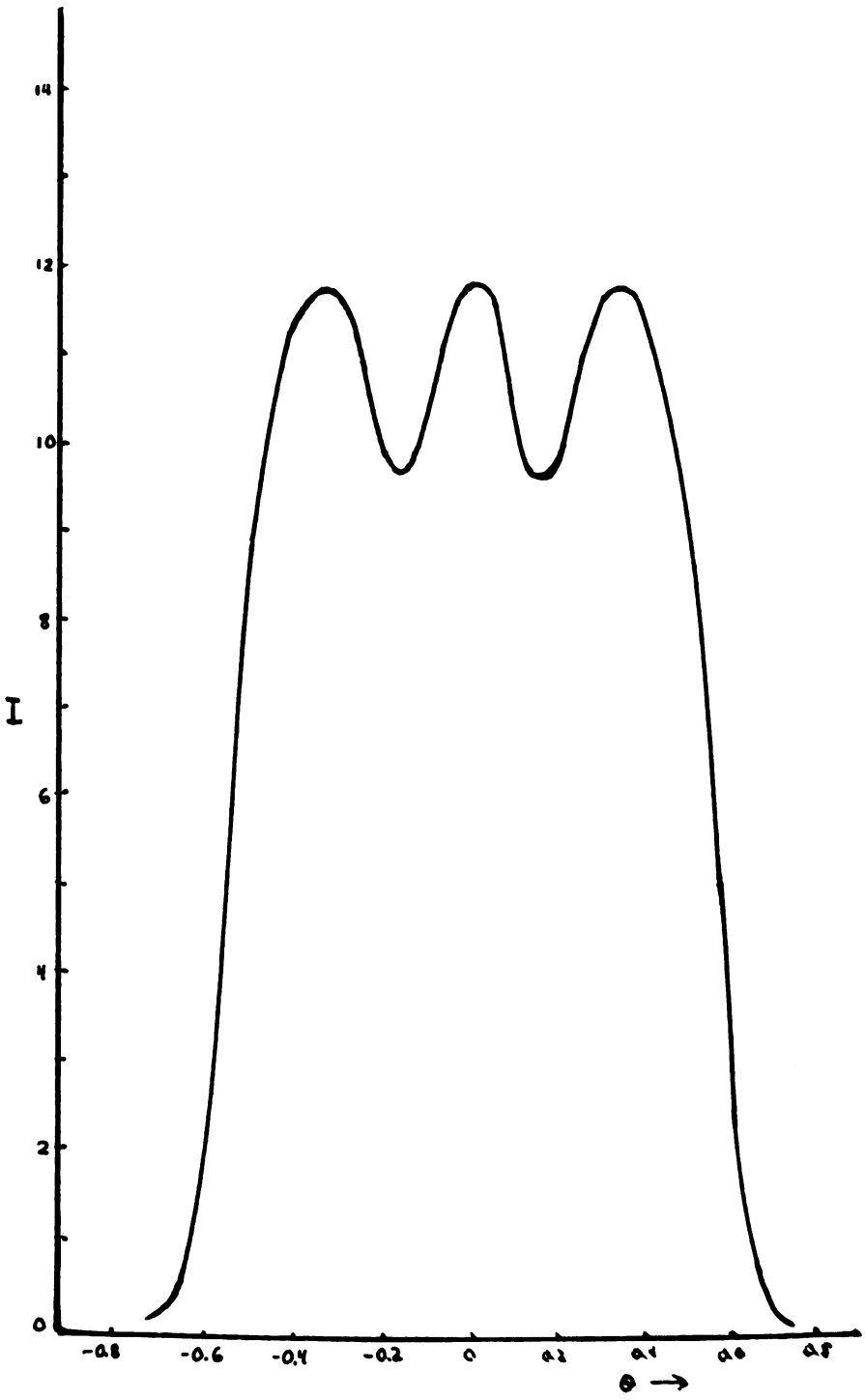

Fig. 31 Grating B. Coherent mode of illumination $\alpha = 6\lambda/Ns$.

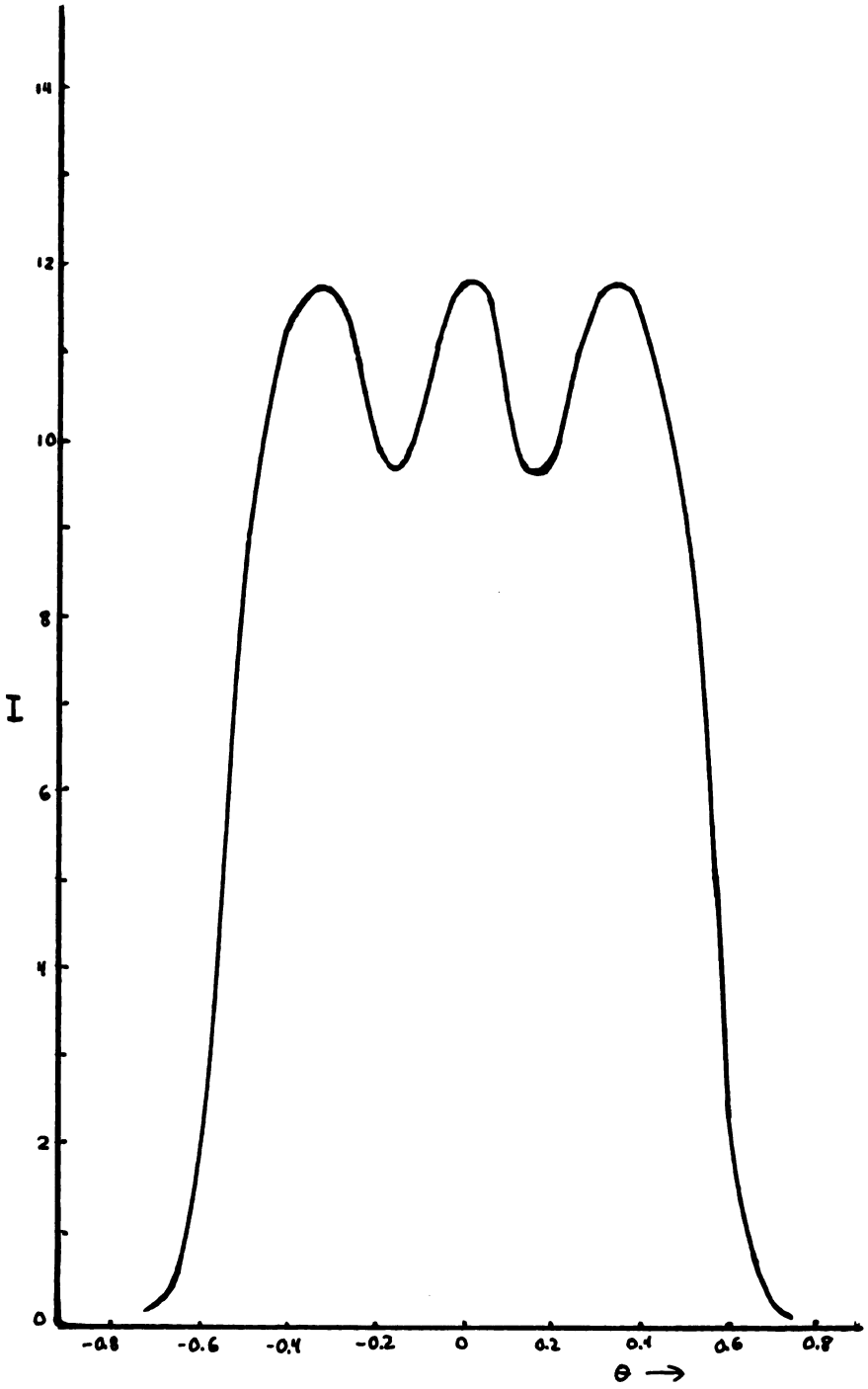

Fig. 31 Grating B. Coherent mode of illumination $\alpha = 6\lambda/Ns$.

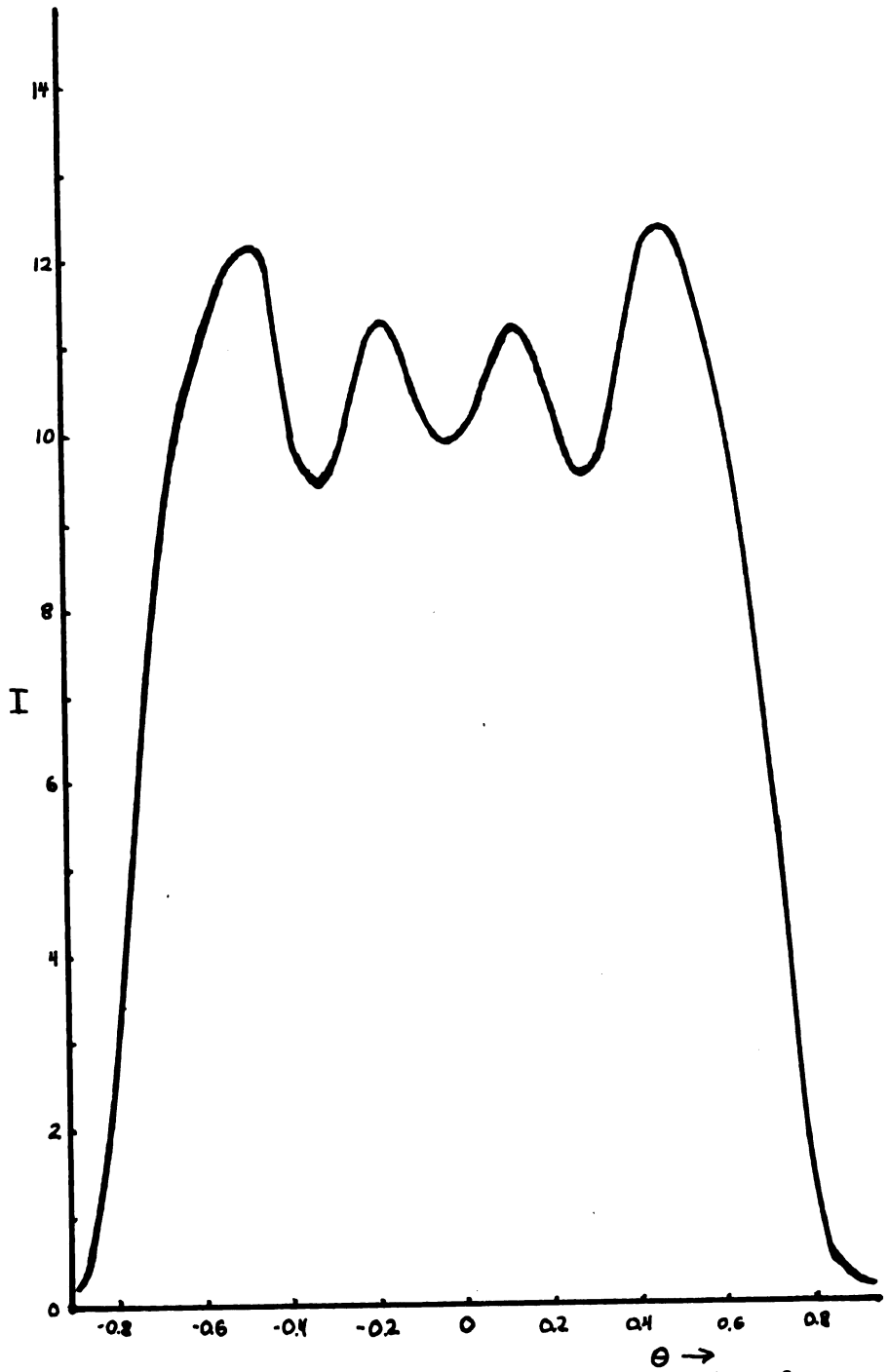

Fig. 32 Grating B. Coherent mode of illumination $\alpha = 8\lambda/Ns$.

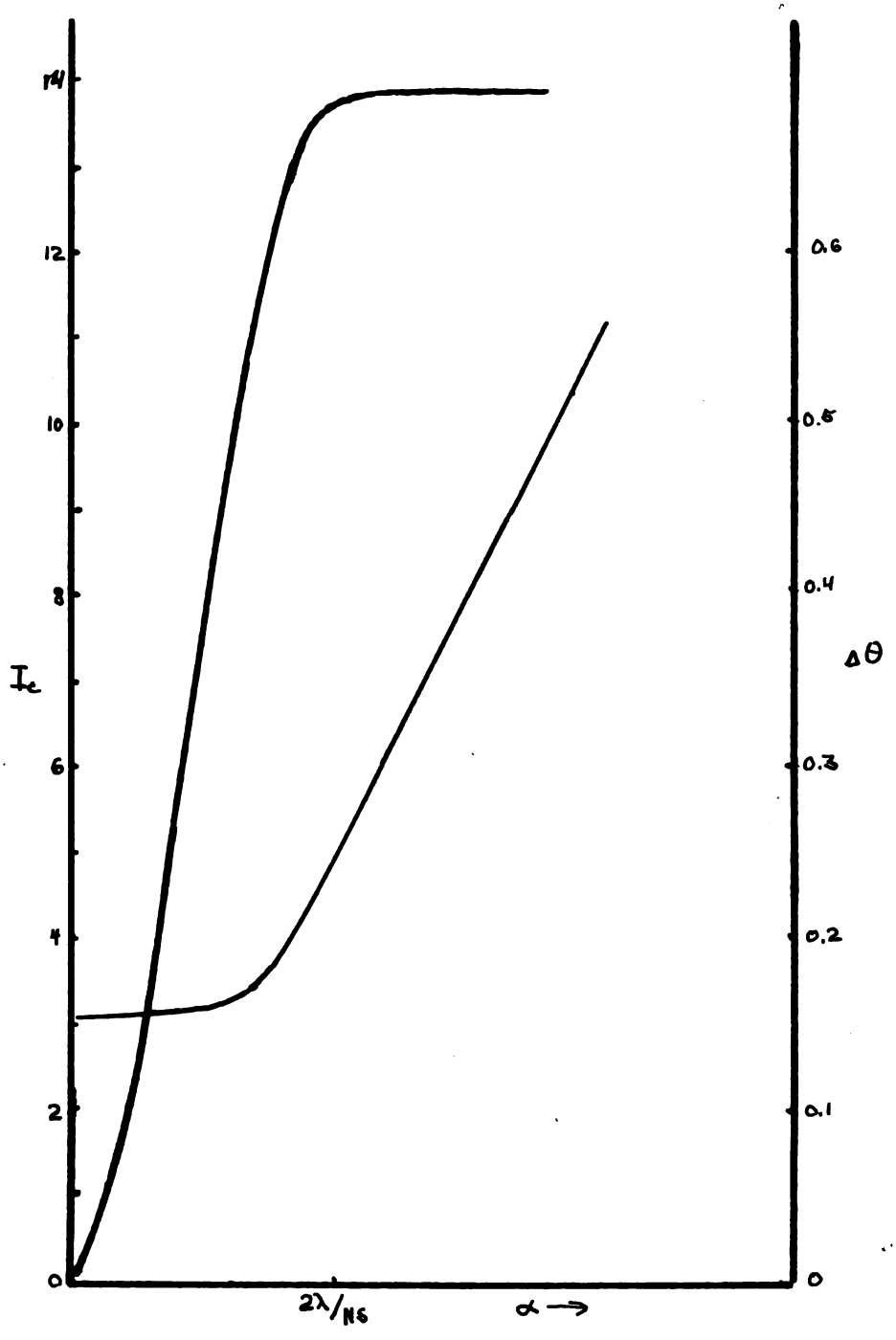

Fig. 33 Grating B illuminated in the broad source mode. Intensity in the center of the image and half-intensity breadth as functions of the angular source width.

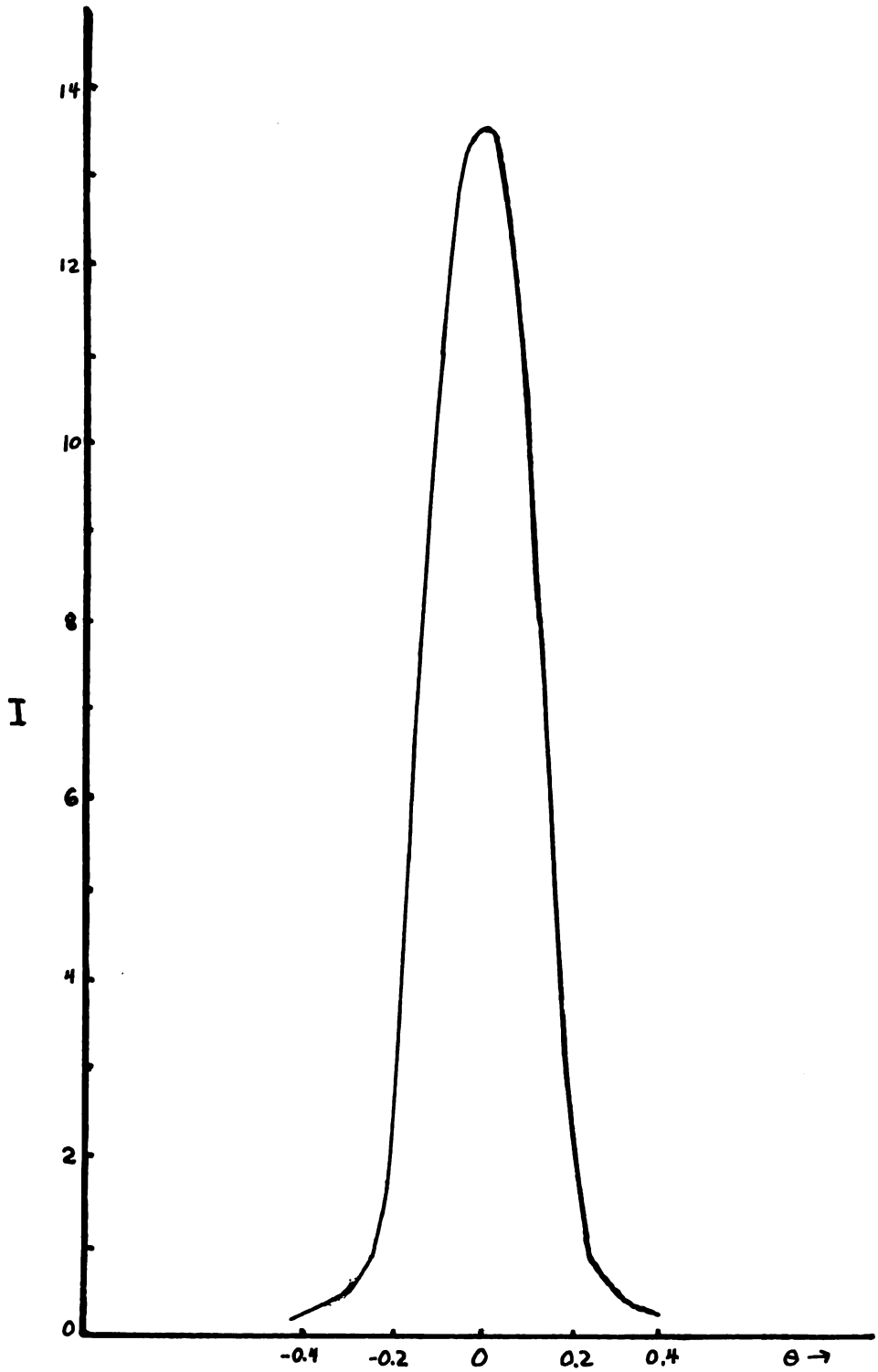

Fig. 25 Grating C. Broad source mode of illumination $\alpha = 2\lambda/Ns$.

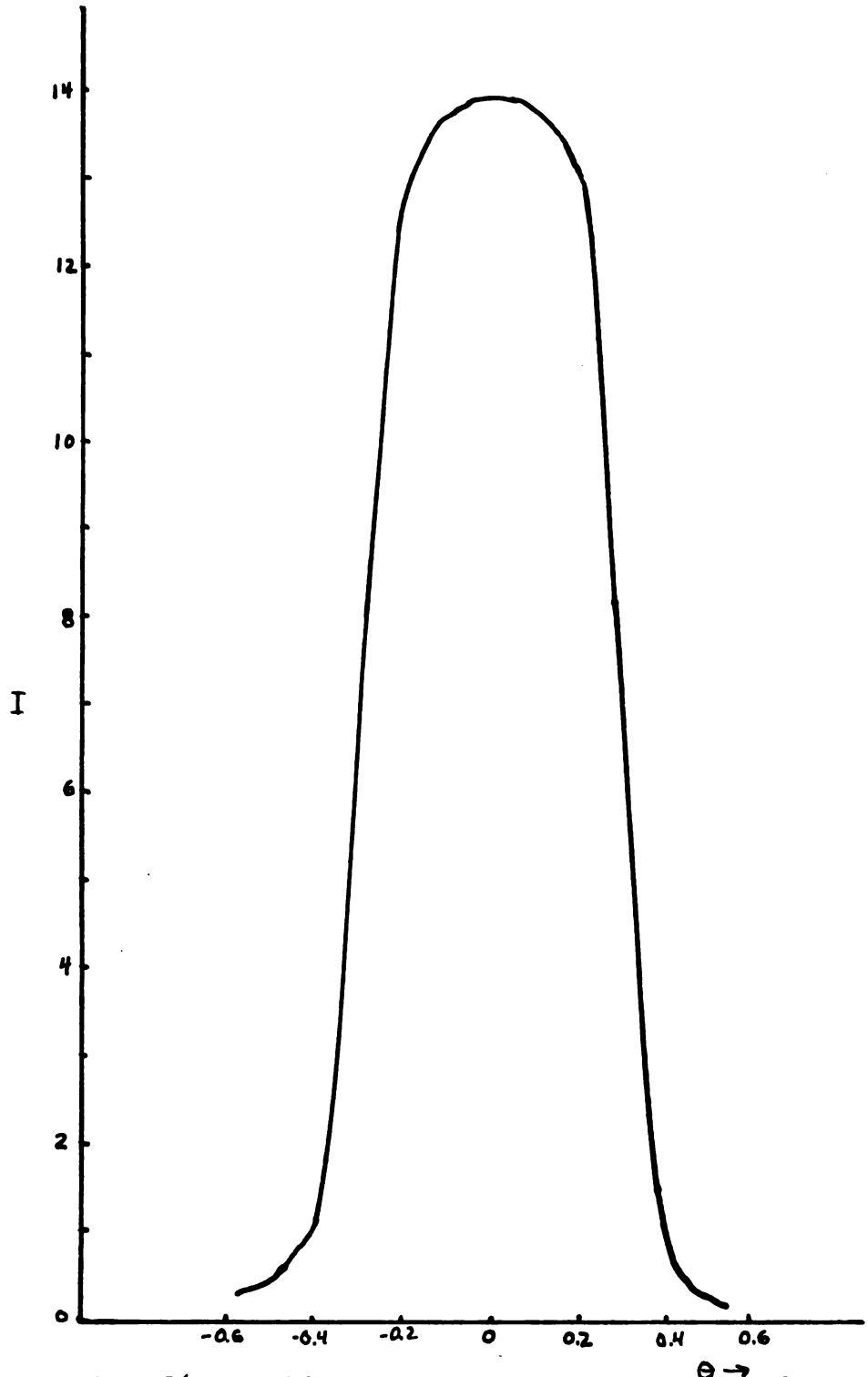

Fig. 26 Grating C. Broad source mode of illumination $\alpha = 4\lambda/Ns$.

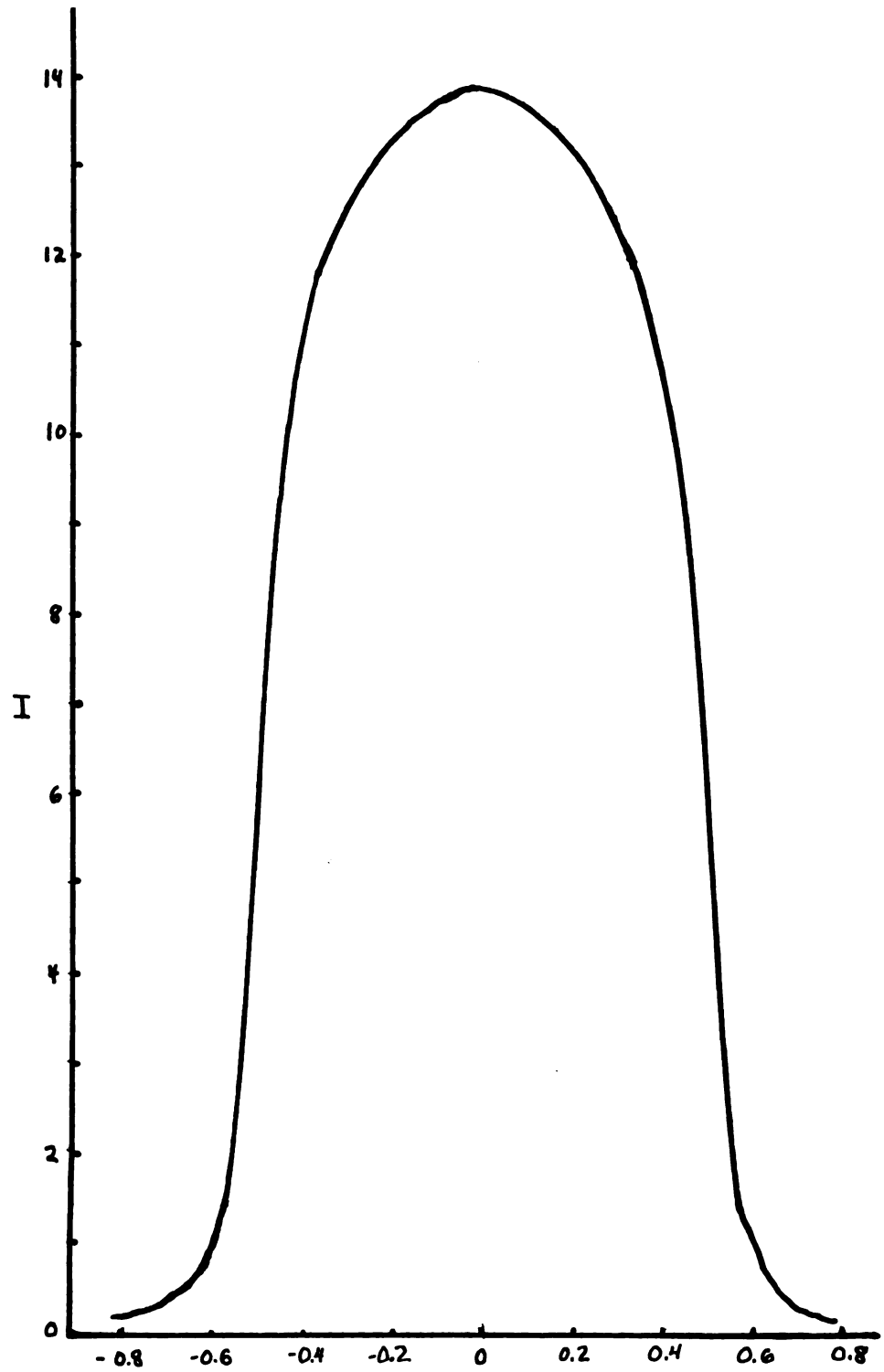

Fig. 27 Grating C. Broad source mode of illumination $\alpha = 6\lambda/Ns$.

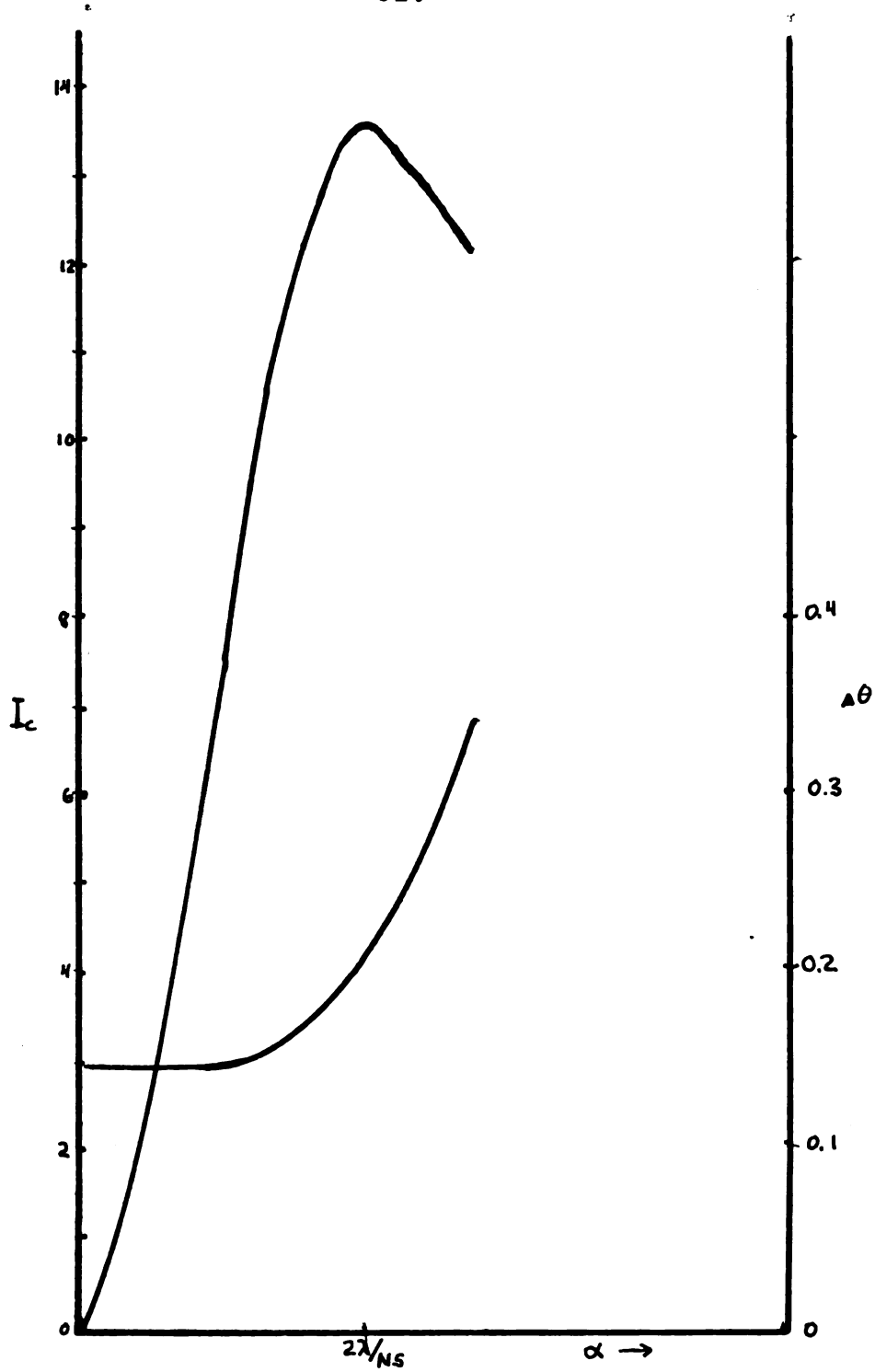

Fig. 28 Intensity at center of image and half-intensity breadth as functions of angular source breadth. Grating B - 90 lines/mm; grating aperture 3.50 mm; coherent mode. $\Delta\theta$ is expressed in units of 10^{-3} radians.

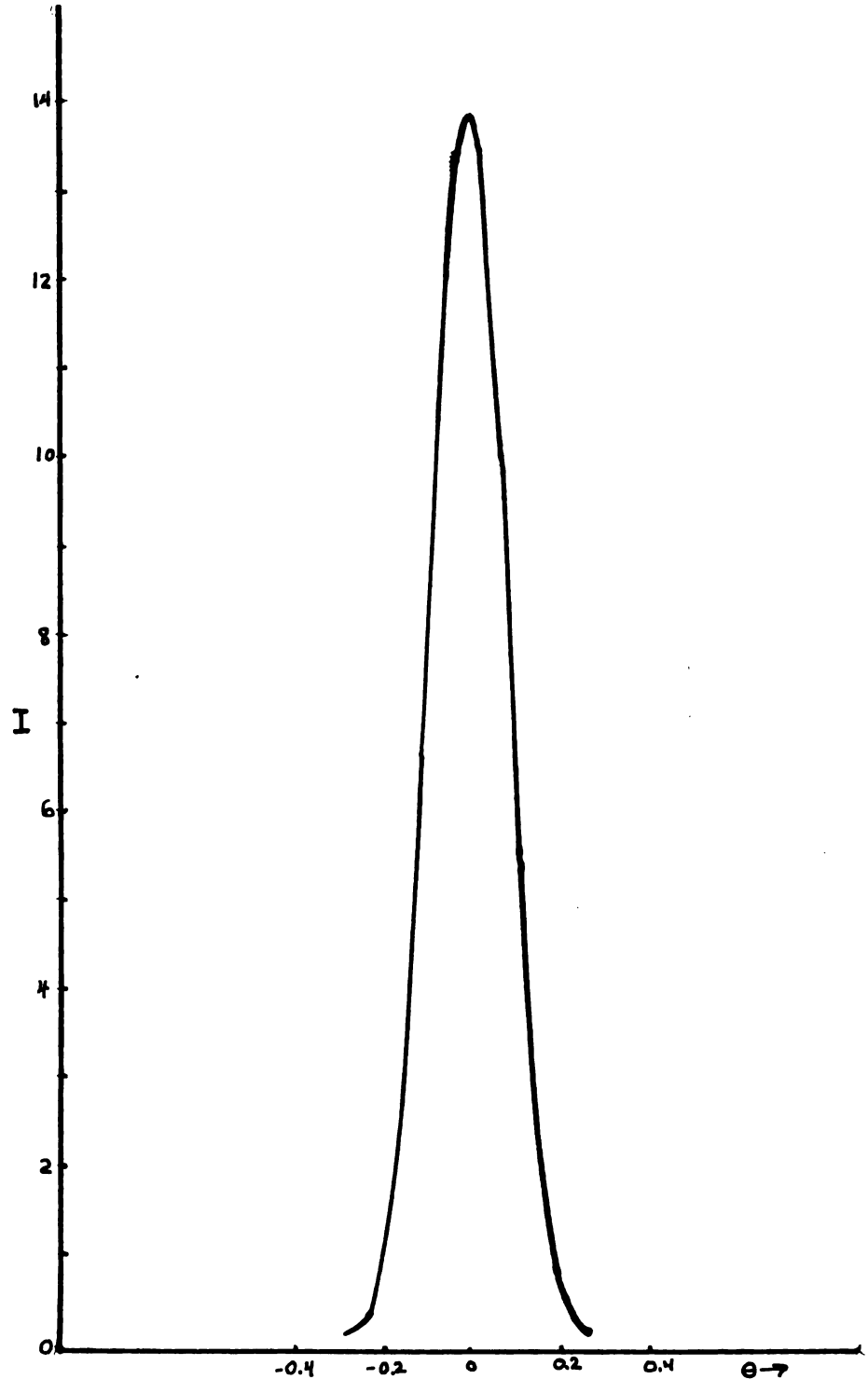

Fig. 29 Grating B. Image formed by coherent mode of illumination. Source aperture of angular breadth $\alpha = 2\lambda/Ns$. is expressed in units of 10^{-3} radians.

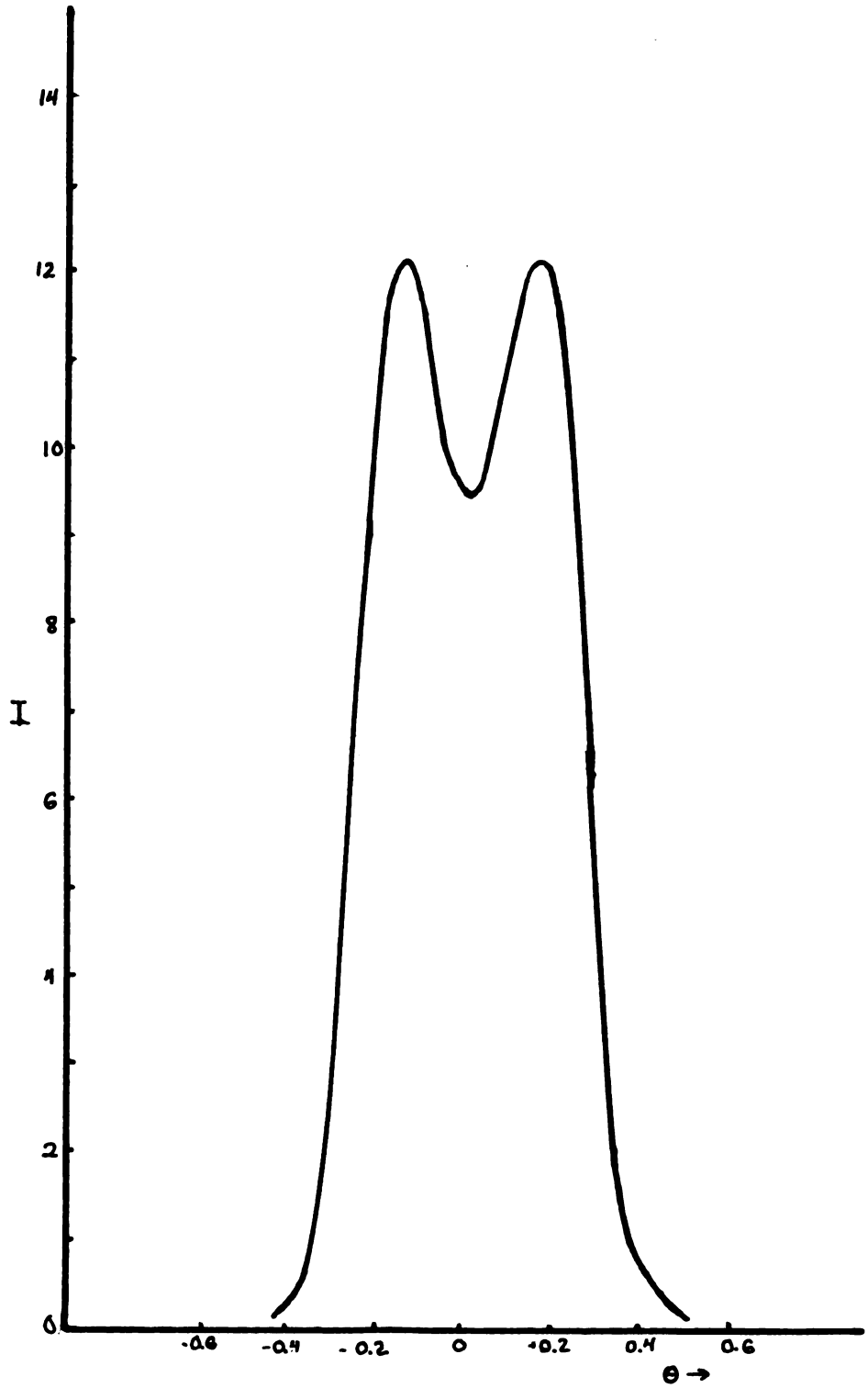

Fig. 30 Grating B. Coherent mode of illumination $\alpha = 4\lambda/Ns$.

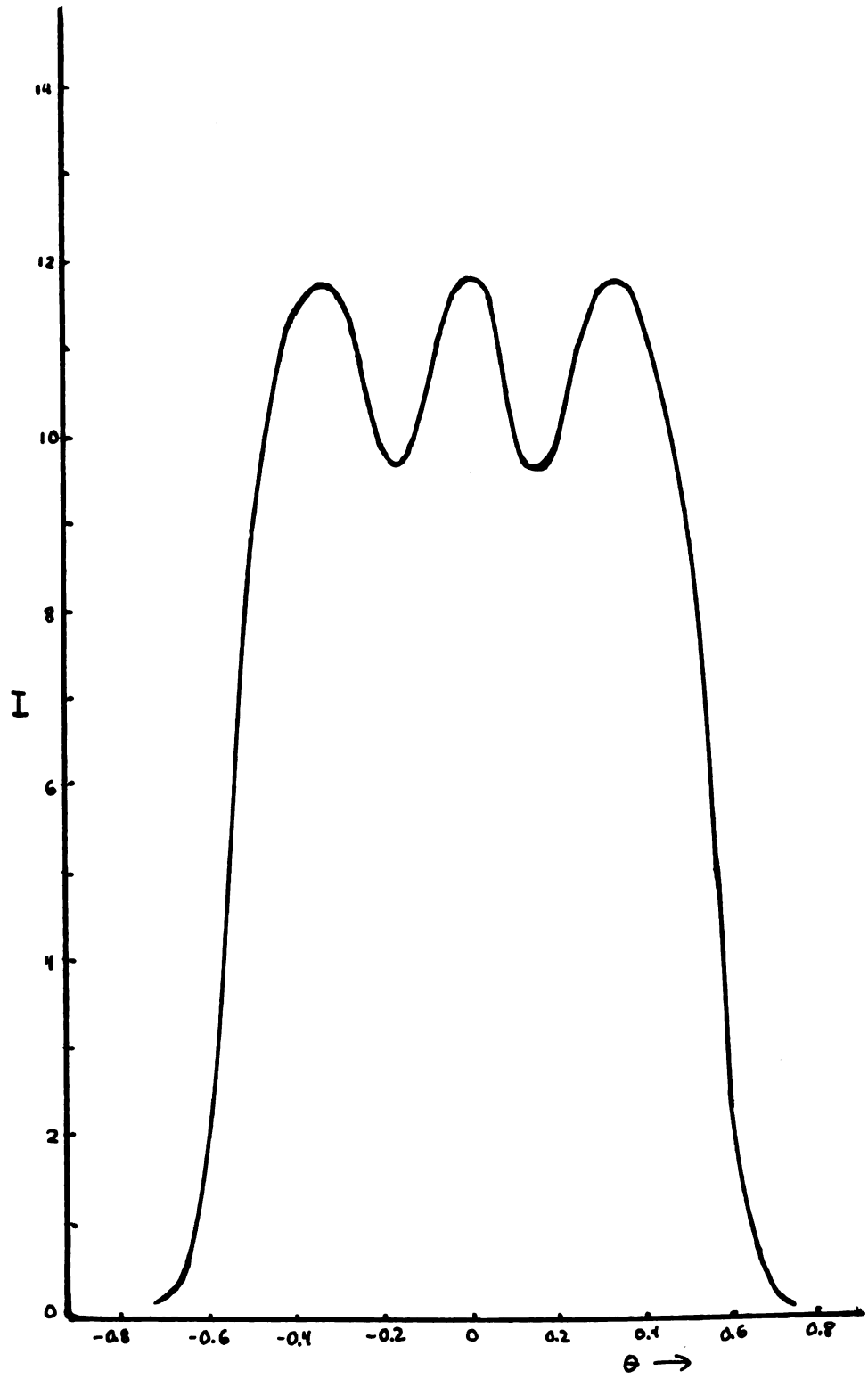

Fig. 31 Grating B. Coherent mode of illumination $\alpha = 6\lambda/Ns$.

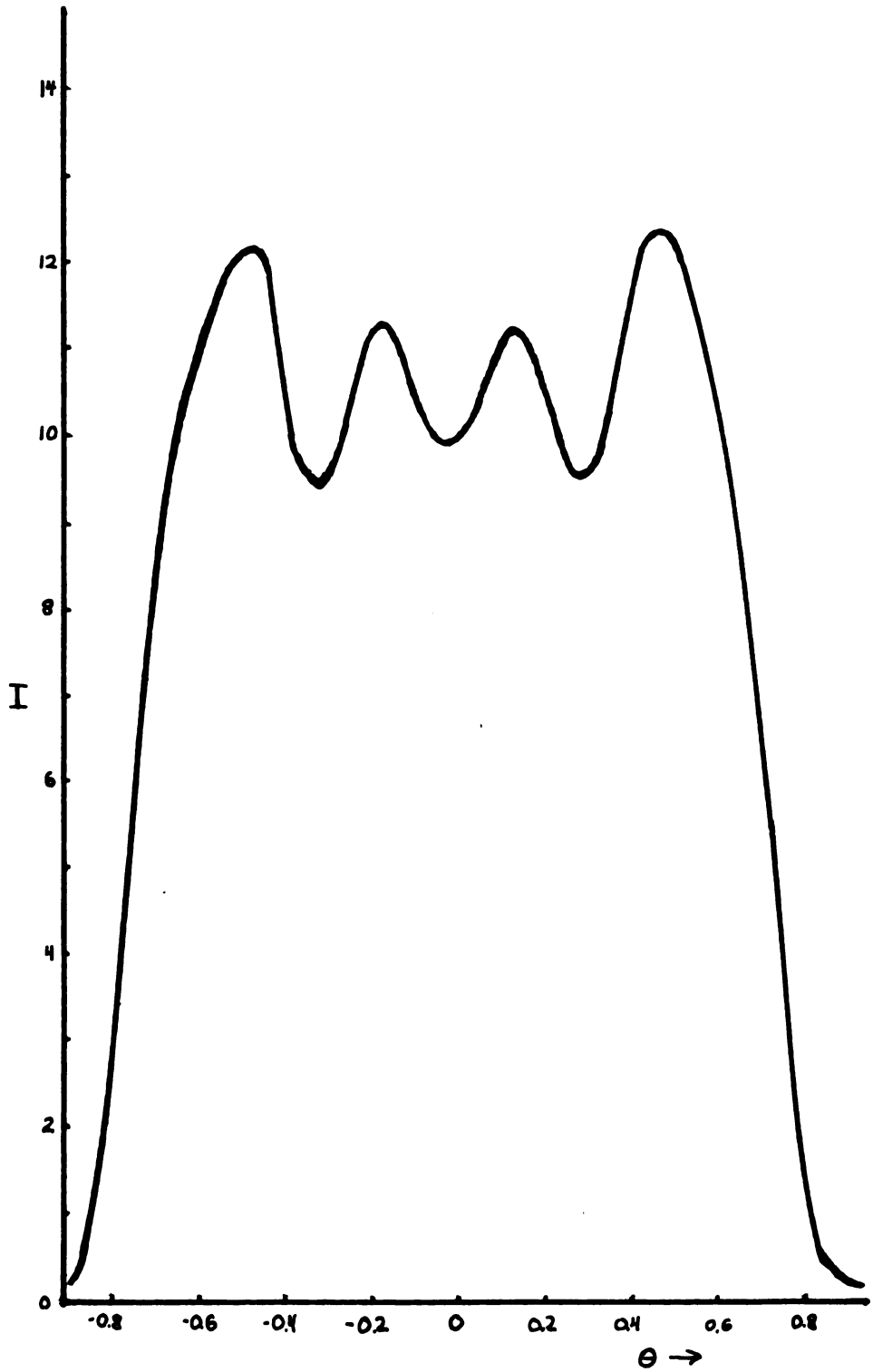

Fig. 32 Grating B. Coherent mode of illumination $\alpha = 8\lambda/Ns$.

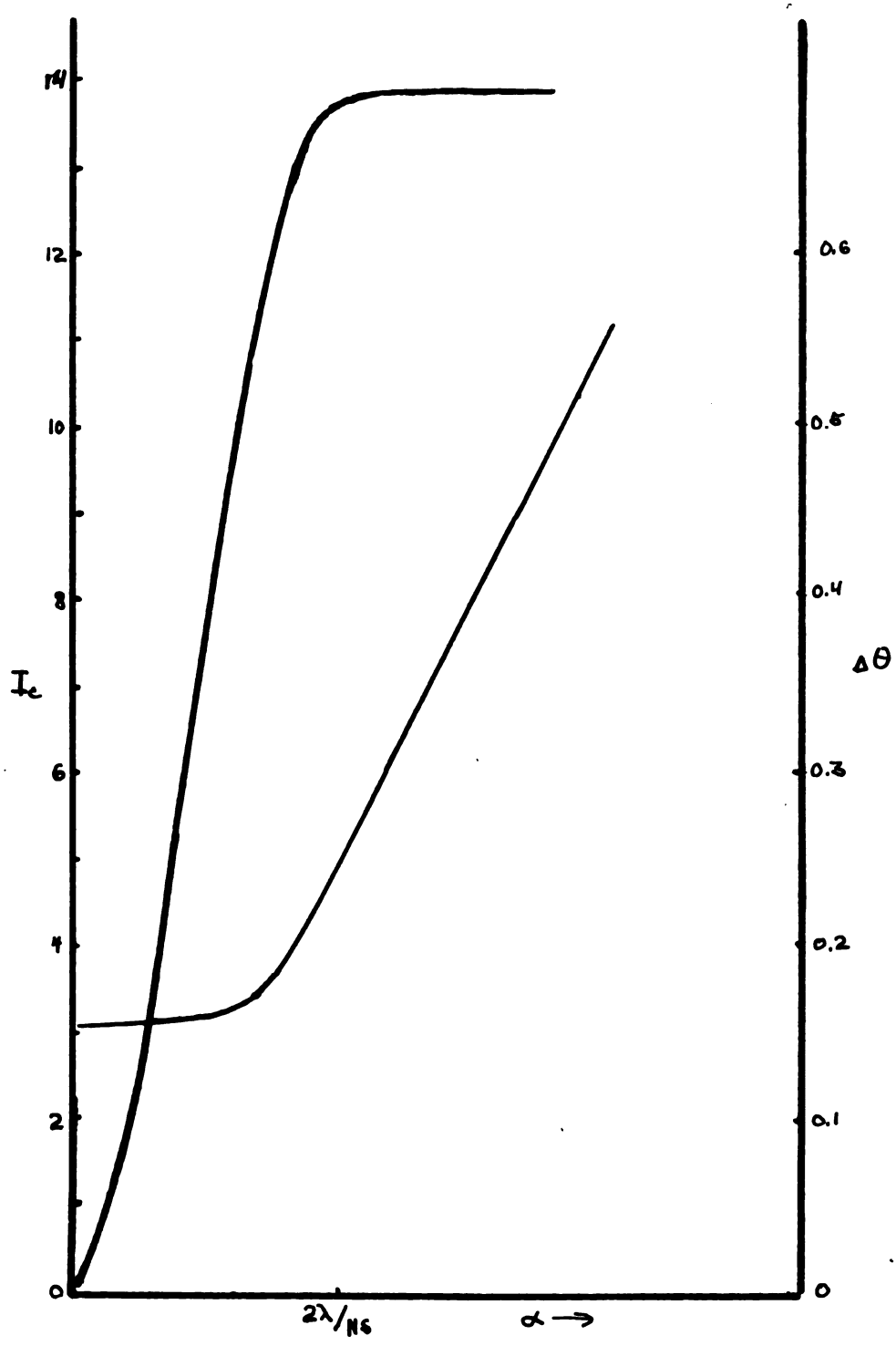

Fig. 33 Grating B illuminated in the broad source mode. Intensity in the center of the image and half-intensity breadth as functions of the angular source width.

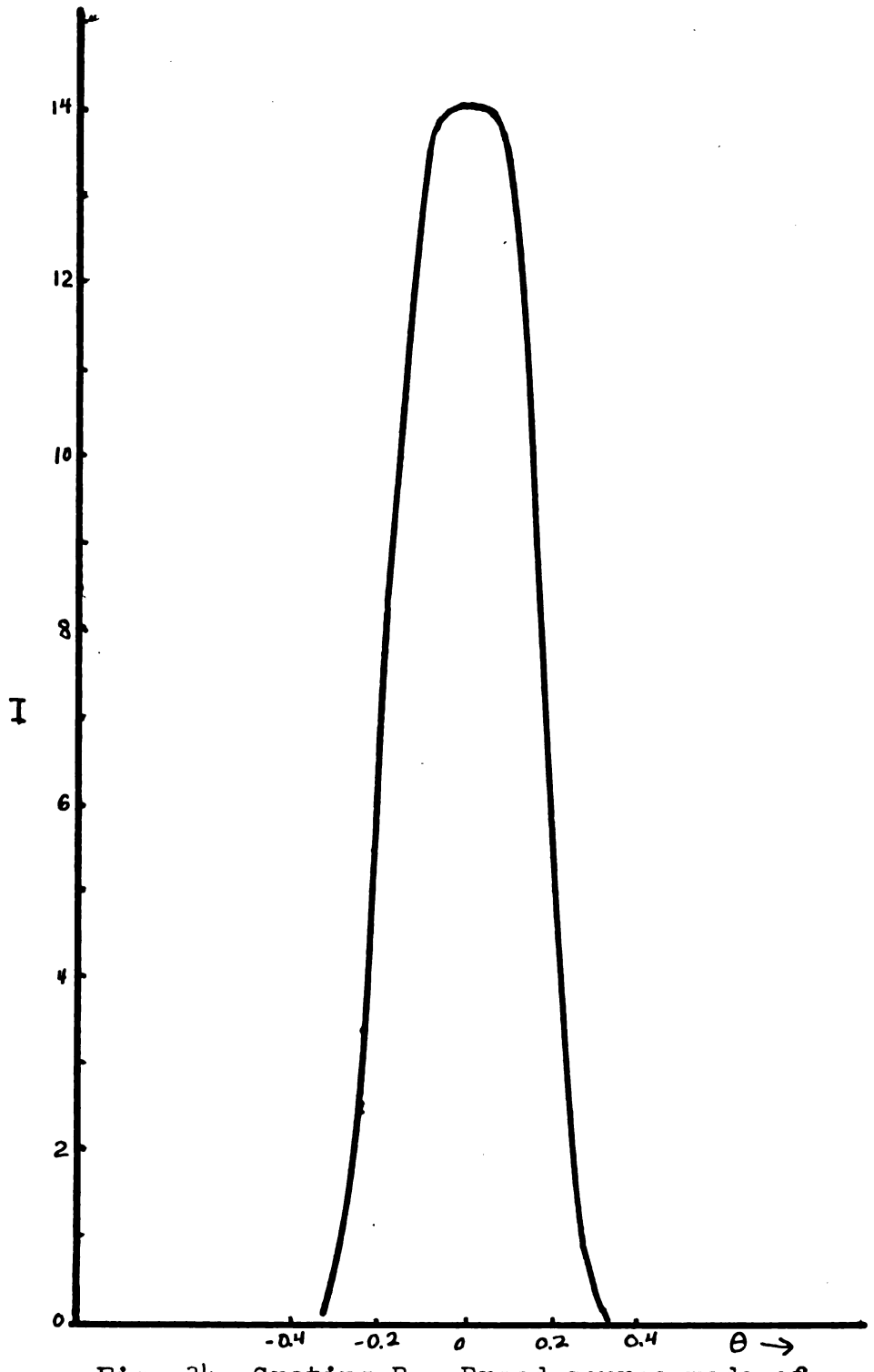

Fig. 34 Grating B. Broad source mode of illumination $\alpha \doteq 2.7^{1}/_{2}$Ns.

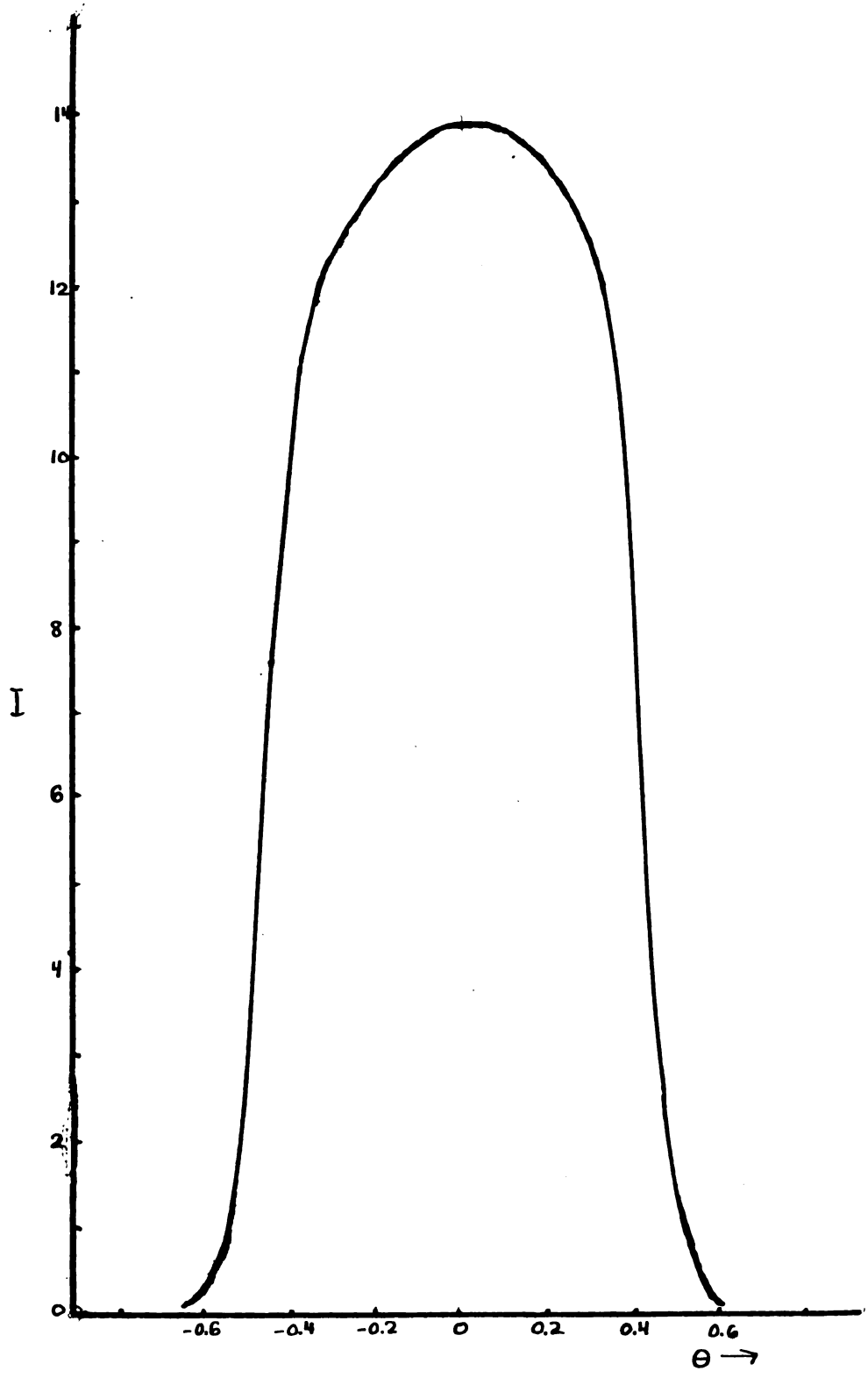

Fig. 35 Grating B. Broad source mode of illumination $\alpha = 5.4\,N/Ns$.

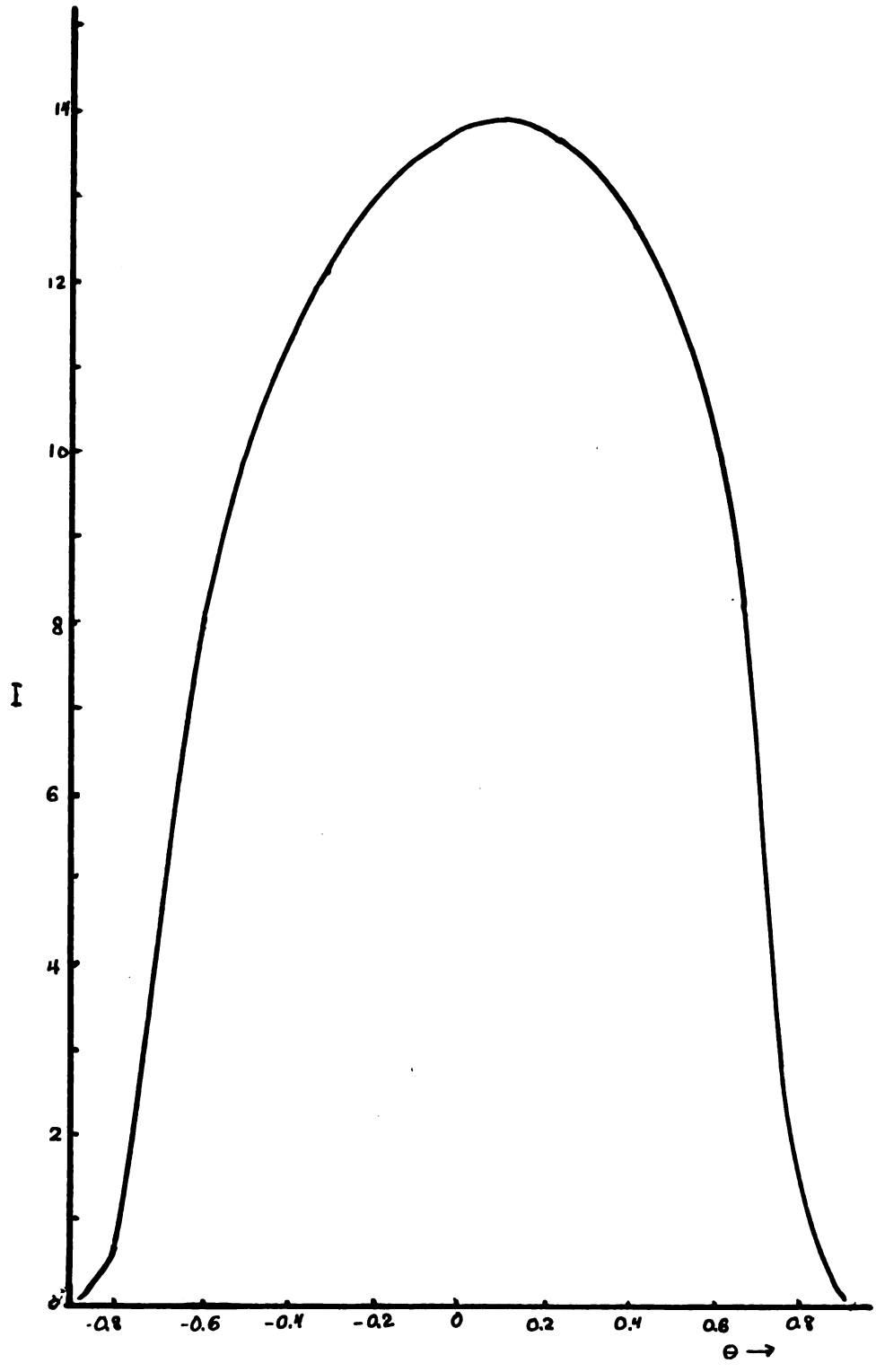

Fig. 36 Grating B. Broad source mode of illumination α = 8.1λNs.

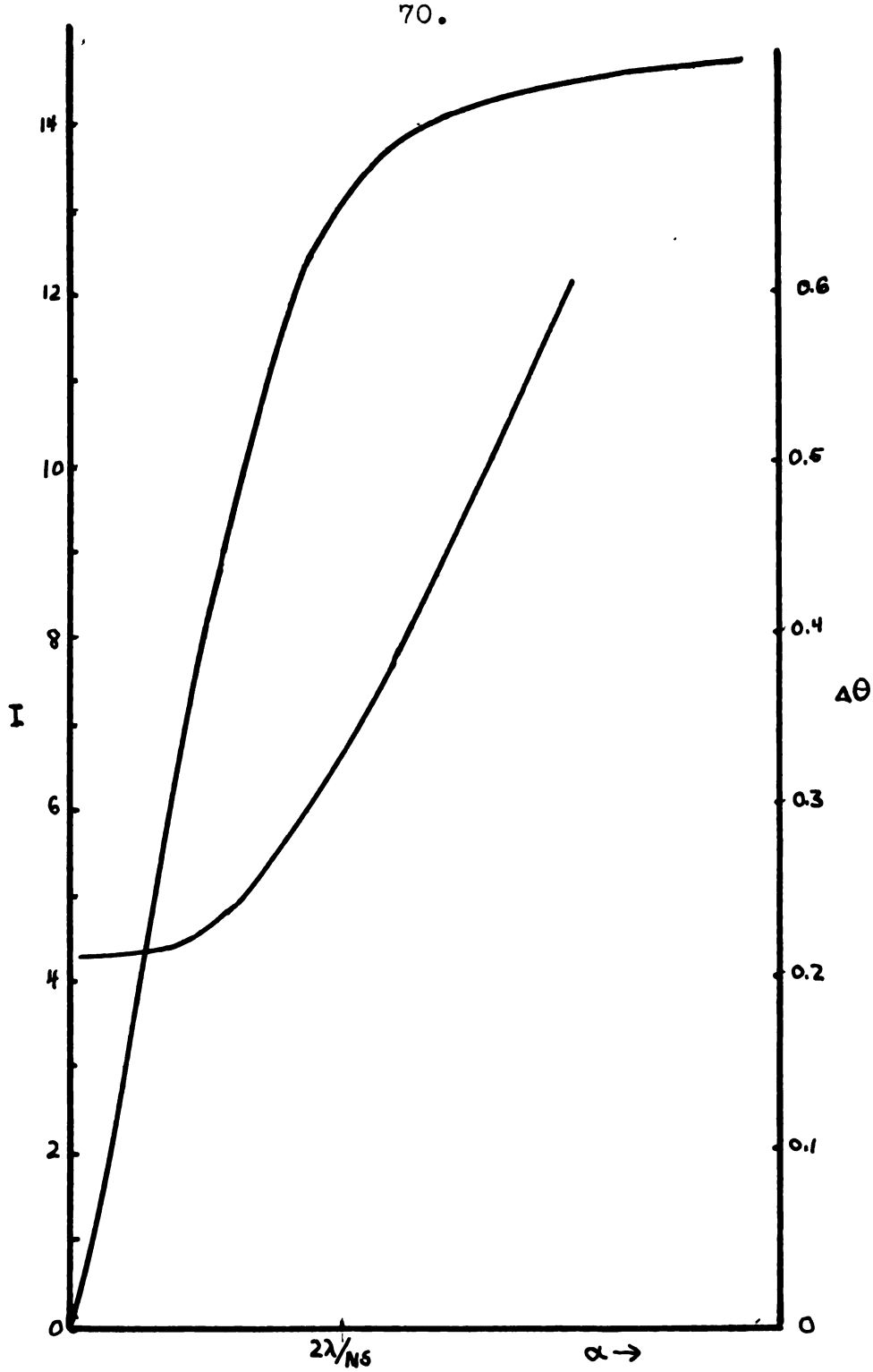

Fig. 37 Grating B illuminated in the lens mode. Intensity at the center of the image and the half-intensity breadth as functions of the angular source width.

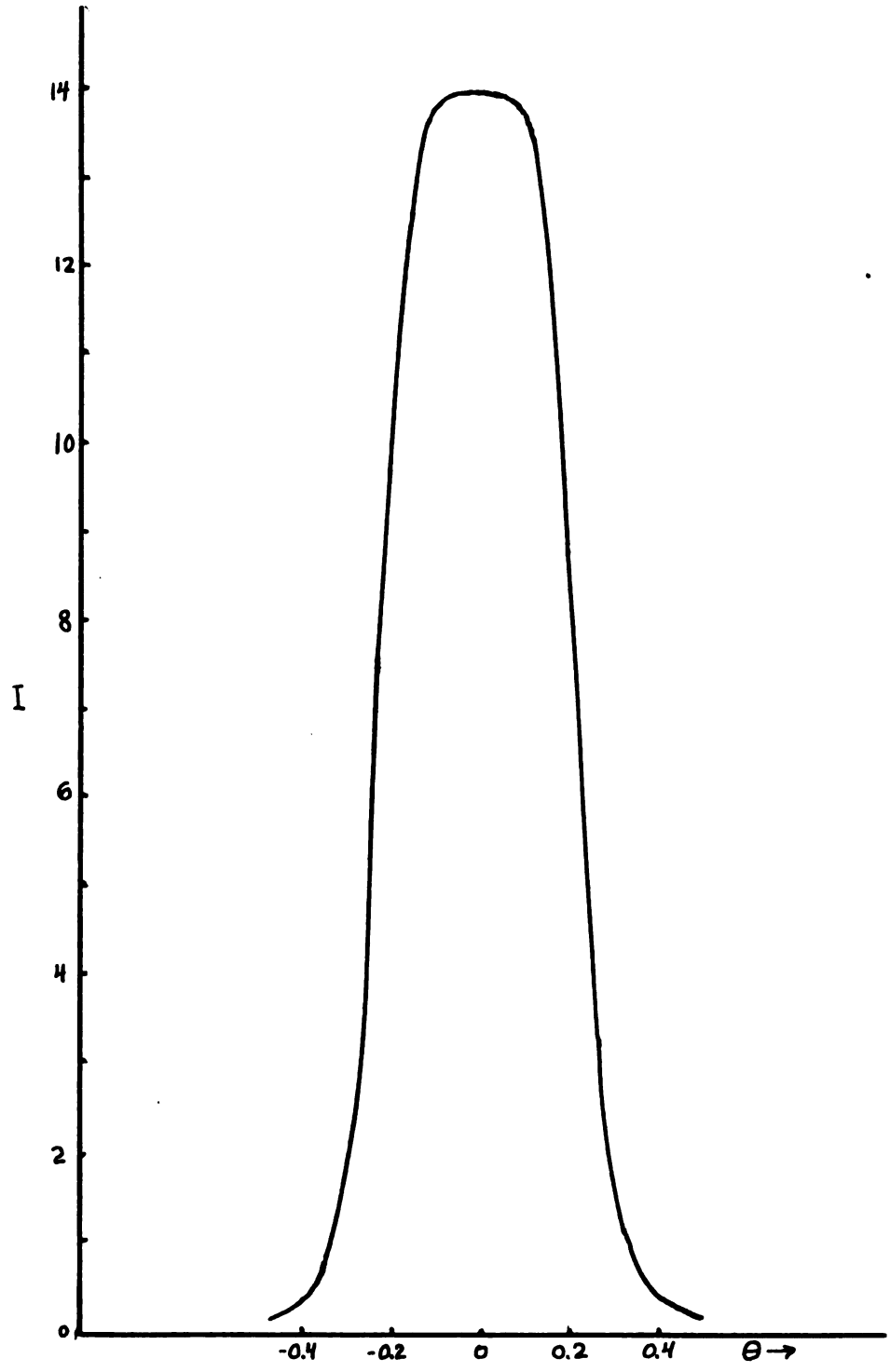

Fig. 38 Grating B. Lens mode of illumination $\alpha = 2.7\lambda/Ns$.

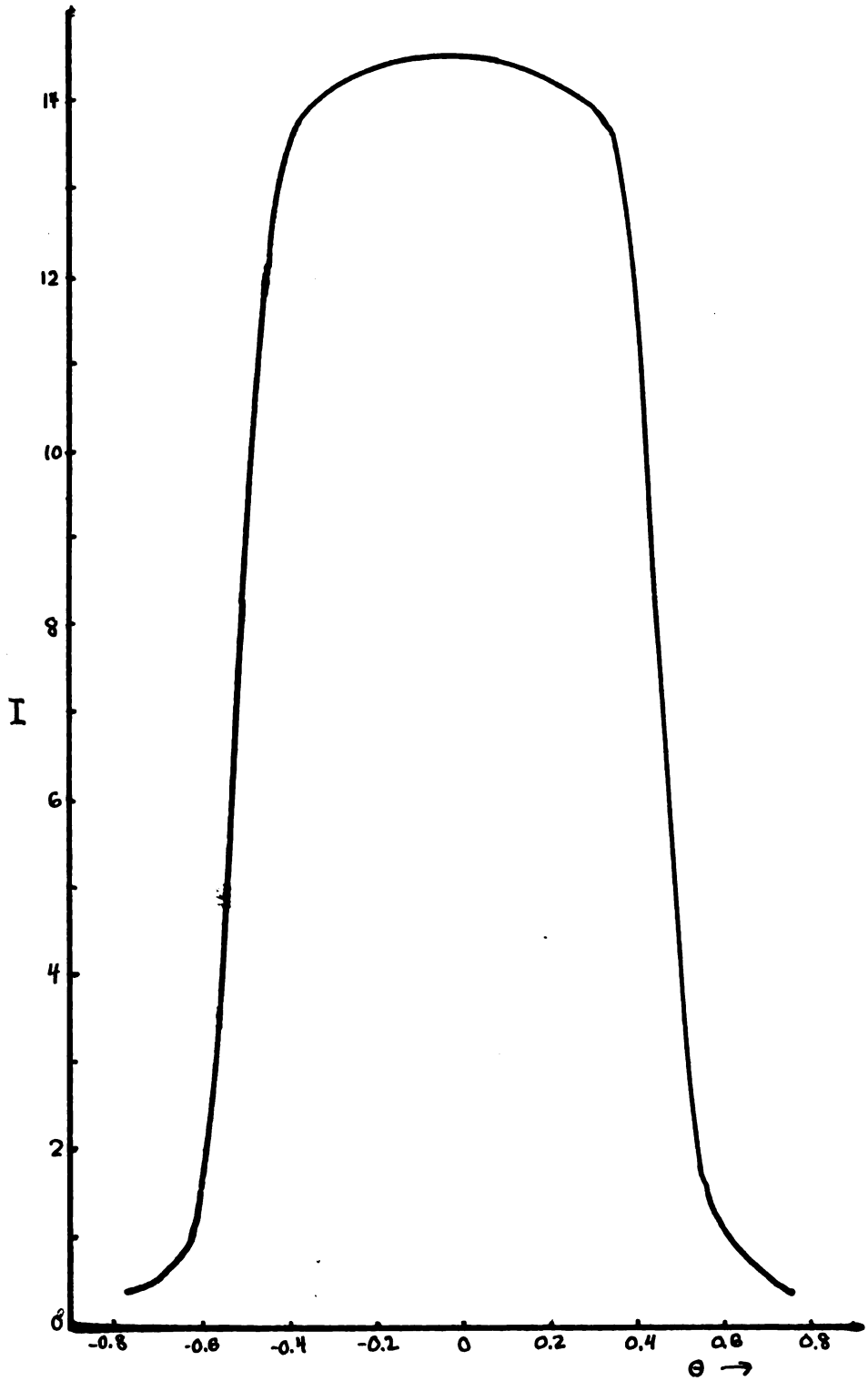

Fig. 39 Grating B. Lens mode of illumination $\alpha = 5.4\lambda/Ns$.

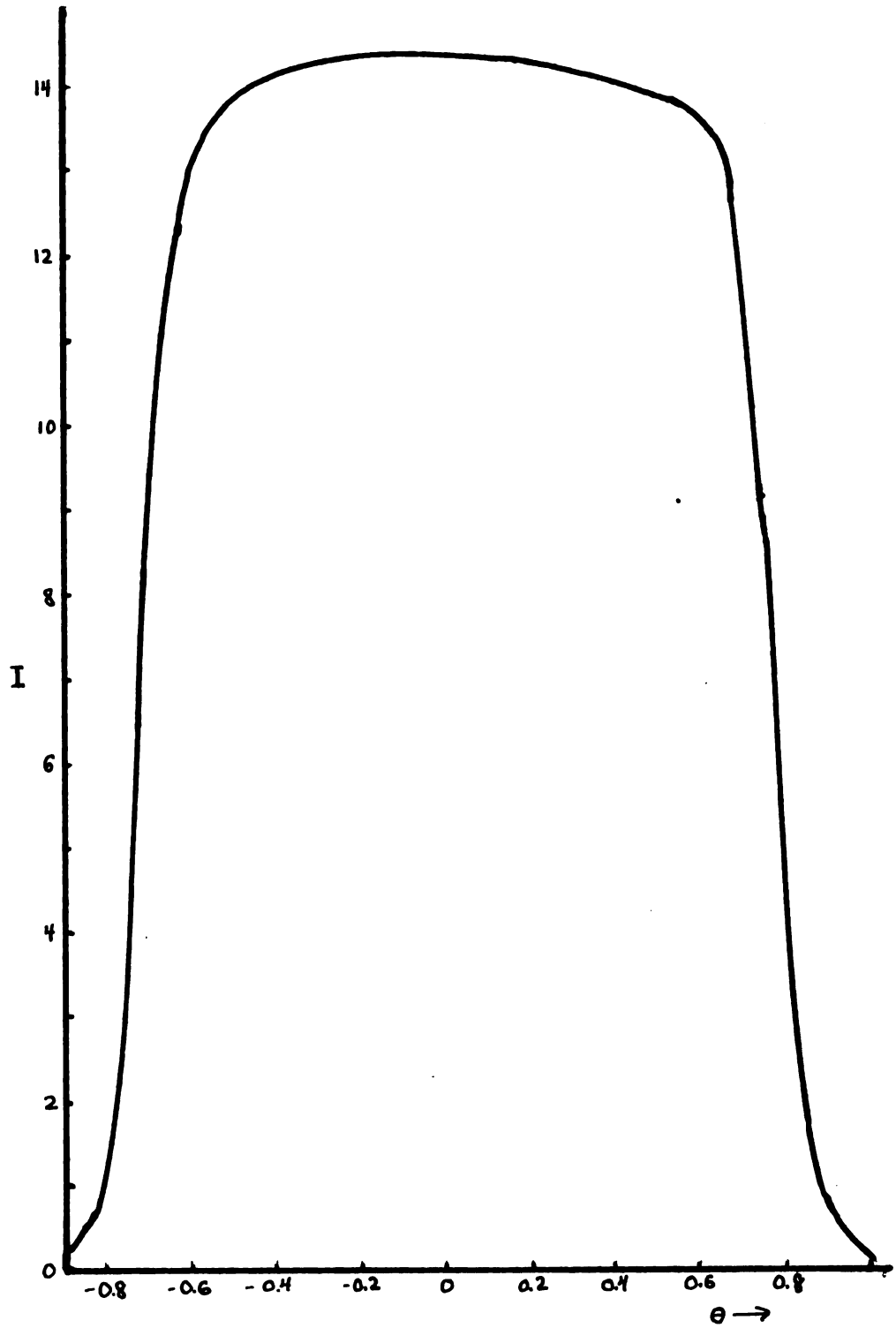

Fig. 40 Grating B. Lens mode of illumination $\alpha = 8.1\lambda/Ns$.

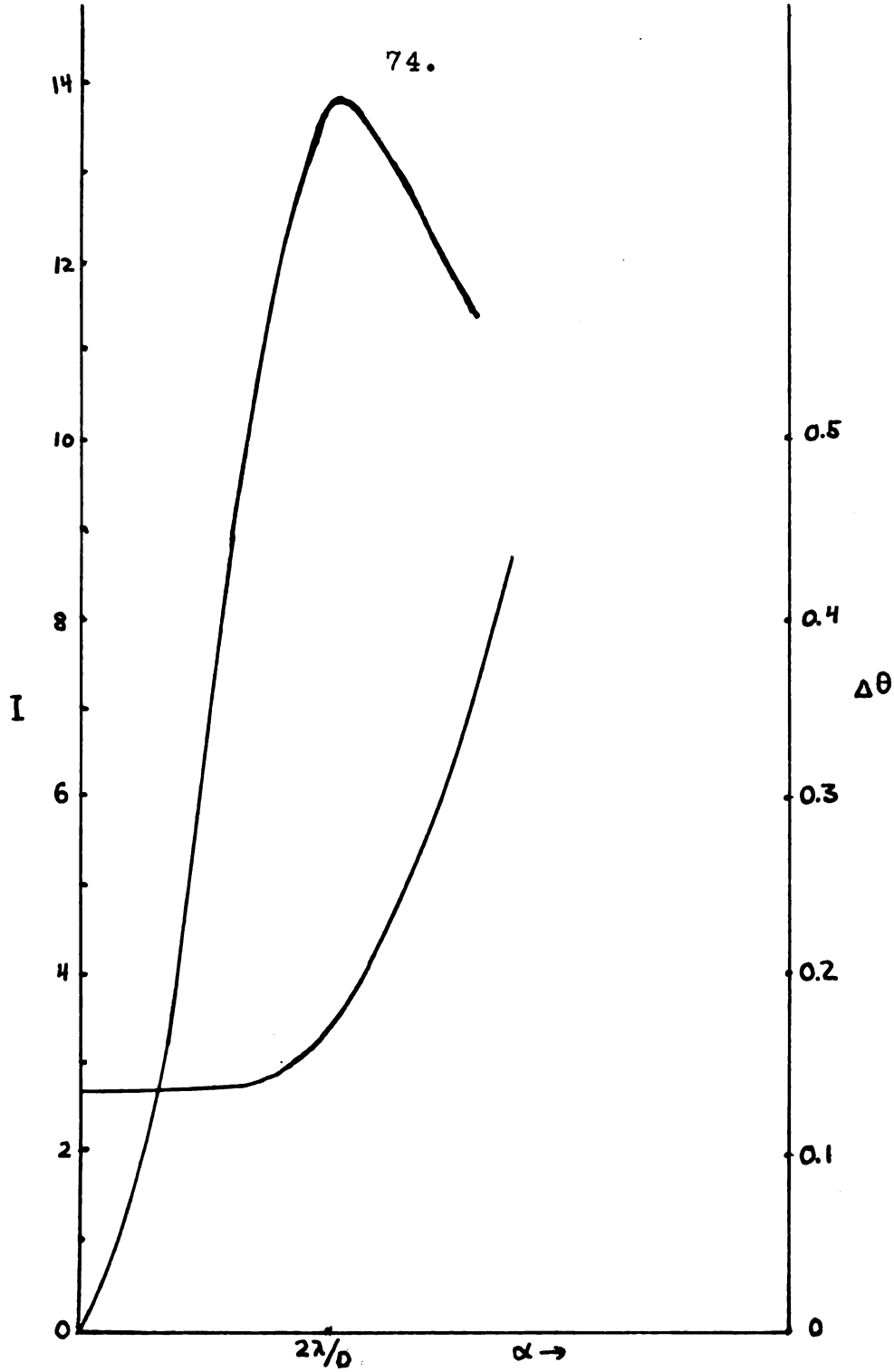

Fig. 41 Single aperture of 4.10 mm width illuminated in the coherent mode. Intensity at the center and half-intensity breadth as functions of the angular source width $\Delta\theta$ is expressed in units of 10^{-3} radians.

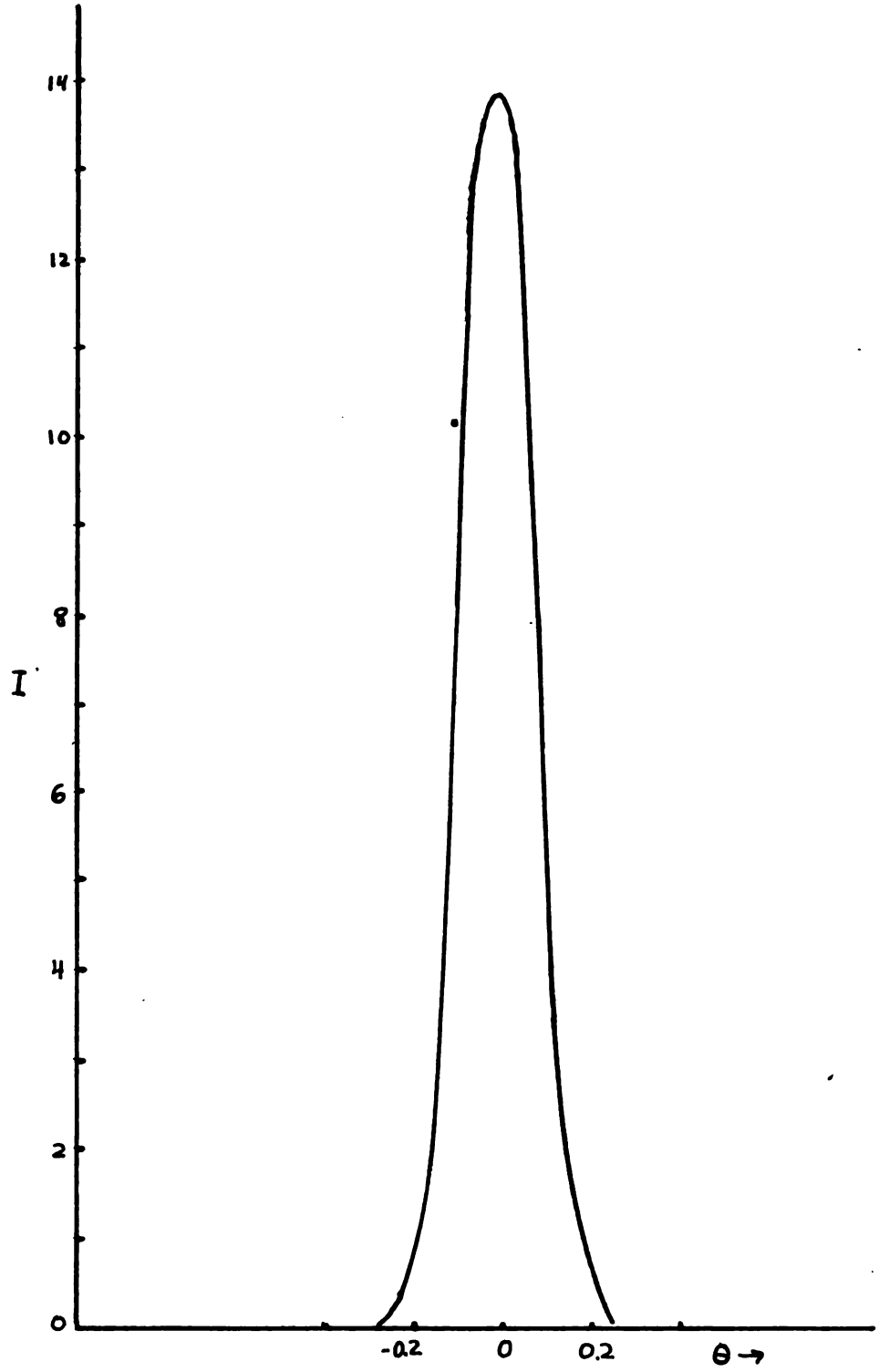

Fig. 42 Single aperture illuminated in the coherent mode. Source aperture of angular breadth $\alpha = 2\lambda/D$. θ is expressed in 10^{-3} radians.

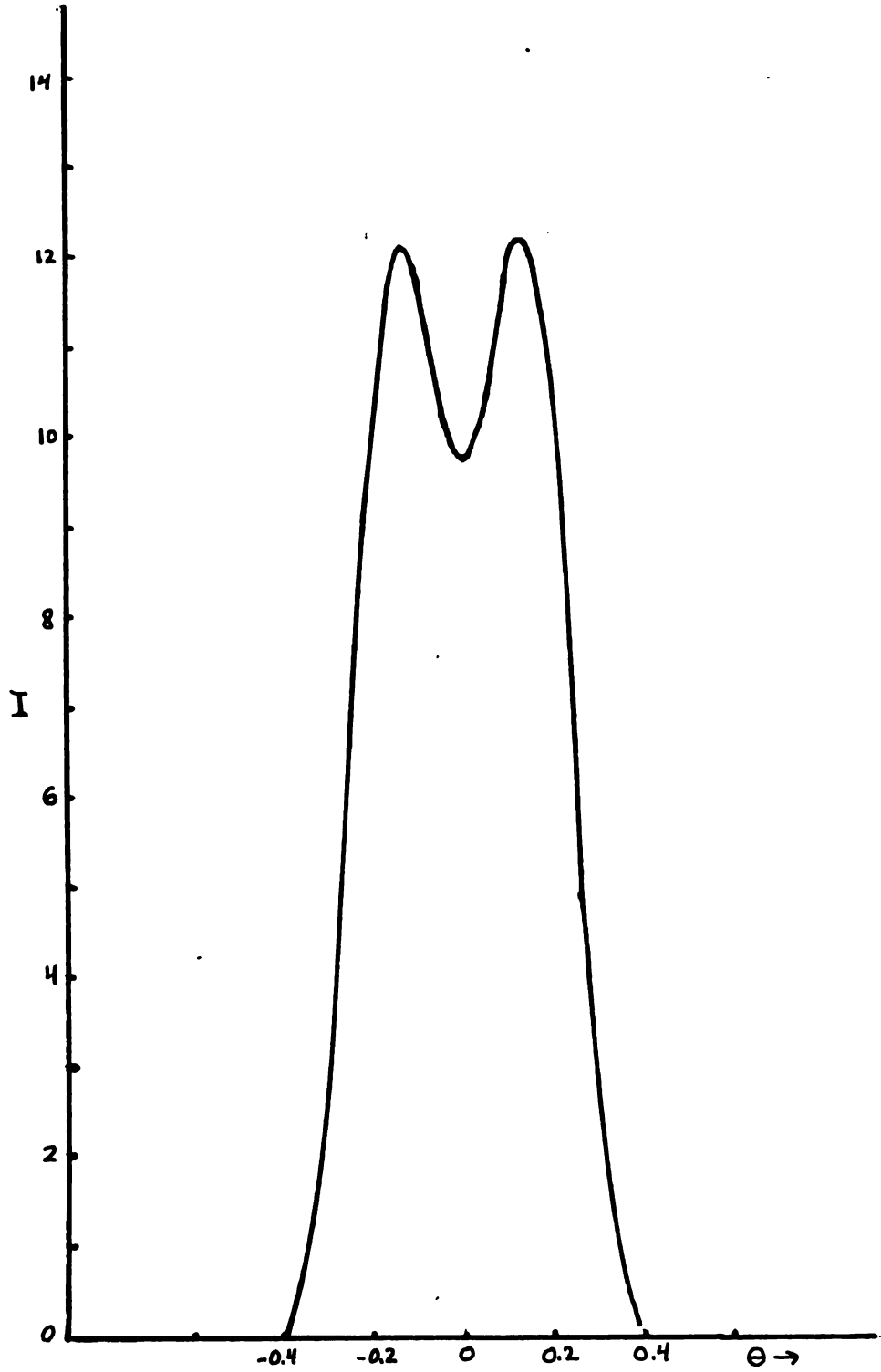

Fig. 43 Single aperture. Coherent mode of illumination $\alpha = 4\lambda/D$.

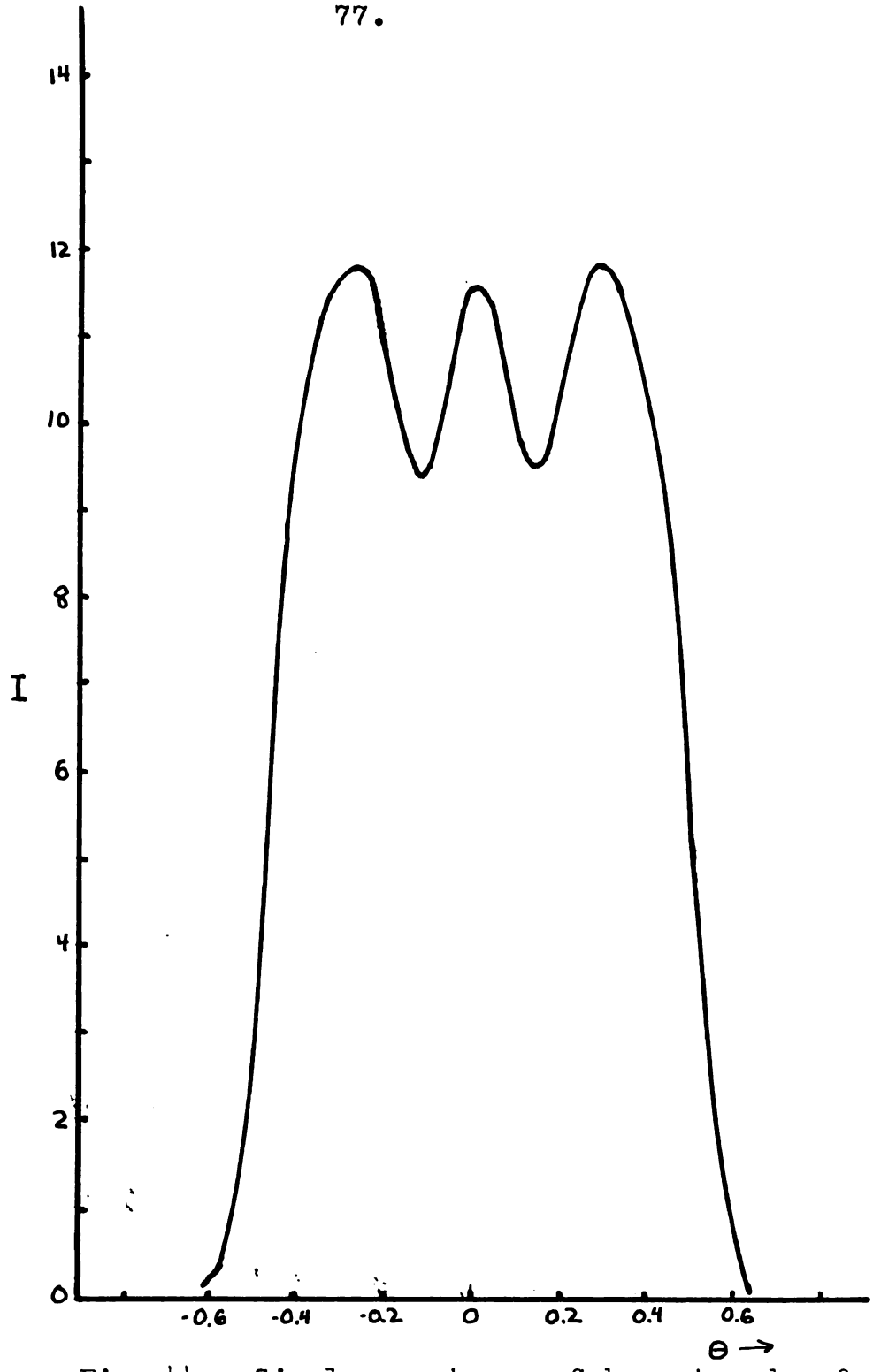

Fig. 44 Single aperture. Coherent mode of illumination $\alpha = 6\lambda/D$.

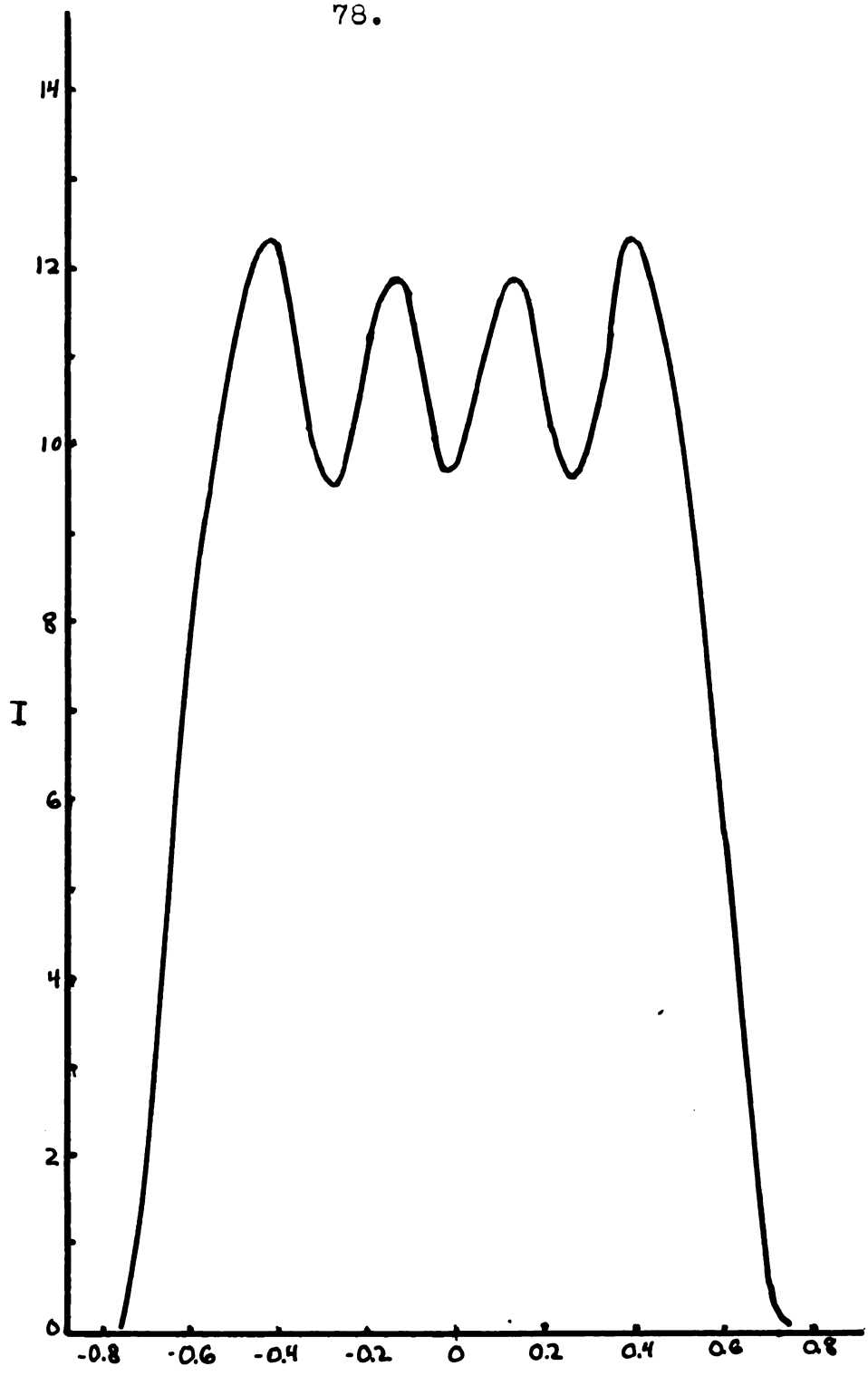

Fig. 45 Single aperture. Coherent mode of illumination $\alpha = 8\lambda/D$.

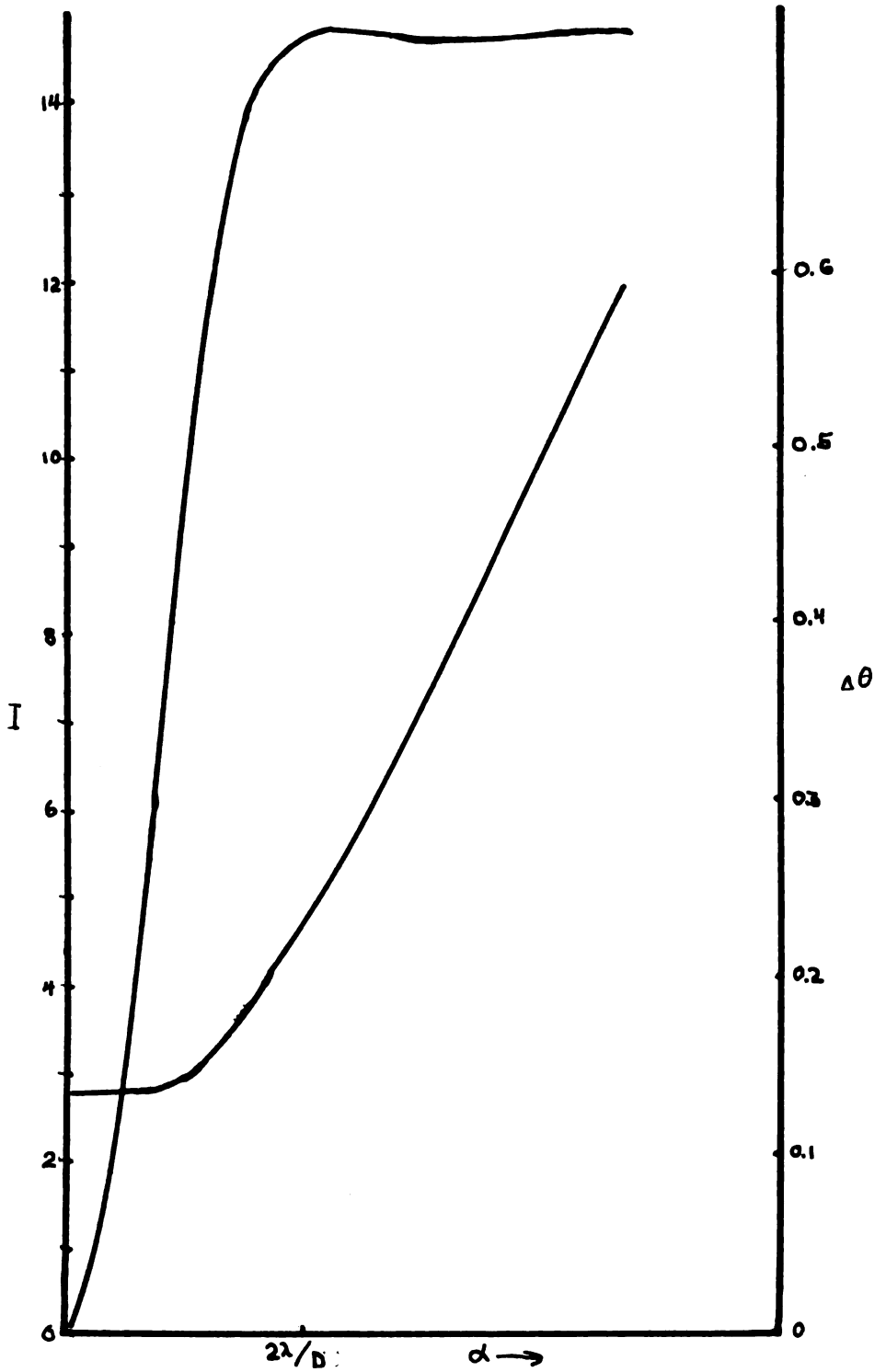

Fig. 46 Single aperture of 4.10 mm width illuminated in the broad so.mode. Intensity at the center and half-intensity breadth as functions of angular source width.

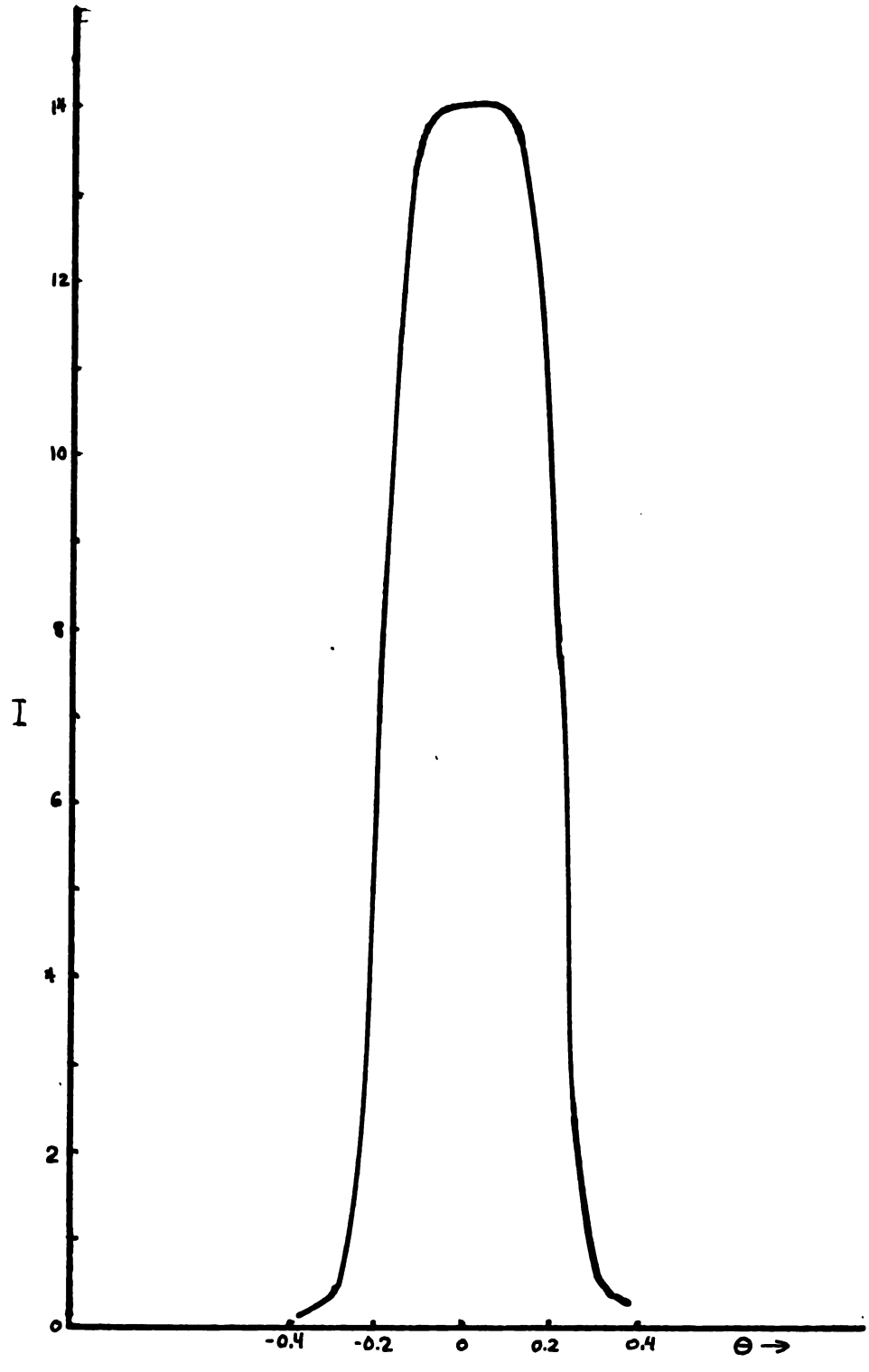

Fig. 47 Single aperture illuminated in the broad source mode. Source of angular breadth $\alpha = 2.8\lambda/D$. θ is expressed in 10^{-3} radians.

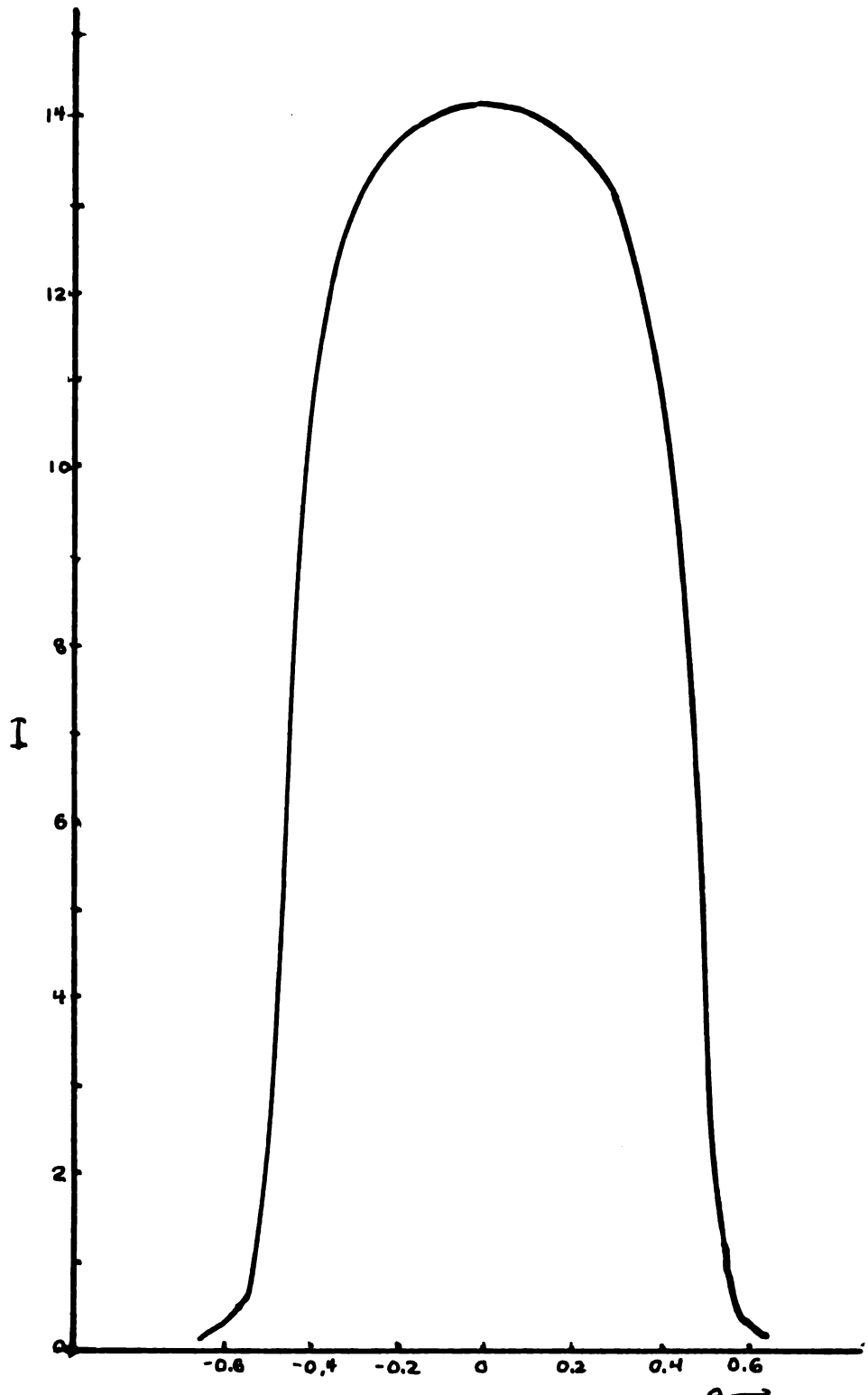

Fig. 48 Single aperture. Broad source mode of illumination $\alpha = 5.6\lambda/D$.

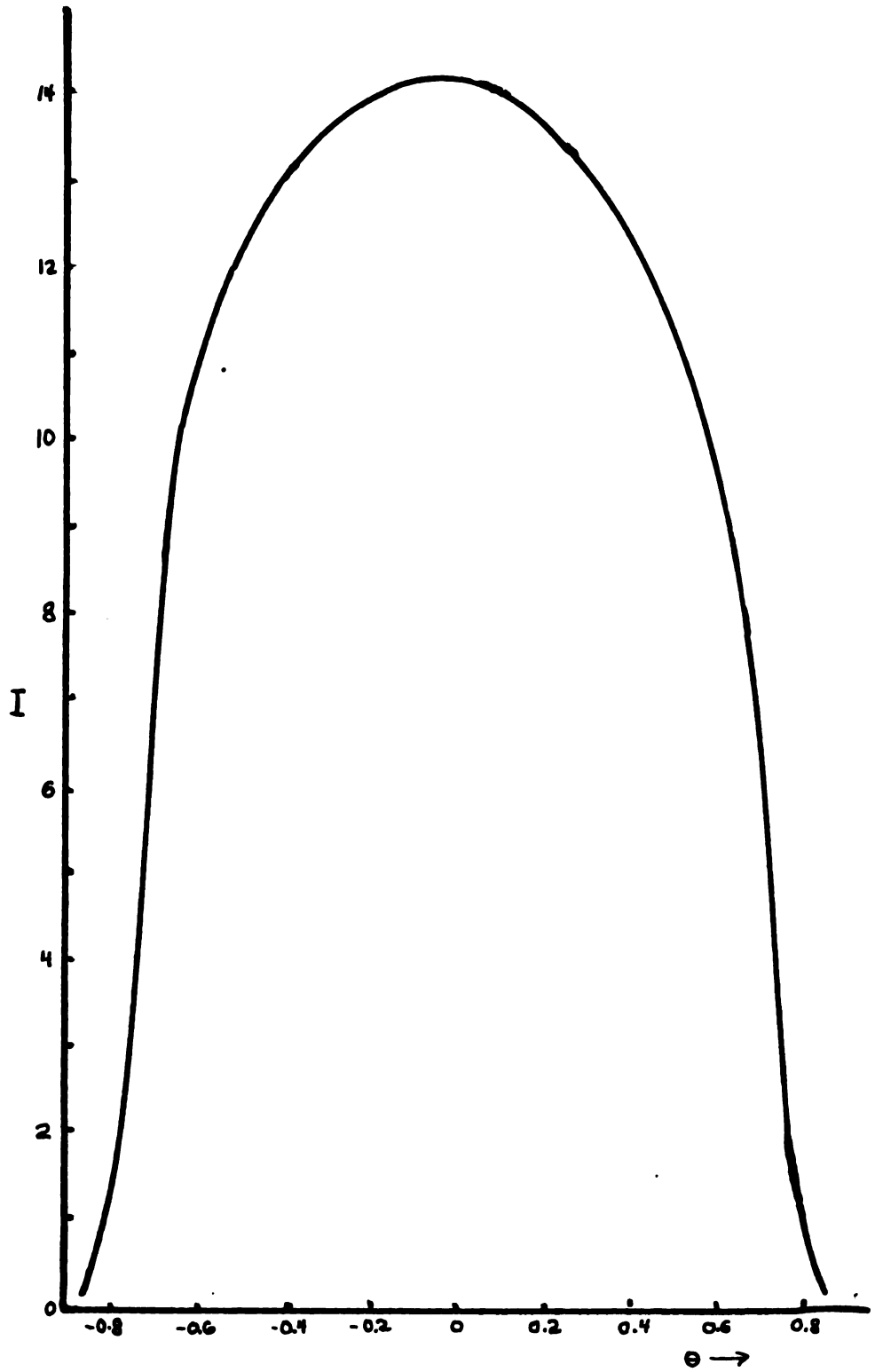

Fig. 49 Single aperture. Broad source mode of illumination $\alpha = 8.4\lambda/D$.

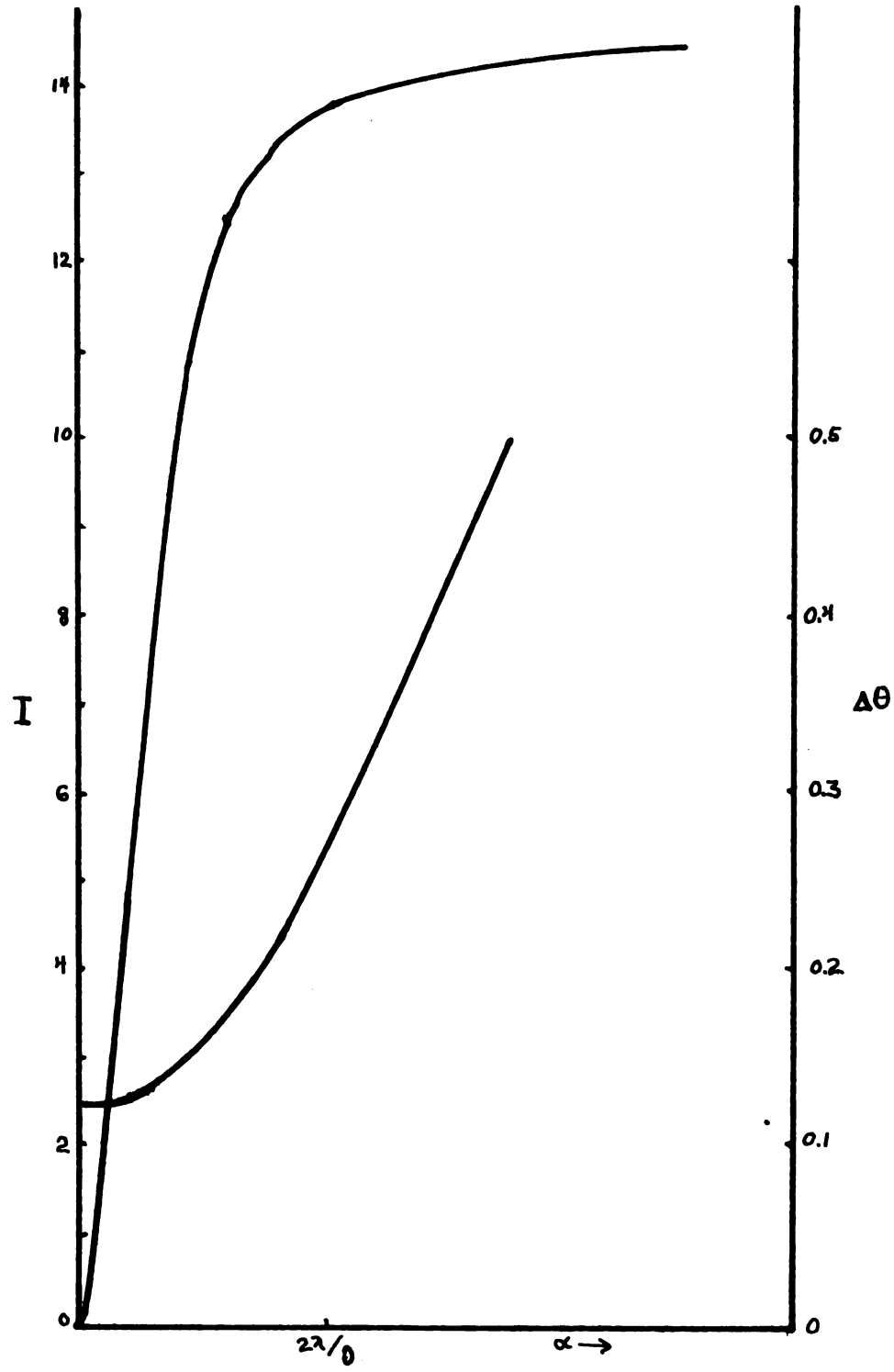

Fig. 50 Single aperture illuminated in the lens mode. Intensity at the center and half-intensity breadth as functions of angular source breadth.

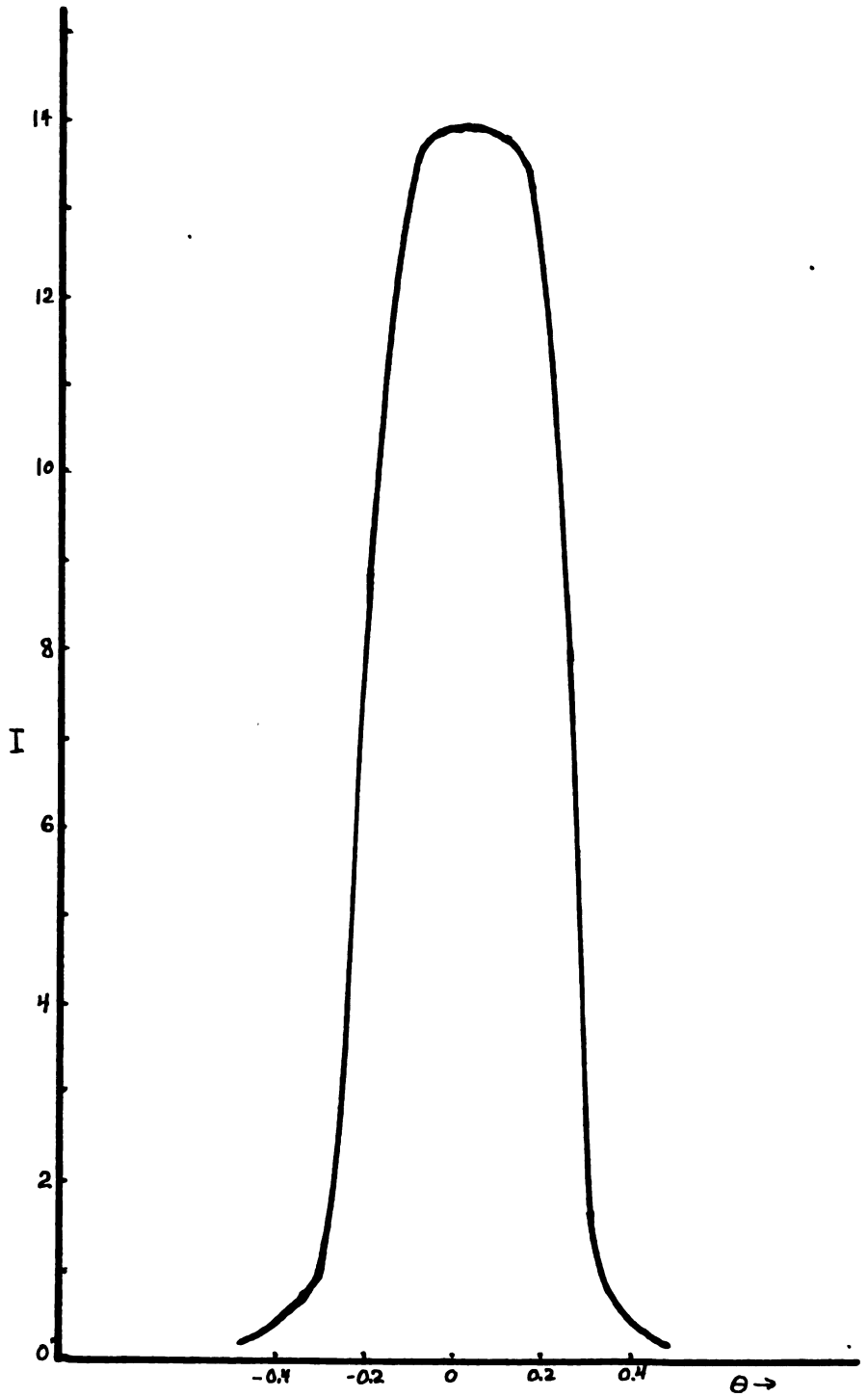

Fig. 51 Single aperture illuminated in the lens mode. Source aperture of angular breadth $\alpha = 2.8\lambda/D$. θ is expressed in 10^{-3} radians.

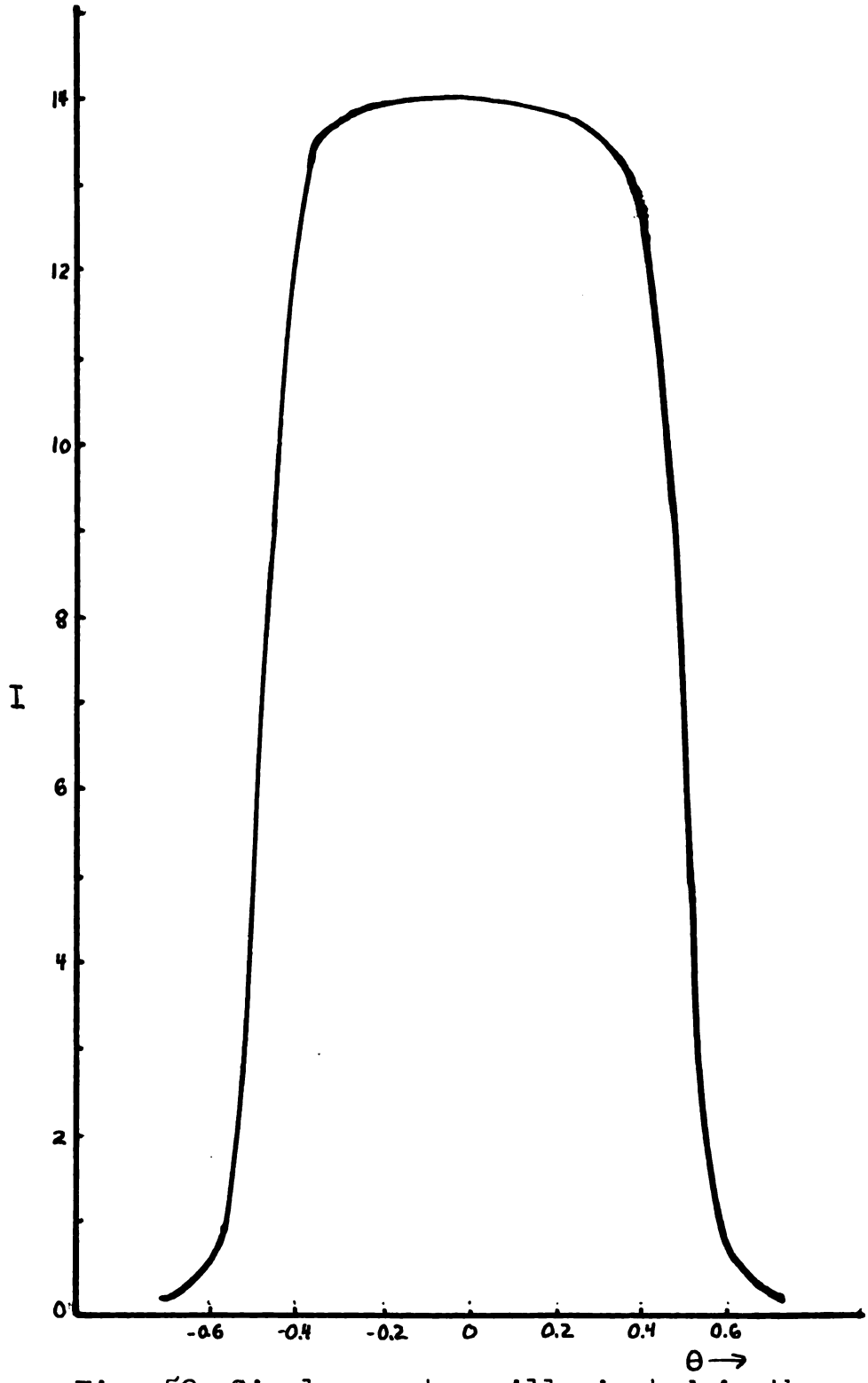

Fig. 52 Single aperture illuminated in the lens mode $\alpha = 5.6\lambda/D$.

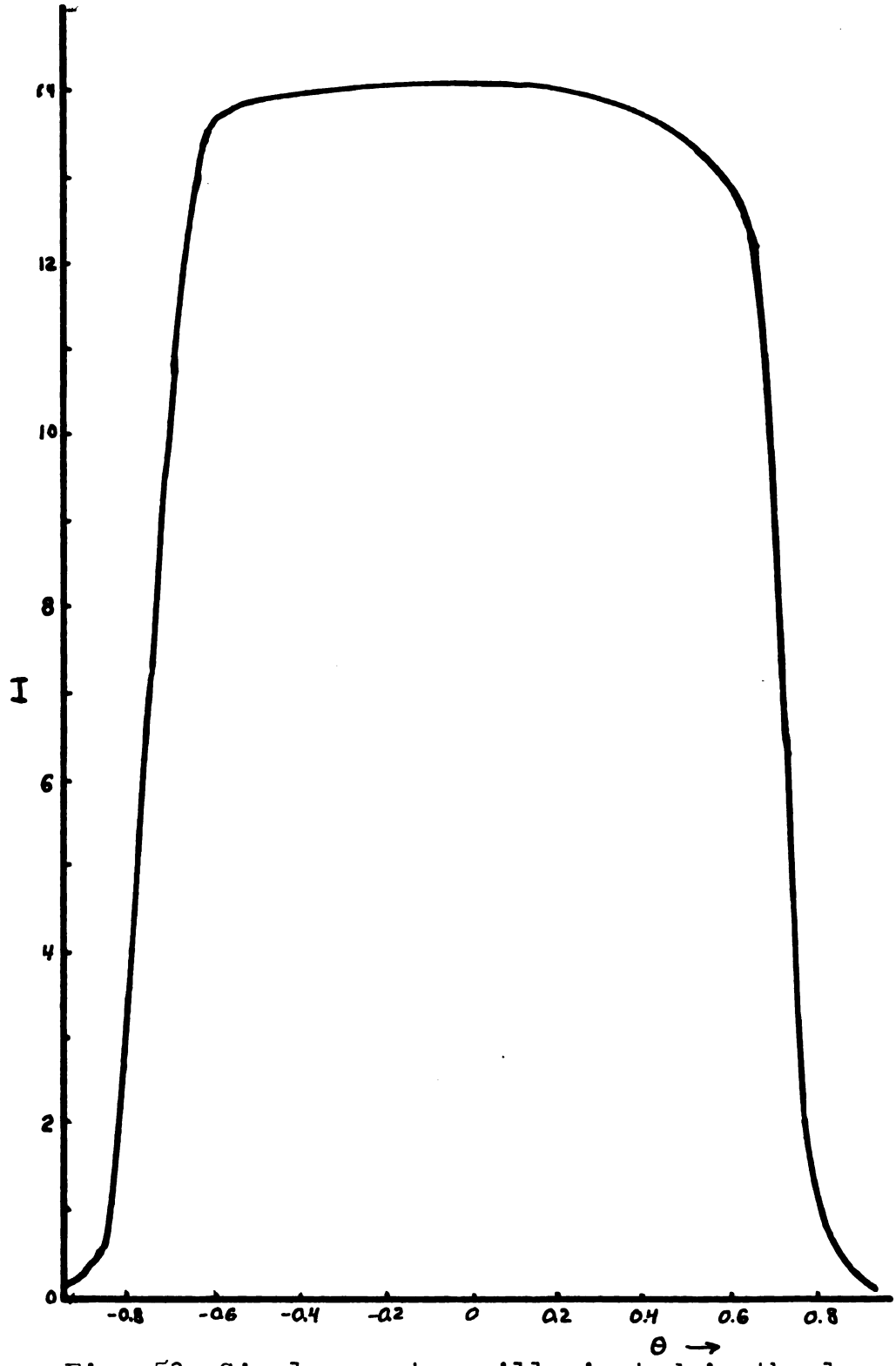

Fig. 53 Single aperture illuminated in the lens mode $\alpha = 8.4\lambda/D$.

V SUMMARY

Starting with the basic relations for a diffraction grating illuminated by a line source under Fraunhofer conditions the theory was extended to include a source of finite breadth. Two different modes of illumination of this finite source were assumed, the radiation in the plane of the source being either completely coherent or completely noncoherent. The results for a diffraction grating of many apertures were extremely cumbersome. But with the limiting assumptions of a large number of apertures and small incidence angles the results were simplified to give expressions for the intensity distributions in the images as functions of the angular breadth of the source aperture, the dimensions of the diffraction grating, and the wavelength of the incident radiation.

The results were compared with the relations which Van Cittert (1) found for single diffracting apertures illuminated in the modes prescribed for the grating. Within the limitations of the theory no difference was found to exist. It is believed, however, on the basis of a previous work (10) that slight differences exist for a grating with a small number of apertures.

Experimental verification of the theory was obtained by illuminating the source aperture in ways which more or less approximate the assumed conditions. The experimental images found were compared with the images expected from the calculation. It was found that in most details the experimental and theoretical results were in agreement. Differences were ascribed to a lack of complete coherence or noncoherence in the source aperture, to the narrow beam of radiation present in the coherent mode of illumination, and to the fact that the source aperture contributes to the system in some ways as a diffracting element.

The images formed with the diffraction grating are compared experimentally with images formed with a single diffracting aperture as a means of checking the identity of the two theoretical results. No observable difference was found. These latter observations also serve as a check on the theory of the single aperture.

Two different experimental arrangements have been suggested (5) as approximating the noncoherent mode of illumination, see Figs. (14) and (15). It was found that the lens mode of illumination more nearly fits the results of the noncoherent theory.

VI LIST OF REFERENCES

(1) Van Cittert, P. H., Zum Einfluss der Spaltbreite auf die Intensitatsverteilung in Spektrallinien. Z. Physik, 65, 547-563, (1930)

(2) Schuster, A., Optics of the Spectroscope. Astrophys., 21, 197-210, (1905)

(3) Wadsworth, F.L.O. On the Resolving Power of Telescopes and Spectroscopes for Lines of Finite Width. Phil. Mag. 43, S5, 317-343, (1897)

(4) Godfrey, G. H. Diffraction of Light from Sources of Finite Dimensions. Austral. Jour. Sci. Res. A, 1, 1-17, (1948)

(5) Stockbarger, D. C. and L. Burns, Line Shape as a Function of Spectrograph Slit Irradiation J. Opt. Soc. Am. 23, 379-384, (1933)

(6) Michelson, A. A. On the Application of Interference Methods to Astronomical Measurements. Phil. Mag. 30, 1-21, (1890)

(7) Munster, C. Unahnliche Abbildung und Ausmessung von Nichtselbstleuchtern Ein Beitrag zum Äquivalenzprinzip Ann. Physik, 15, 619-644, (1932)

(8) Michelson, A. A. and F. G. Pease, Measurement of the Diameter of -Orionis with the Interferometer Astrophys. 53, 249-259, (1921)

(9) Gerhardt, U. Application of the Michelson Stellar Interferometer to the Measurement of Small Particles. Zeits. f. Phys. 35, 697-717, (1926)

(10) Smith, A. E. and C. D. Hause Fraunhofer Multiple Slit Diffraction Patterns with Finite Sources. J. Opt. Soc. Am. 42, 426-430, (1952)

(11) Takeyama, H., T. Kitahara, and T. Matubayasi. On the Mathematical Treatment of the Effect of the Width of the Slit on Fraunhofer's Diffraction Phenomenon (Part II). J. Sci. Hirosima Univ. (S.A.) 15, 139-146, (1951)

(12) Born, M. Optik Julius Springer; Berlin (1933) (Lithoprint by Edwards Bros., Ann Arbor) p. 163

(13) Bôcher, M. Introduction to the Theory of Fourier's Series. Ann. of Math. 7 (S.2) 81-147, (1905-'06)

(14) Carslaw, H. S. Introduction to the Theory of Fourier's Series and Integrals ed. 3, Dover Pub., New York, 289-310, (1930)

(15) Hopkins, H. H. On the Diffraction Theory of Optical Images Proc. Roy. Soc. A 217, 408-432, (1953)

APPENDIX

The difficulties which were experienced in the case of coherent illumination were mentioned briefly under the description of experimental results. In order to show the limitations of the theory it would appear advisable to describe these difficulties in more detail with graphical illustration. Possible explanations for the causes of the characteristics will be offered.

In the coherent case it was observed that when the total expanse of the diffracting element used was smaller than the width of the source aperture that some anomalies were present in the resulting image. In particular, it was found that the structure of the image lags behind the predicted structure, that is, the amount of structure in terms of numbers of observed local maxima was not as great as was predicted by the theory. In addition there appeared for diffracting elements of small expanse and relatively wide source apertures a small peak on each side of the image which moved out from the image and became more distinct as the source aperture was opened.

In the first situation it was found that the maximum visibility of the structure predicted in the pattern always appeared at source breadths slightly

greater than those expected. The difference between predicted and observed source widths was completely negligible for small source apertures but became the dominant factor as the source aperture breadth became broader than the total expanse of the diffracting element. It was further found that if the slit used as the source aperture was completely removed, the slit immediately in front of the lamp now becoming the source, that the pattern was only slightly influenced. In no case could more structure be found in the presence of the source aperture than was found with the source aperture removed. This would indicate that when the source aperture was wider than the diffracting element the aperture had little influence upon the resulting pattern. The image observed was a Fresnal pattern with the source at the lamp acting as the source for the pattern. In intermediate situations it would appear reasonable to expect the pattern to be a mixture of the two types. This problem is illustrated in Figs. (54) and (55). Fig. (54) is a diffraction grating of aperture 3.5 mm illuminated by a source of angular breadth =14 /Ns, which would predict a pattern of seven maxima on the basis of the coherent theory. It is seen in Fig. (55) that there are only six maxima in the pattern with

source aperture removed. When the source aperture was widened beyond its width in Fig. (54) the six peaks appeared, but not clearly, and they are therefore not pictured.

In the second situation where the diffracting element was quite narrow at the start the pattern with the source slit removed as in Fig. (59) only showed two definite maxima. The number of maxima and the general outline of the image depend upon the dimensions of the system and the diffracting element.

The peaks which appear at each side in Figs. (56) and (57) but which are not present in Fig. (59) can be explained in terms of the source element which can be said to exist at each edge of the aperture. The peaks appear at the positions predicted by the Fraunhofer theory, which assumes that they are images of line sources located at the aperture edges. These line elements are noncoherent with respect to the other elements of the aperture plane. This structure is absent when the source aperture is removed.

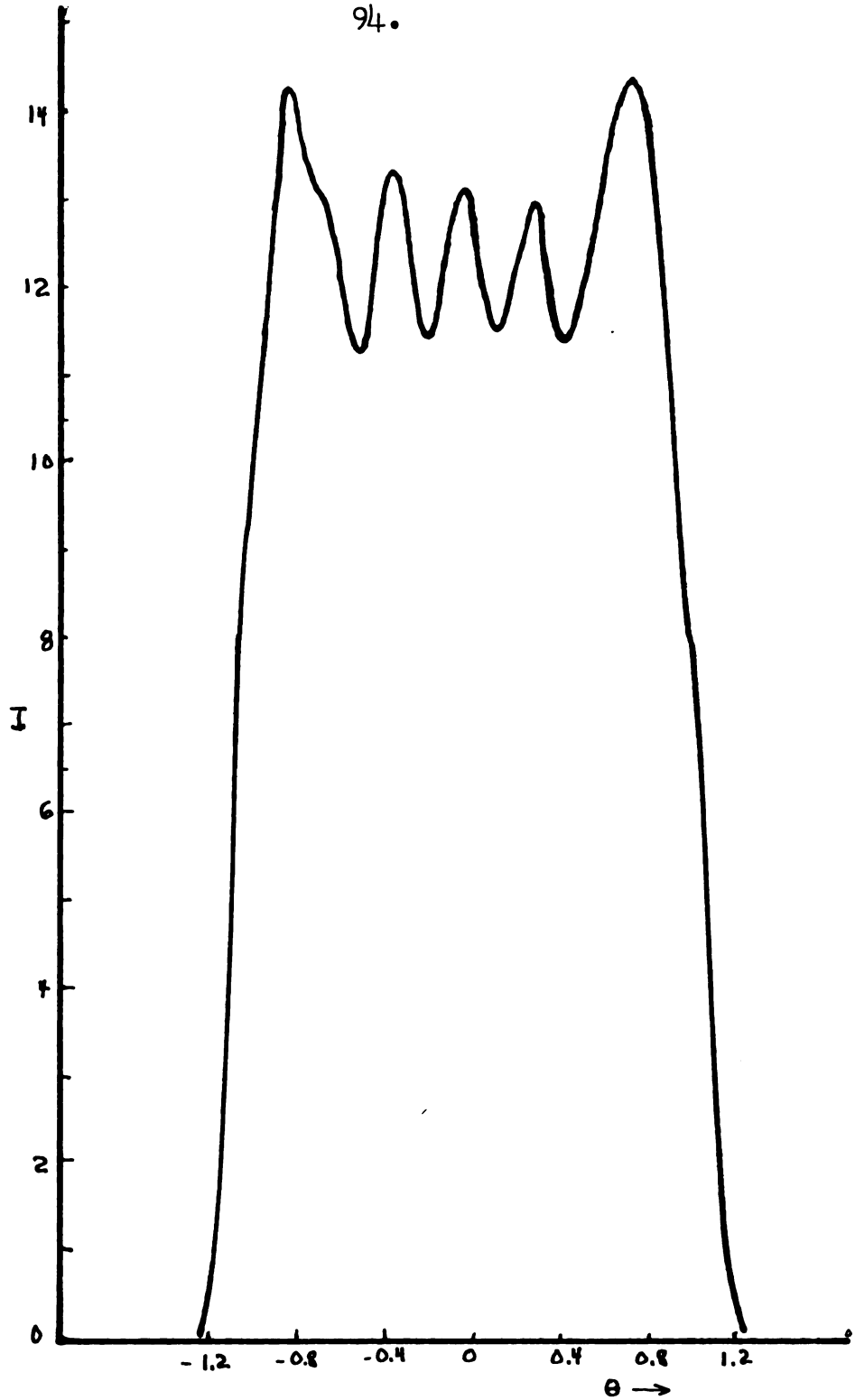

Fig. 54 Grating B illuminated in the coherent mode $\alpha = 14\lambda/Ns$.

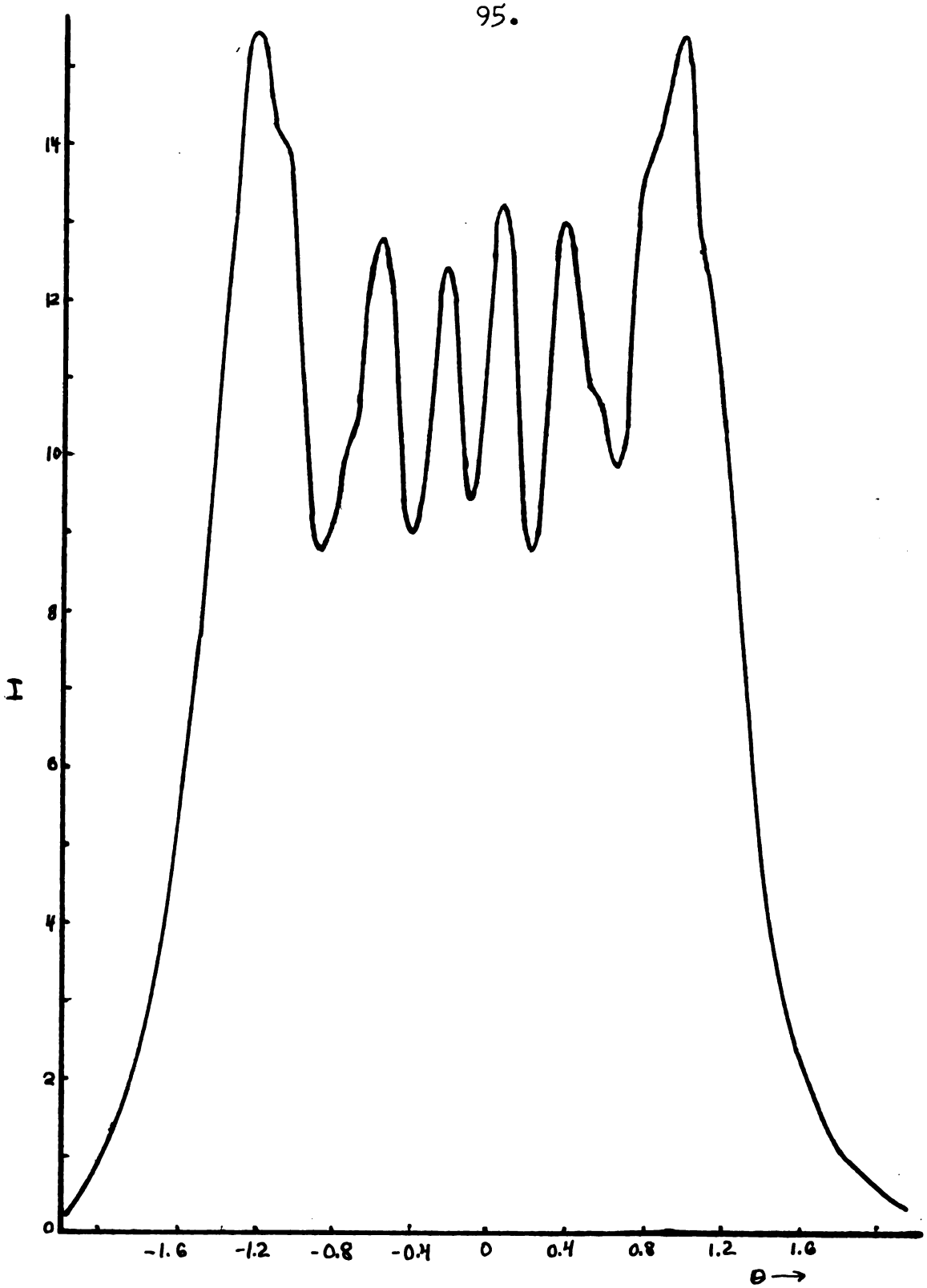

Fig. 55 Grating B with source aperture removed. Note similarities to Fig. 54

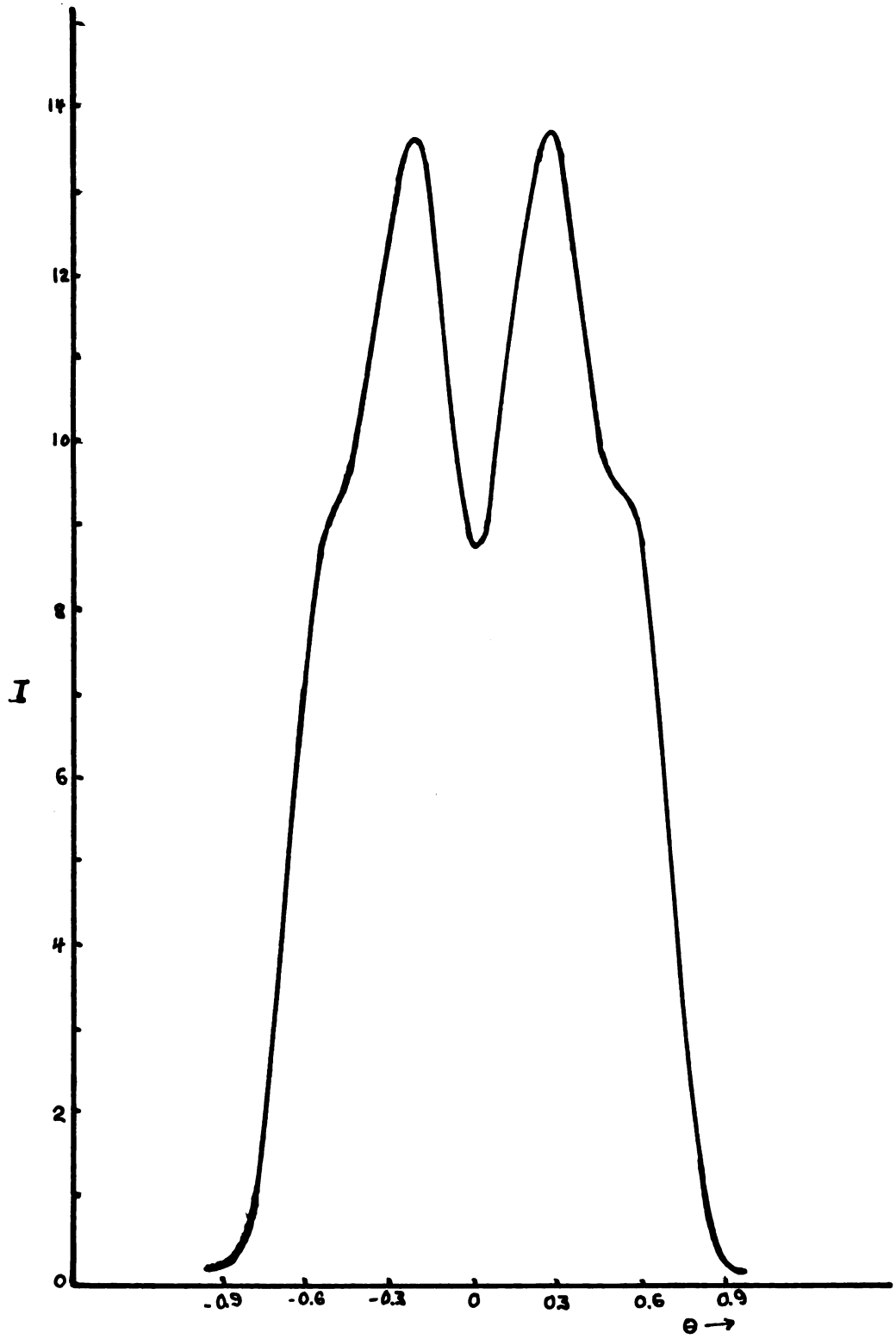

Fig. 56 Single aperture illuminated in the coherent mode. Note the structure beginning to appear at each side of the image $\alpha = 5.5\lambda/D$.

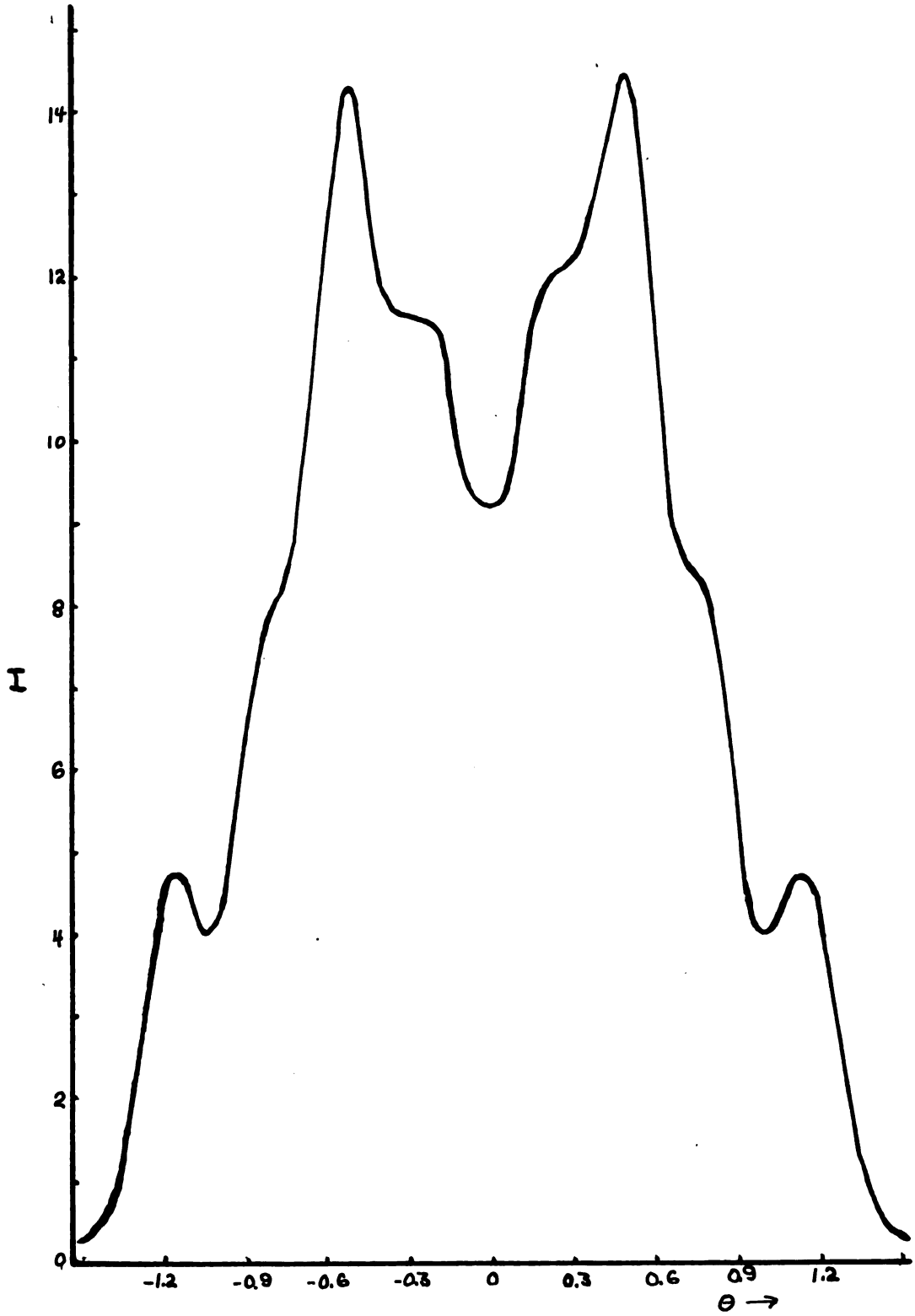

Fig. 57 Single aperture illuminated in the coherent mode as in Fig. 56. $\alpha = 9.42\lambda/D$.

Fig. 58 Single aperture as in Figs. (56) and (57) with source aperture removed.